BIOMASS ASPECT AND AIR VELOCITY MODELING FOR COMBUSTION AND HEAT TRANSFER ENHANCEMENT IN GRATE FIRED BOILER

By

J.Elamathi Raja

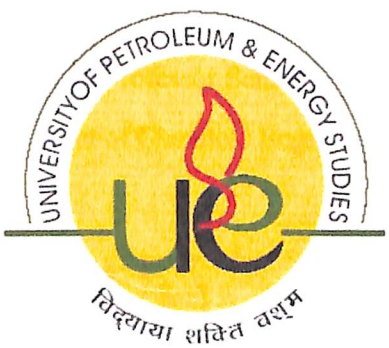

College of Engineering

University of Petroleum & Energy Studies

Dehradun

April, 2011

BIOMASS ASPECT AND AIR VELOCITY MODELING FOR COMBUSTION AND HEAT TRANSFER ENHANCEMENT IN GRATE FIRED BOILER

A thesis to be submitted in partial fulfillment of the requirements for the Degree of

Master of Technology

(Energy Systems)

By

J.Elamathi Raja

Under the guidance of

.....

Mr.Sanjay Dashrath Dalvi

Assistant Professor Senior Scale

Department of Chemical Engineering

Approved

.....

Dr. Shrihari

Dean

College of Engineering

University of Petroleum & Energy Studies

Dehradun

April, 2011

CERTIFICATE

This is to certify that the work contained in this thesis titled **"Biomass aspect and air velocity modeling for combustion and heat transfer enhancement in grate fired boiler"** has been carried out by **J.Elamathi Raja** under my supervision and has not been submitted elsewhere for a degree.

Mr.Sanjay Dashrath Dalvi
Assistant Professor - Senior Scale
Department Of Chemical Engineering
College of Engineering Studies
University of Petroleum and Energy Studies
Dehradun – 248 007

Date: 27/01/2011

Human Resources Department

Forbes Marshall

P B: 29, Mumbai-Pune Rd.,
Kasarwadi, Pune 411 034
Tel: 91 (0) 20-27145595

Fax: 91 (0) 20-27147413
Website: www.forbesmarshall.com

Ref: PN/HRD/189

Dt: 15.04.2011

TO WHOMSOEVER IT MAY CONCERN

This is to certify that **Mr. J.Elamathi Raja**, Final year M.Tech (Energy Systems) of University of Petroleum and Energy Studies, Dehradun, has done Project Works in our organization during the period from 20th January 2011 to 20th April 2011.

20/4/11

Manager – HR

Forbes Marshall Pune

Acknowledgement

ACKNOWLEDGEMENT

I would like to solicit my earnest gratitude to my beloved Dean **Dr. Shrihari**, Department of Chemical Engineering, College of Engineering Studies, University of Petroleum & Energy Studies, Dehradun, who devised me this golden opportunity.

It's my immense pleasure to thank my guide **Mr. Sanjay Dashrath Dalvi**, Assistant Professor Senior Scale, Department of Chemical Engineering, for tracing out the field of combustion and heat transfer and for his intend reference made during the course of study and valuable suggestion offered for the successful completion of project and presentation within the prescribed time.

I am in a position in expressing my gratefulness to **Dr. Kamal Bansal**, Professor, Department of Electrical, Electronics & Instrumentation Engineering and **Mrs. Madhu Sharma**, Assistant Professor - Senior Scale, Department of Electrical, Electronics & Instrumentation Engineering for their appraisal and acceptance made at the early stage of this project work.

I express my sincere thanks to University of Petroleum & Energy Studies for encouraging the Master degree students to undergo six month project in the field of their interest.

I wish to place my deep sense of gratitude to my parents and family members for their inspiration and support

J.Elamathi Raja

Contents

CONTENTS

SI.NO.	Particulars	Page No
	Acknowledgement	
	List of tables	II
	List of figures	IV
	Nomenclature	VI
	Abstract	IX
I	Introduction	01
II	Review of Literature	05
III	Model Development	21
IV	Results and Discussion	62
V	Summary and Conclusions	109
	References	
	Annexure	

LIST OF TABLES

SI.NO.	Particulars	Page No
1.1	Preferred pressure temperature combinations at inlet to steam turbines	2
1.2	Recommended Flue Gas Temperatures at Furnace Outlet for achieving Various superheat Steam Temperatures	3
3.1	Combustion Regime of biomass	30
3.2	Typical Value of Volumetric Heat Release Rate (q V) in MW/m^3	43
3.3	Typical Value of Upper Limit of qF in MW/m^2	44
3.4	Recommended values of burner region heat release rate, qb	45
4.1	Burning rate and burning time of different wood piece size	74
4.2	Burning rate and burning time of different wood piece size	75
4.3	Behavior of burning rate with impinging primary air pressure	76
4.4	Mass flow rate of flue gas	83
4.5	Flue gas composition by weight basis	84
4.6	The partial pressure ratio and molecular weight of flue gas species	84
4.7	Calculated property of flue gas for selected boiler design over wide range of temperature	87
4.8	Fuel bed temperature Vs. Fuel bed heat release rate	88
4.9	Fuel bed density Vs. Heat release rate	89

4.10	Mean Beam Length for furnace dimension	92
4.11	Non-luminous radiative coefficient of flue gas	95
4.12	Primary Super Heater tube diameter Vs. Convective Coefficient	99
4.13	Air preheater internal tube diameter Vs. Internal heat transfer Coefficient	100
4.14	Pressure drop across fuel bed in grate with initial staged void fraction	105
4.15	Pressure drop across fuel bed in grate with varied void fraction with Respect to varying primary air velocity	106
4.16	Behavior of void fraction with respect to primary air velocity in fuel bed	106

LIST OF FIGURES

SI.NO.	Particulars	Page No
2.1	Schematic of the experimental rig	9
2.2	Calculated bed height and solid temperature profile vs. time	10
2.3	Calculated rate as the function of time	11
2.4	Burning rate as a function of both primary air flow rate and moisture content in the fuel	13
2.5	Volatile release rate as a function of both primary air flow rate and moisture content in the fuel	15
2.6	Peak bed temperature as a function of both primary air flow rate and moisture content in the fuel	16
2.7	Effect of particle size	18
2.8	Effect of bed porosity	19
3.1	General scheme for carbon combustion showing global heterogeneous and homogeneous reaction	23
3.2	Species and Temperature Profile of Carbon Particle of Biomass	26
3.3	Species mass flux at the carbon surface and at an arbitrary radial location	27
3.4	Energy Flow at the surface of Biomass Carbon Particle burning in air	31
3.5	Chain Grate assembly Fired Boiler	35
3.6	Different representations of a non-regular shaped particle	36

4.1	Furnace different level	64
4.2	Two stage superheater - Primary and Secondary	64
4.3	Boiler Bank - Cross Flow (Typical)	66
4.4	Boiler Bank Screen (Typical)	66
4.5	Economizer	67
4.6	Behavior of particle burning time with respect to biomass size	75
4.7	Variation of burning rate as the function of biomass aspect and pressure	77
4.8	Variation of heat release from bed with corresponding bed temperature	90
4.9	Fuel bed density Vs. Fuel bed heat release to near furnace wall	90
4.10	Variation of Non-luminous radiant coefficient with gas temperature	95
4.11	Primary super heater tube OD vs. Convective Coefficient	99
4.12	Air preheater internal diameter Vs. Internal heat transfer coefficient	101
4.13	Pressure drop in fuel bed with initial staged void value of wood particle	107
4.14	Pressure drop in fuel bed with varying void value with respect to primary air velocity	107
4.15	Bed void fraction Vs. Velocity of primary air	108

NOMENCLATURE

Symbol	Abbreviation
PA	Primary Air
dv	Volume Diameter,m
ds	Surface Diameter,m
dp	Sieve Size
dsv	Surface-Volume Diameter,m
Ø	Sphericity
qv	Heat Release Rate per unit volume, Kcal/m^3
qF	Heat Release Rate per Unit Cross Sectional Area, Kcal /m^2
qb	Heat Release Rate per Unit Wall Area of the Burner Region
Yo_2,s	Concentration of oxygen in particle surface
Yo_2, ∞	Concentration of oxygen in away from surface
Ts	Temperature at surface, K
T∞	Temperature away from surface, K
ϑ_1	Mass stoichiometric coefficient
Kc	Kinetic rate constant coefficient (m/s)
ρD	Product of density and mass diffusitivity
Tsur	Surroundings Temperature, K
Cpg	Specific Heat of gas (J/Kg-K)

KB	Burning Rate Constant, m^2/s
t_c	Burning time of biomass particle, s
Do	Diameter of Biomass Particle, m
LHV	Lower Heating Value of fuel, KJ/Kg
V	Furnace Volume, m^3
B	Designed fuel consumption rate, Kg/s
F	Cross sectional area of the furnace grate m^2
Nu	Nusselt Number
Re	Reynolds Number
Pr	Prandtl Number
ρ_{avg}	Average density of fuel bed in furnace, Kg/m^3
T_b	Average temperature of fuel bed, K
K_g	Thermal conductivity of the flue gas in W/m° C
μ_g	Dynamic viscosity of flue gas in kg/ms
h_r	Non-Luminous Radiative Coefficient, KJ/m^2h °C
t_g	Gas temperature in ° C
MBL	Mean beam length in m
Tw	Log mean wall temperature in ° K
KE	Wall emissivity correction factor
D	Outside diameter of tube in m
t_f	Film temperature in ° C

R	Fire bed (grate) surface area, m^2
H	Surface area of heat transfer (water wall), m^2
ε_{red}	Emissivity of bed
ε_{eff}	Emissivity of wall
ε_g	Emissivity of furnace gas
a_g	Absorptivity of furnace gas
ρ_a	Pressure of species A
N_a	Total number of moles of species A in the volume V
p	Total pressure exerted by the gas mixture
$\frac{\Delta P}{L}$	Pressure drop across fuel bed , N/m^2 per m of fuel depth
ε	Void fraction in the bed
U	Gas flow rate per unit cross section of the bed, m/s
OD	Outer Diameter of tube, mm

Abstract

ABSTRACT

BIOMASS ASPECT AND AIR VELOCITY MODELING FOR COMBUSTION CUM HEAT TRANSFER ENHANCEMENT IN GRATE FIRED BOILER

By

J.Elamathi Raja

Degree : **Master of Technology**

Guide : **Mr.Sanjay Dashrath Dalvi**

Assistant Professor - Senior Scale

Department Of Chemical Engineering

College of Engineering Studies

University of Petroleum and Energy Studies

Dehradun – 248 007

April, 2011

The biomass combustion in the furnace is depend on physical (Moisture content and particle size) and chemical property (fuel composition) of fuel as well as furnace design and its environment like mass flow rate of oxygen, particle residential time, temperature, turbulence and velocity of combustion air.Mostly physical and chemical property of fuel cannot be greatly controlled but the biomass particle size and the combustion velocity can be handled manually to have the change in combustion behavior.

Also the heat transfer inside the furnace is the function of fuel combustion rate and furnace components design parameters. The combustion rate of wide biomass aspect was calculated whose result shows the burning rate will increases with increase in pressure of impinging primary air. The fuel bed heat release rate have minimal changes from 87.94 W/m^2 K to 86.30 W/m^2 K over wide range of the fuel bed temperature from 1900 K to 1200 K.

But when the fuel bed density vary from 800 to 500 Kg / m^3, the heat release have wide variation of about 92.8 W/m^2 K to 77.27 W/m^2 K. The Non-luminous radiative coefficient at

adiabatic flame temperature of wood (1627 ° C) is 108.18 W/m^2 °C, but in actual it is about 71.64 W/m^2 °C at 1100 ° C of fuel bed temperature.

The convective coefficient tends to increase about 15 % (From 14.72 to 17.09 W/m^2 ° C) with about 30 % reductions in OD of superheater (From 50.8 mm to 35 mm) and its observed that the maximum heat absorption takes place by heat radiation. The wood piece of 6 cm long and 3 cm diameter have customized pressure drop between 3mm to 5 mm of WC per mm of fuel bed depth between 11 m/s to 15 m/s of air velocity which will result in enhanced combustion.

Key words: Biomass combustion; particle size; air velocity; fuel bed heat rate; Non-luminous radiative coefficient; Convective coefficient; fuel bed pressure drop.

Introduction

CHAPTER I

INTRODUCTION

1.1 Biomass Combustion

Biomass combustion represents a possibility to lower regional emissions of the greenhouse gas CO_2, especially in countries with large wood resources. In India, potential of energy generation through biomass is about 22000 MW out of which we achieved only 2437 MW (MNRE, 2010). Despite the ecological advantages of renewable energies, a techno-economic optimization of the combustion unit is necessary in order to make biomass-fired heating plant competitive with fossil fuel-fired systems. The major goal of the development and optimization of biomass grate furnaces is the reduction of investment and operating costs. This can be achieved by a compact furnace design, an increased availability of the plant, by reduced emissions (CO and NO_x) as well as by reduced air and flue gas fluxes in the furnace. The design of biomass furnaces is still usually based on experience and empirical data.

1.2 Grate boiler in glance

Boiler is the mean to have combustion of fuel & transferring the resulting energy of combustion to working fluid called water which is converted in to steam after absorbing the energy which again used for driving a mechanical device or process heat application. Grate fired boiler are widely used in industrial application for its ability to handle high moisture content fuel and wide range of fuel input. While operation of this boiler about 15 – 20% of energy is loosed through heat along flue gas (7 to 10%), evaporation of water formed as a result of hydrogen oxidation (7%) and surface radiation & unaccountable loss (2%) (BEE, 2005).

This study is about bringing down the energy loss in flue gas to maximum extent by increased heat transfer of hot gas to working fluid & achieving complete combustion with least excess air by experimenting the biomass combustion phenomena with different biomass aspect (size) and combustion air velocity there by its effect on carbon burnout, excess air requirement, residential time for particle combustion, heat release rate, composition of gas, distribution path of hot gas within the furnace geometry and temperature distribution of hot gas is examined and optimized biomass size & air velocity is chosen with respect to achieve less excess air

requirement, maximum heat release rate, maximum heat transfer between hot gas & water wall tubes within furnace geometry. The effectiveness of biomass combustion mainly depends on its particle size (exposed surface area) & mass flux of oxygen which have relation with its velocity. So these two main factors are going to be analyzed in this study.

Grate fired boiler have to handle wide range of fuel with different bandwidth of moisture content, so it's necessary to establish the optimum size of biomass and combustion air velocity to achieve maximum combustion efficiency. These grate boilers are characteristics with slow response to load swing because of high fuel loading on grate. To overcome this problem detail study upon various fuel factors (like Moisture content, particle size, mass flow rate of oxygen, composition, residential time, velocity of combustion air) and its influence on combustion need to be done. But invariably control of particle size and combustion air parameters are only left to us to make regulation upon combustion. So these parameters are selected for the analysis.

1.3 Biomass power plant

The most efficient method of using bio-mass would be for power generation purposes. The bio-mass boilers would produce steam which will be fed to steam turbine producing electrical power. The steam turbines work on the Rankine Thermo Dynamic Cycle. Rankine Cycle gives better efficiencies with the increase in pressure and temperature of the steam fed to the turbine. The turbine designs have their own special features which make certain steam temperature regimes attractive with certain specific steam pressure regimes. These ranges of steam pressure and their corresponding ranges of steam temperature are given in Table 1.1.

Table 1.1 Preferred pressure temperature combinations at inlet to steam turbines

S.No	Steam inlet pressure (ATA)	Preferred steam inlet temperature (Deg C)
1	32	435
2	41	455
3	62	485
4	86	510 / 538
5	103 and above	538 / 635

It should always be desirable to go in for as high a steam pressure and temperature as possible. However, going in for higher steam temperature for certain specific pressure values have limitations with regard to boilers firing bio-mass fuels (Sridharan, 2008).

With higher steam temperatures and pressures, it becomes necessary that greater percentage of total heat of steam generation be given in the super heater. It then becomes necessary that the flue gasses leaving the furnace must have higher and higher temperatures, in order to cater to this higher percentage of super heat requirements (Sridharan, 2008).

Table 1.2 Recommended Flue Gas Temperatures at Furnace Outlet for Achieving Various Superheat Steam Temperatures

S.No	Super heat steam temperature (^{o} C)	Required furnace exit gas temperature (^{o} C)
1	Up to 380 °C	Above 600 °C
2	380 – 420 °C	Above 650 °C
3	420 – 480 °C	Above 700 °C
4	480 – 520 °C	Above 750 °C
5	520 – 540 °C	Above 980 °C

It becomes evident from the Table 1.2 that the ash fusion characteristics of the bio-mass fuel will have a definite influence on the allowable flue gas temperature on furnace outlet. The flue gas temperatures at furnace outlets should be 100°C less than the ash fusion temperature. This feature imposes restriction on the super heat temperature that can be achieved in a boiler with a given bio-mass fuel. Most of the bio-mass fuels are therefore not amenable for super heat temperature of 515°C and above. They are also non-amenable for adoption with re-heat cycles

The higher moisture content in the biomass fuels lead to higher moisture content in the flue gas evolved. The non-luminous radiation characteristics of flue gas are greatly influenced by the quantity of water content in them. Flue gasses with high water content give raise to higher non-luminous radiation. The bio-mass fuel fired boilers should take this into consideration while assessing the total heat transfer across various heating surfaces in such boilers.

The higher moisture content of flue gasses also lead to higher dew point of these flue gasses. The low temperature heating surfaces in biomass fired boilers are therefore susceptible to low temperature corrosion due to moisture. The design of air pre-heaters for biomass fired boilers should take this aspect into account (Sridharan, 2008).

The biomass is a promising fuel alternative for power generation. Since, the biomass is created by "Carbon fixation" the combustion of biomass is not disturbing the delicate "carbon di-oxide balance" of the atmosphere. The adoption of bio-mass as a fuel for power generation should therefore be encouraged.

1.4 Objectives

1. To optimize operational loading of boiler for enhancing boiler Combustion & heat transfer
2. Experimenting combustion with different biomass aspect cum combustion air velocity for optimizing biomass size and primary air supply pressure
3. To study the radiative heat transfer and convective heat transfer from fuel bed and flue gas to furnace water wall surface
4. To study the design of selected boiler components and its influence on heat transfer coefficient

Review of Literature

CHAPTER II

REVIEW OF LITERATURE

This chapter consists of previous work carried out in the field of biomass combustion modeling with respect to primary air velocity, biomass size distribution and heat release rate and their studies are categorized under the following subtopics.

2.1 Combustion of biomass in packed bed

2.2 Mathematical description of biomass and solid waste combustion on a packed bed

2.3 Experimental facilities

2.4 Bed height, solid temperature and reaction zone thickness vs. time

2.5 Process rates vs. time and combustion stages

2.6 Time-averaged burning rate vs. primary air flow rate and moisture level

2.7 Devolatilisation rate vs. primary air flow rate and moisture level

2.8 Char burning rate vs. primary air flow rate and moisture level

2.9 Effect of particle size

2.10 Effect of bed porosity

2.1 Combustion of biomass in packed bed

Combustion of biomass and municipal solid wastes can be accomplished in packed beds, either static or moving. The design, operation and maintenance of such combustion equipment require detailed understanding of the burning process inside the bed. There have been many researches into packed bed combustion of solid fuels, mainly biomass and wastes during the last two decades. The propagation of a reaction front in a packed bed for thermal conversion of municipal waste and biomass was investigated by Gort (1995). The distribution of temperature and gas composition in a bench-top packed bed burning simulated waste (SW) fuels has been measured by Goh *et al.*, (1999). Other researchers include Zakaria *et al.*, (2000) who investigated

the reduction of NOx emission from the burning bed in a municipal solid waste incinerator and Ro¨nnba¨ck *et al.,* (2000) who studied experimentally the influence of primary airflow and particle properties on the ignition front, its temperature and on the composition of the exiting gases in a biomass fuel bed.

Measurements on medium or large-scale moving beds were also carried out by Sharifi (1990) in which detailed measurements of waste properties, bed temperature and gas composition profiles were reported. Measurements on gasification of waste materials in a medium-scale grate system were done by Beckmann *et al.,* (1997). The latest full scale experiments on moving grates were reported by Thunman *et al.,* (2001) and Yang *et al.,* (2002).

However, there is still a lack of detailed and systematic theoretical study on the packed bed burning of biomass and municipal solid wastes. The advantage of theoretical study lies in its ability to reveal the detailed structure of the burning process inside a solid bed, such as reaction zone thickness, combustion staging, gas emission and char burning characteristics, thus contributing to better understanding and controlling of the process. These parameters are hard to measure by conventional experimental techniques.

The authors have previously investigated the effects of fuel devolatilisation and moisture level on the combustion of wood chips and incineration of simulated municipal solid wastes in a packed bed by Yang *et al.,* (2002) and it was found that the kinetic devolatilisation rate has noticeable effects on the ignition time, peak flame temperature, CO and H_2 emissions at the bed top and the proportion of char burned in the final stage (char burning only) of the combustion; and also a wetter fuel results in a thinner reaction zone in the bed. In this paper, the work is extended to the effect of primary airflow rate for biomass and municipal solid wastes.

Primary airflow is employed as a major controlling parameter to maintain the stability of the combustion and achieve the desired burning rate, temperature and gas composition. In this paper, the same mathematical model as in previous work by Yang *et al.,* (2002) is employed and extensive calculations carried out to assess the combined influence of the primary airflow and moisture level on the burning behavior of biomass and simulated municipal solid wastes in a

static bed. Limited experimental work was also done to validate the calculations. The current research contributes to better understanding of the biomass and waste combustion processes

2.2 Mathematical description of biomass and solid waste combustion on a packed bed

Peters (2003) summarized the previous mathematical models on packed bed combustion. Those models can be generally classified into four categories: continuous-medium models where the solid bed was treated as a continuous medium; neighboring-layers models where the packed bed above the grate was divided into four layers representing fuel, drying, pyrolysis and ash; well stirred reactor models where the bed was simulated by a cascade of well-stirred reactors; and the 1d + 1d model where a one-dimensional and transient single-particle model in spherical coordinates was implemented in a transient one-dimensional fuel-bed model.

A packed bed, either stationary or moving, consists of numerous individual particles and the gaps between them through which combustion air flows. Ideally, calculations should be made both outside and inside the solid particles. But the shear number of the individual particles in the bed prevents such delicate calculations to be performed on the whole bed due to an unrealistic requirement for CPU speed and computer memory. In fact, the temperature profile inside a particle is three-dimensional (not one-dimensional in respect of the radial distance) and this further adds to the difficulty. In the light of this, in this study the whole bed is treated as a continuous porous medium and numerical calculations are carried out by dividing the bed into many cells. Inside each cell the concerned parameters (e.g. temperature, percentage of moisture, carbon, etc.) are assumed uniform and by reducing the cell size (hence increasing the cell number), calculation can be made on a size-scale much smaller than the fuel particles. For the fuels used in this work (size around 12 mm), the Biot number is calculated as being around 1.0. So no significant errors are expected to occur due to the non-isothermal behavior of the solids. The solid fuel is assumed to consist of four components, moisture, volatile matter, fixed carbon and ash (Yang *et al.*, 2003).

The incineration process of solid wastes can be divided into four successive sub-processes: evaporation of moisture from the solids, volatile release/char formation, burning of

the hydrocarbon volatiles in the gaseous space, and the combustion of char particles. The transport equations for the gas and solid phases are summarized in the following.

Peters (1995) has summarized the basic governing equations for both the gas and solid phases in a moving bed. Full description of the model and equations as well as the model parameters employed in this study can be found in the authors' earlier work . The whole bed height is discretized into 460 sections and time-dependent solutions are sought. The particle size is taken as 12 mm in diameter. The waste fuel is assumed to be ignited by over-board radiation at fixed heat flux of 88 kW/m^2.

This radiation source is present for the whole combustion period. Primary air at 20 $^{\circ}C$ enters the bed from under the grate. Initial bed height is taken at 480 mm. The combustion starts at the bed top and the bed height falls as the flame front travels down towards the grate. Apart from the fuel properties, all other model parameters maintain the same for all the calculated cases, like those for kinetic devolatilisation rate, mixing of the volatile gases and under-grate air in the bed, char burning, in-bed radiation, etc.

Boundary conditions: at the upper boundary, gradients of the gaseous temperature, concentrations and velocity are assumed to be zero (the second-type boundary). For the solid phase, the third-type boundary is assumed at both the bottom of the bed and the top surface for temperature (conduction and radiation heat exchange with the grate and over-bed radiation source are considered) (Yang *et al.*, 2003).

2.3 Experimental facilities

A fixed-bed reactor was employed to burn wood chips and simulated solid wastes Yang *et al.*, (2002). The reactor was a vertical cylindrical combustion chamber suspended from a weighing scale (Fig. 2.1). The height of the chamber was 1.5 m with an inner diameter of 200 mm. It consisted of an interior tube surrounded by a thick layer of insulating material and an external casing (Yang *et al.*, 2003).

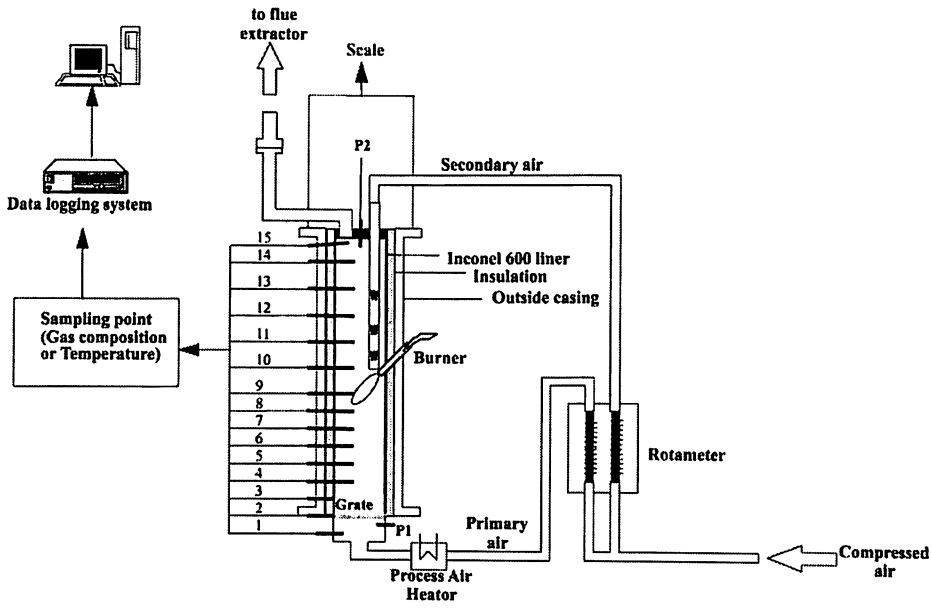

Fig 2.1 Schematic of the experimental rig

The grate was located at the bottom of the chamber and consisted of a perforated plate made from stainless steel, with approximately 700 holes of 2 mm diameter, representing 7% open area.

Thermocouples were used to monitor the temperature of primary airflow, temperature inside the bed at different height levels and temperature of the flue gases. There was a gas-sampling probe inside the chamber at 430 mm above the grate. A gas burner was placed at a 458 angle toward the waste at 750 mm above the grate. The gas burner was used to initiate the burning process of the waste sample and for maintaining the free-board combustor temperature during the experiment. Primary air was fed from the bottom of the fixed-bed reactor through the grate without preheating (Yang *et al.*, 2003).

2.4 Bed height, solid temperature and reaction zone thickness vs. time

Fig. 2.2 shows the calculated bed height and solid temperature profile vs. time for the combustion of SW containing 31% moisture in the bench-top incinerator. The initial bed height is 480 mm above the grate and the primary air flow rate is 0.13 kg/m^2 s. The inlet air temperature

is 15 ° C. It is seen that the bed top begins to fall at t = 200 s as the local bed temperature rises from room level to above 900 K.

Later the temperature at the bed top increases to 1300 K while the height of the bed decreases linearly. From around t = 400 s, the bed-top temperature begins to fall to around 1100 K and remains at that level for a considerable time period. During this time, the height of the bed continues to drop linearly. It is also seen that the flame front reaches the bottom of the bed (the grate) at around t = 1100 s.

After that, the bed becomes very hot for a short period of time and the maximum temperature goes up to 1500 K. This lasts about 200 s during which time the height of the bed undergoes only a slight fall. Further on, the bed residual material cools down as the combustion completes at t = 1450 s. It is also interesting to note the development of the reaction zone as time goes on (Yang *et al.*, 2003).

The thickness of the reaction zone is defined as the distance from the bed top downward to where the bed temperature begins to rise from the original room temperature. Fig. 2.1 shows that as the bed gets ignited from the top at around t = 100 – 200 s, the reaction zone thickness increases quickly to about 14 mm or roughly one particle diameter.

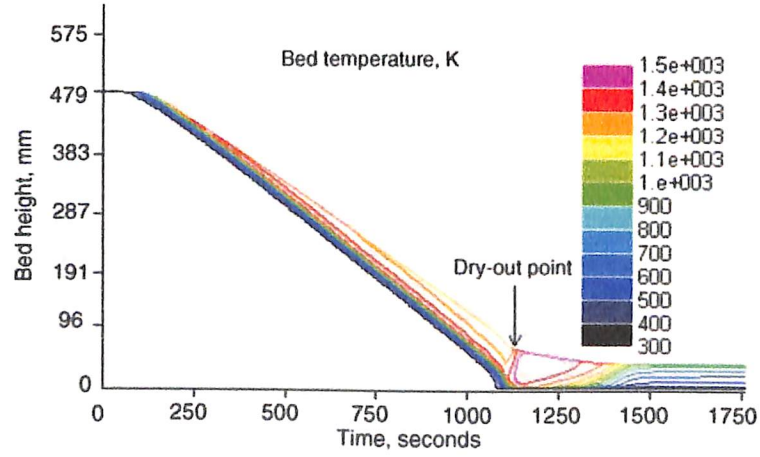

Fig 2.2 Calculated bed height and solid temperature profile vs. time (SW, 30% moisture, initial bed height = 480 mm, primary air = 0.13 kg/m^2 s at 15 8C).

With the combustion proceeding, the reaction zone thickness increases and reaches a maximum level of 96 mm or 8 times of the original particle diameter when the flame front touches the bed bottom. After that, the reaction zone extends to the whole bed height for a while before receding towards the bed top as the char burns out (Yang *et al.*, 2003).

2.5 Process rates vs. time and combustion stages

Fig. 2.3 shows the corresponding calculated individual process rates as a function of time for the case shown in Fig. 2.2. The individual process rates are for moisture evaporation, devolatilisation and char combustion. Three stages are identified. The first is the initial or ignition stage (t = 0 – 100 s) where only moisture evaporation occurs (Yang *et al.*, 2003).

The moisture inside the solids is driven out at temperature of 100 ° C by strong radiation from the over-bed ignition source. When all the moisture in the top layer has been evaporated, the local bed temperature then rises quickly to the onset point of devolatilisation (taken as 260 ° C or 533 K) at t = 100 s and the bed is ignited. There is a temporary fall in the moisture evaporation rate just before the bed ignition. This is because the over-bed heat input to the evaporation front inside the bed decreases as the front moves away from the bed top downward. After that, the moisture evaporation rate recovers as the heat supply shifts from over-bed to the newly established flame-front at the bed top (Yang *et al.*, 2003).

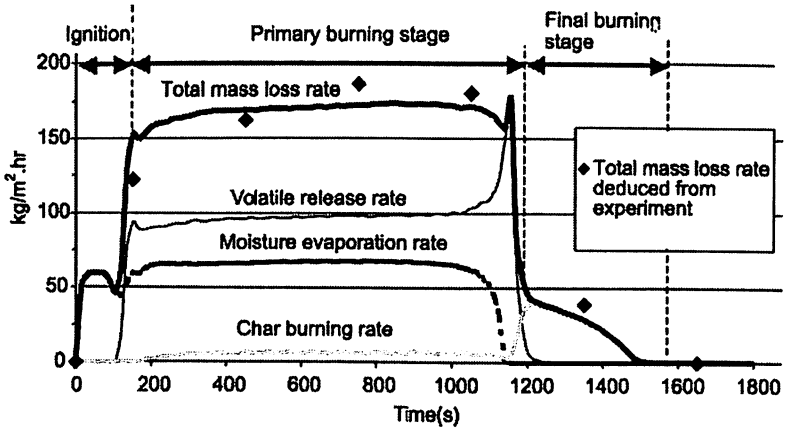

Fig 2.3 Calculated rate as the function of time

(SW,30% moisture, initial bed height = 480 mm, primary air = 0.13 kg/m^2 s at 15 ^{0} C).

The primary burning stage starts after the bed gets ignited at t = 100 s and extends to where both the moisture and the volatiles in the whole bed have been completely driven out at t = 1200 s. It takes over 70% of the total combustion time. During this period, moisture evaporation, devolatilisation and char burning rates maintain a relatively constant level, respectively (the formed char begins to burn at t = 200 s as the local solid temperature reaches a preset onset temperature of 600 ° C or 873 K). Towards the end of this primary stage, the devolatilisation rate shows a sharp rise before falling to zero (Yang *et al.*, 2003).

This is because all the moisture has evaporated at this point, causing an upsurge in the bed temperature. The final stage of combustion follows where only char burning occurs. An initial sharp increase in the char burning rate is shown and this is due to the increased O_2 availability to the char burning (in the primary stage, most of the O_2 is consumed by volatile gas burning). The char burning rate falls gradually as time goes on until the whole combustion process completes at t = 1500 s. The final stage comprises 20% of the total combustion time. Fig. 2.3 also shows the calculated total mass loss rate as a function of time compared to experimental measurement. Agreement between the two is reasonably good. The total mass loss rate is a summation of moisture evaporation, volatile release and char burning (Yang *et al.*, 2003).

2.6 Time-averaged burning rate vs. primary air flow rate and moisture level

Fig. 2.4 shows the time-averaged burning rate on a dry basis as a function of primary air flow rate at different moisture levels for SW, wood cubes and forest wastes. The particle size ranged from 10 to 20 mm though for theoretical calculations it was fixed at 12 mm. Experimental data, especially from Gort (1995) have clearly established the patterns for the relationship between the burning rate and the air flow rate at different moisture levels.

However, a systematic theoretical calculation employing proper mathematical models has not been done previously and the results shown here are intended to demonstrate the reasonably good agreement between the modeling predictions and experimental measurements. This gives validity for the following detailed. Theoretical analysis of the combustion processes.

The airflow rate spans a range from 0.03 to 0.6 kg/m^{2}s without preheat (around 15 $^\circ$C) and the moisture level covers from 10 to 50% on a wet basis.

At a certain moisture level, the burning rate increases as the airflow rate increases until a peak point is reached, beyond which a further increase in the air flow results in a fall in the burning rate. This is defined as the critical air flow rate and reflects the balance between the burning heat absorbed by the solids and the heat loss to the cooler gas stream from the particles. Thus at lower air flow rates, more heat is generated than that carried away by the gas flow.

At higher flow rates, however, the heat carried away by the gas flow exceeds the heat generated by combustion. The effect of moisture level in the fuel is obvious. At a fixed airflow rate, drier fuels have higher burning rates while wetter fuels have lower burning rates. For example, at 10% moisture the maximum burning rate obtainable (the peak point at the critical air flow rate) by experiments was 0.07 kg/m^2 s while at 50% moisture it was only 0.018 kg/m^2 s, nearly 4 times lower.

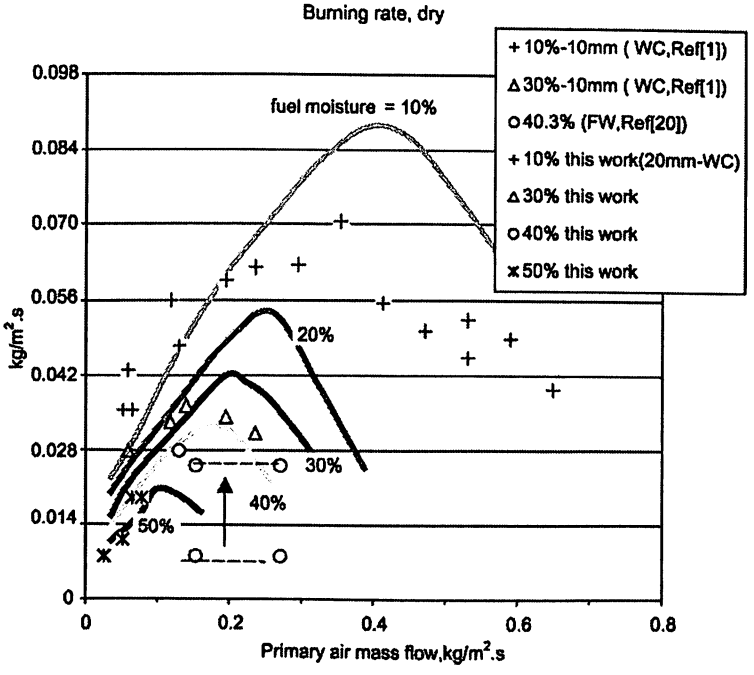

Fig 2.4 Burning rate as a function of both primary air flow rate and moisture content in the fuel.

The critical air flow rate corresponding to each of the peak burning rates is also affected by the level of moisture. Calculations show that a drier fuel has a higher rate and a wetter fuel has a lower one. Results of the theoretical calculation and the experiments can be compared. Agreement is satisfactory to good in terms of the general trends. However, the calculated burning rate is higher than the measured one at high primary air flow rates. This might be caused by the channeling phenomenon at a high airflow rate in an actual bed. The local bed structure (porosity, particle size distribution and the orientation of particles) cannot be made perfectly uniform in an actual bed. The effect of such structure non-uniformity on the flow distribution inside the bed can become significant at high flow rates and channeling occurs as a consequence, where some of the combustion air would bypass the solids and flows out of the bed without reacting, thus reducing the burning efficiency. The current mathematical models did not take the channeling into account (Yang *et al.*, 2003).

2.7 Devolatilisation rate vs. primary air flow rate and moisture level

Fig. 2.5 shows the calculated time-averaged devolatilisation rate as a function of both air flow rate and moisture level. Similar trends to the situations of the burning rate are found for the devolatilisation rate in relation to the change in the air flow rate. The moisture level also demonstrates a strong effect and the drier the fuel, the higher its devolatilisation rate. For example, the maximum devolatilisation rate for 10% of moisture is obtained as 0.08 kg/m^2 s, compared to only 0.028 for 40% of moisture.

The volatile release rate is a strong function of temperature. Drier fuels require less heat for moisture evaporation and the reaction zone is thicker Yang *et al.*, (2002). The moisture evaporation front is moved away from the devolatilisation front so that less heat is transferred from the devolatilisation zone downward to the moisture evaporation zone, resulting in a higher temperature in the devolatilisation zone which enhances the devolatilisation rate.

2.8 Char burning rate vs. primary air flow rate and moisture level

There are two stages involving char burning, the primary stage and the final stage. In the primary stage, the char burning rate is affected by both the primary air flow rate and the moisture

level in the fuel. It is seen that at any fixed moisture level greater than 10%, the char burning rate in the primary stage rises as the primary air flow increases and reaches a peak point at the critical air flow rate. After that the rate declines as the air flow is further increased.

This is in line with the total burning rate shown in Fig. 2.4. For the moisture level at 10%, however, the char burning rate undergoes a continuous rise as the primary air increases in the whole covered range. The moisture level also affects the char burning rate in the primary stage. Firstly, the critical air flow rate at which the char burning rate reaches a maximum shifts to a greater value for a drier fuel. For example, the critical air rate is 0.2 kg/m^2 s for 40% moisture, but increases to 0.32 kg/m^2 s for 20% moisture. Secondly, in the range where the air flow is lower than the critical rate (at a given moisture level), a wetter fuel, surprisingly, has a higher char burning rate than a drier fuel at the same air flow rate. This is not clear for the cases of 10 and 20% moisture, however (Yang *et al.*, 2003).

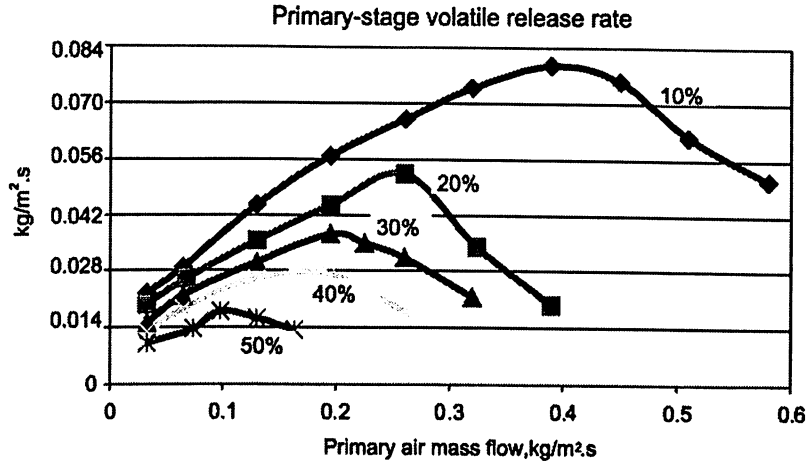

Fig 2.5 Volatile release rate as a function of both primary air flow rate and moisture content in the fuel. The moisture level ranges from 10 to 50% on a wet basis. The fuels are 12-mm simulated wastes (SW). The over-bed radiation heat flux is fixed at 88 kW/m^2.

It is also interesting to look at the percentages of char burned in the primary and final stages. The amount of char burned in the final stage takes the balance. It is seen

that the percentage of char burned in the primary stage increases roughly linearly with increase in the primary air flow (Yang *et al.*, 2003).

At each moisture level, there is a critical air flow rate at and beyond which all the char is burned in the primary stage and the final or the char-burning-only stage no longer exists. The moisture effect is significant. The wetter the fuel, the higher the percentage of char burned in the primary stage. For the wettest fuel, all the char is burned in the primary stage even at small air flow rates. The char burning depends on three factors: the amount of formed char, the O_2 availability and the temperature. The relationship between its rate and the primary air flow can be explained in terms of those three factors. In the range of air flow smaller than the critical rate (at a given moisture level), an increase in the air flow makes more O_2 available to the char burning. It also increases the devolatilisation rate as demonstrated in Fig. 2.5 (so more char is produced) as well as the flame temperature (as shown later in Fig. 2.6).

When the air flow rate is further increased beyond the critical point, the flame temperature undergoes no further increase (Fig. 2.6) and the devolatilisation rate starts to decrease (Fig. 2.5) so less char is produced, though more air is available to the char burning. The moisture effect can be explained in the following way (Yang *et al.*, 2003).

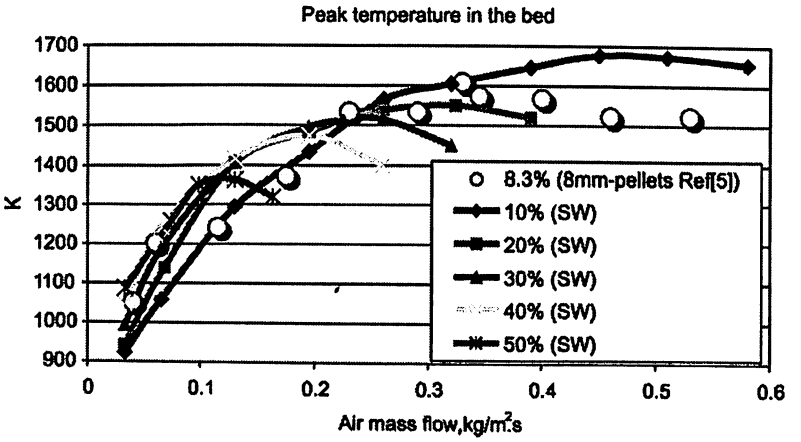

Fig 2.6 Peak bed temperature as a function of both primary air flow rate and moisture content in the fuel. The moisture level ranges from 10 to 50% on a wet basis. The fuels are 12 mm

simulated wastes (SW) unless indicated otherwise. The over-bed radiation heat flux is fixed at 88 kW/m^2 for the calculations (Yang *et al.*, 2003).

A wetter fuel reduces the devolatilisation rate and hence the O_2 consumption by the burning of the volatile gases. This makes more O_2 from the air supply available to the char burning in such a way that overweighs the effect caused by decreasing char formation, so the net effect is an increase in the char burning rate compared to a drier fuel (Yang *et al.*, 2003).

2.9 Effect of particle size

The particle size covered in the calculations ranges from 2 to 35 mm. Fig. 2.7(a) shows the burning rate as a function of particle size at different primary air velocities. Generally, larger particle size results in lower burning rate. For instance, 5 mm particles have a burning rate of 0.06 kg mK2 sK1 at a primary air velocity of PA3, which is 1.5 times of the burning rate with 30 mm particles at the same primary air velocity. One exception is for the particle sizes of 4 and 5 mm at the primary air velocity PA2 where the 5 mm particles demonstrate a higher burning rate than the 4 mm particles. Fig. 2.7(b) shows the combustion stoichiometry as a function of particle size. Generally, larger-size particles result in a higher air-to-fuel stoichiometric ratio or less fuelrich combustion. For instance, 5 mm particles have an airto- fuel stoichiometric ratio of 0.49 at PA3 compared to the ratio being 0.74 with 30 mm particles at the same conditions.

One exception is for particle sizes of 4 and 5 mm at the primary air velocities PA2 and PA3 where the 5 mm particles produce a slightly fuel-richer condition than the 4 mm particles. Fig. 2.7(c) shows the bed-top gas composition as a function of particle size.For CO, the volumetric percentage ranges from around 12 to 17% and larger particles have lower CO levels at the bed top; for CH_4, the volumetric percentage ranges from 5 to 9% and a noticeable change in the relationship with the particle size is only obtained for particles smaller than 5 mm at PA1, for particles smaller than 10 mm at PA2 and for particles smaller than 15 mm at PA3. Generally, increasing particle size reduces the methane concentration at the bed top. For H2, the volumetric percentage ranges from 1.5 to 7% and generally an increase in particle size results in higher hydrogen concentration at the bed top (Yang *et al.*, 2003).

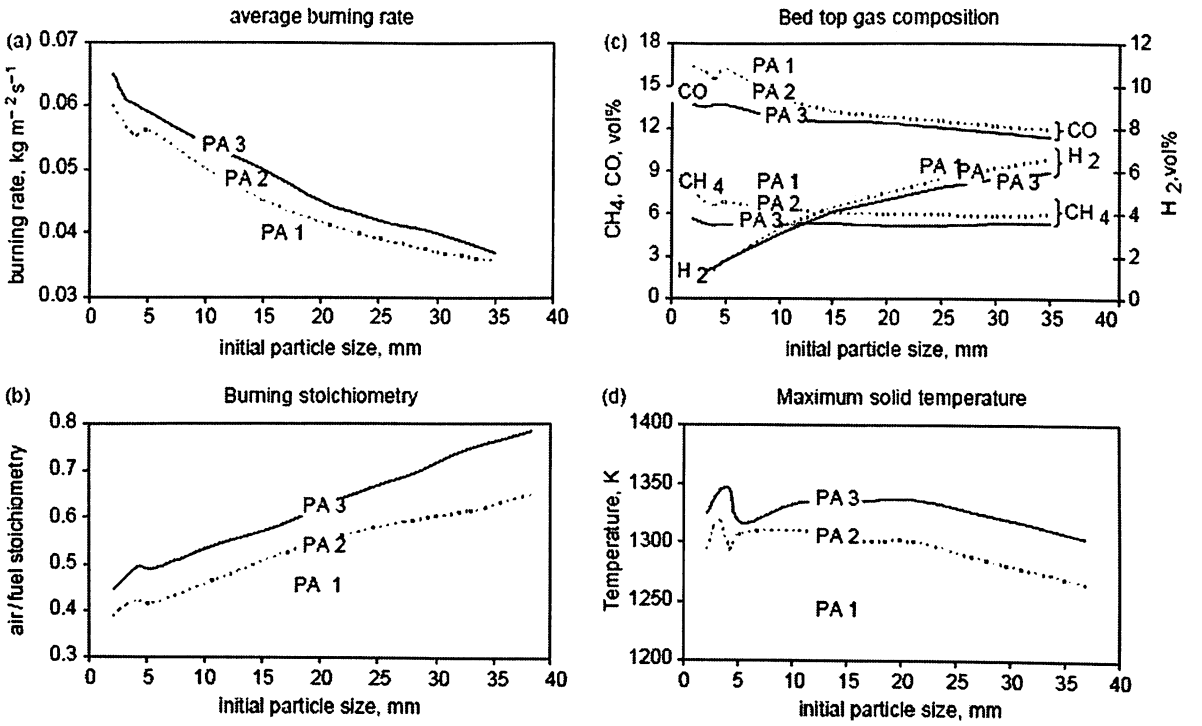

Fig 2.7 Effect of particle size: (a) average burning rate; (b) combustion stoichiometry; (c) gas composition at the bed top; (d) maximum solid temperature.

The primary air velocity has negligible effect on H_2 when particles are smaller than 10 mm. It also has negligible effect on CO when particle size is greater than 20 mm. Fig. 2.7(d) shows the maximum solid temperature inside the bed as a function of particle size. It is seen that at PA1 the maximum solid temperature increases as particle size increases from 2 to 3 mm, then drops down 30 K at 4 mm, rises again at 5 mm to the maximum level of 1270 K. Beyond 5 mm, the general trend is decreasing solid temperature as particle size increases. At 35 mm, the maximum solid temperature is 70 K lower than the peak value obtained at 5 mm.

At PA2, the maximum solid temperature pattern in relation to the particle size is similar to the case of PA1, except that the absolute temperature level is about 50 K higher on the whole. At PA3, the maximum solid temperature is obtained at 4 mm (1350 K) but falls to 1320 K at 5 mm. Over the range of 10–20 mm, the maximum solid temperature maintains a constant level of 1335 K.

2.10 Effect of bed porosity

Bed porosity depends on a number of factors, including particle size distribution, particle shape, shaking or pressing of the bed, etc. A bed with a low porosity is called a compact bed and a bed with a high porosity is called a loose bed. In this section, the initial bed porosity is artificially changed while keeping all the other bed parameters the same. The porosity covers a range of 0.35–0.75. Fig. 2.8(a) demonstrates the effect of bed porosity on the burning rate of the bed. It is seen that the effect of bed porosity depends on the level of primary air velocity. At low primary air velocities (PA1 and PA2), the general trend is decreasing burning rate as the bed porosity increases, though in some ranges the burning rate may maintain a more or less constant level (porosity 0.5–0.65 for PA1 and 0.65 onwards for PA2) (Yang *Bin et al.*, 2005).

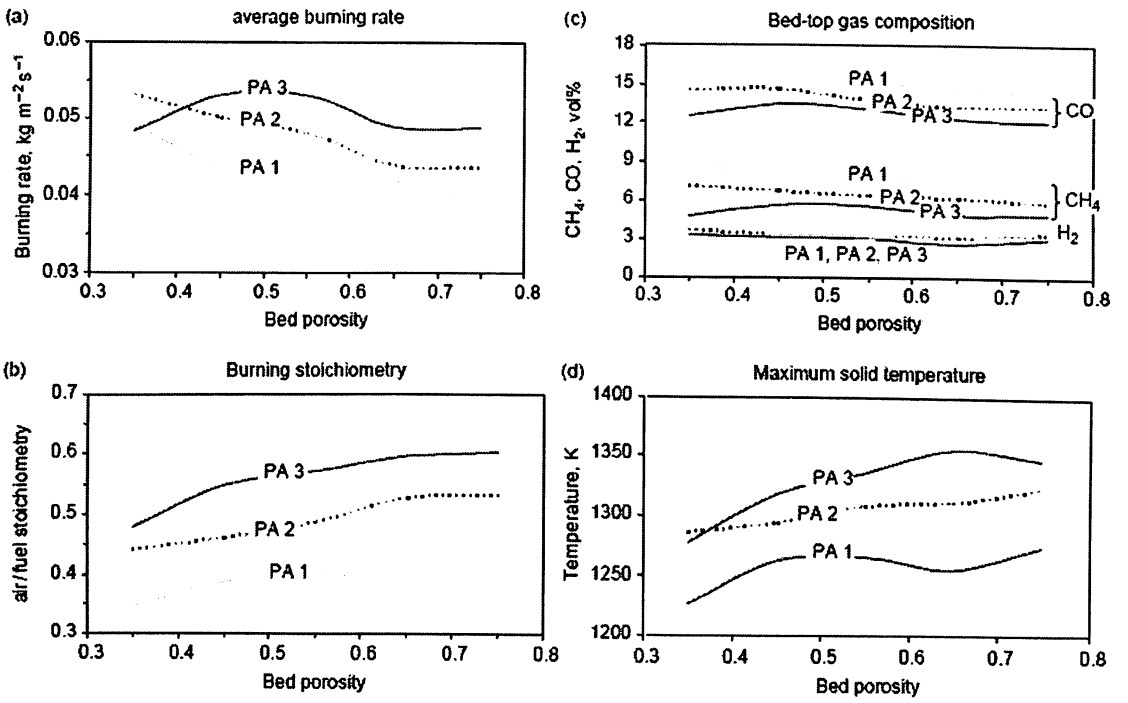

Fig 2.8 Effect of bed porosity: (a) average burning rate; (b) combustion stoichiometry; (c) gas composition at the bed top; (d) maximum solid temperature

At increased primary air velocity (PA3), the maximum burning rate is obtained between bed porosity of 0.45–0.55 and either a looser or denser bed would results in a lower burning rate. However, similar to the situation of PA2, the burning rate keeps constant as the bed porosity

increases beyond 0.65. Fig. 2.8(b) demonstrates the combustion stoichiometry against the initial bed porosity. Generally, the air-to-fuel stoichiometric ratio increases as the bed porosity increases (Yang *Bin et al.*, 2005).

But the air-to-fuel ratio keeps constant in some part along the range, i.e. bed porosity from 0.5 to 0.65 for PA1 and from 0.65 onwards for PA2 and PA3. Fig. 2.8(c) shows the bed-top gas composition as a function of bed porosity. For CO at PA1, very little change in its level is shown for the whole range of porosity variation; for CO at PA2, the volumetric level in the flue gases exiting the bed top falls in the range of 0.45–0.6 of the bed porosity, otherwise, it keeps a constant value; for CO at PA3 the maximum level is obtained around a bed porosity of 0.45 and either a looser or denser bed results in a lower CO concentration at the bed top. For CH_4 at PA1 and PA2, the general trend is reducing concentration level as the bed porosity increases; for CH_4 at PA3, the maximum level is obtained around the bed porosity of 0.5. It is also seen that the H_2 concentration is not affected by either the bed porosity or the primary air velocity. Fig. 2.8(d) demonstrates the maximum solid temperature against porosity variation (Yang *Bin et al.*, 2005).

The pattern of variation depends on the primary air velocity. At the low air velocity of PA1, the maximum solid temperature rises as the bed porosity rises from 0.35 to 0.45, but keeps constant from 0.45 to 0.55, falls from 0.55 to 0.65 and then rises again from 0.65 onwards. At PA2, however, a continuous increase in the solid temperature is obtained as the bed porosity increases from the minimum to the maximum. For the situation of PA3, the solid temperature increases with increasing bed porosity until the porosity reaches 0.65, followed then by a fall in the maximum solid temperature as the bed porosity further increases (Yang *Bin et al.*, 2005).

Model Development

CHAPTER III

MODEL DEVELOPMENT

In this chapter models and methodology used for determining the burning rate of biomass and heat transfer in furnace is discussed under the following sub headings.

3.1 Biomass Combustion rate and burning time model

3.1.1 One film model

3.1.1.a Assumptions

3.1.1.b Overall mass and species conservation

3.1.1.c Energy Conservation Equation application for Biomass Particle

3.1.2 Particle Burning Time

3.2 Modeling of biomass combustion on grate

3.3 Characteristics of solid particle

3.3.1 Solid particles

3.3.2 Equivalent diameters

3.3.3 Volume Diameter (dv)

3.3.4 Surface Diameter (ds)

3.3.5 Sieve Size (dp)

3.3.6 Surface-Volume Diameter (dsv)

3.3.7 Sphericity (Ø)

3.3.8 Packing characteristics

3.4 Biomass Characterizations

3.5 Fundamental of Grate Fired Boiler Design and Operation

3.5.1 Combustion air system and temperature

3.5.2 Moving Grate Boiler Grate Design

3.5.3 Fuel Bed Thickness

3.5.4 Furnace Design

3.5.5 Firing Rate of Furnace

3.5.5. a Heat Release Rate per unit volume (qv)

3.5.5.b Heat Release Rate per Unit Cross Sectional Area (qF)

3.5.5.c Heat Release Rate per Unit Wall Area of the Burner Region (qb)

3.5.6 Furnace Depth

3.5.7 Furnace Height

3.5.8 Furnace Exit Gas Temperature

3.6 Heat and Mass Transfer in Furnace

3.6.1 Furnace Heat Transfer

3.6.2 Determining Heat Transfer Coefficient to the fuel particle in Fuel bed

3.6.3 Heat Transfer to the wall of the furnace near bed

3.6.4 Gas temperature at furnace exit

3.6.5 Determining flue gas property

3.6.6 Thermal Conductivity of flue gas

3.6.7 Determining Dynamic Viscosity of flue gas

3.6.8 Determining Non-luminous radiative coefficient

3.6.9 Determining Convective coefficient for cross flow

3.6.10 Radiative Heat Transfer

3.6.11 Mass Transfer

3.6.12 Diffusion mass transfer; molecular or eddy diffusion

3.6.13 Convective mass transfer: free or forced

3.6.14 Determining Velocity, concentration and flux of flue gas mixture

3.6.14.1 Concentrations

3.6.14.2 Velocities

3.6.14.3 Fluxes

3.7 Determining Pressure drop across bed of fuel in grate

3.1 Biomass Combustion rate and burning time model

Fig. 3.1 schematically shows the burning carbon surface within a reacting boundary layer. At the surface carbon can be attacked by either O_2, CO_2 and H_2O, depending primarily upon the surface temperature, via the following global reaction

$$C + O_2 = CO_2 \quad (3.1)$$

$$2C + O_2 = 2\,CO \quad (3.2)$$

$$C + CO_2 = 2CO \quad (3.3)$$

$$C + H_2O = CO + H_2 \quad (3.4)$$

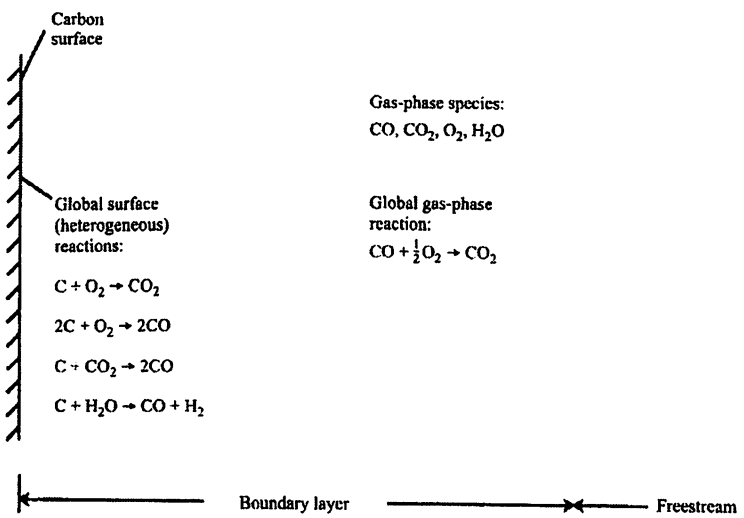

Fig. 3.1 General scheme for carbon combustion showing global heterogeneous and homogeneous reaction

The principle product at the carbon surface is CO. The CO diffuse away from the surface through the boundary layer where it combine with the inward diffusion O_2 according to the following global homogeneous reaction

$$CO + ½ O_2 = CO_2 \qquad (3.5)$$

In principle, the problem of carbon oxidation could be solved by writing the appropriate conservation equations for species, energy and mass, defining all of the elementary reaction steps and then solving these equations subject to appropriate boundary condition at the surface and free stream. The major complication to this scenario, however, is that the carbon surface is porous and the detail nature of the surface changes as the carbon oxidation proceeds. Thus the process of intraparticle diffusion plays the major role in combustion under certain condition.

Simplified model of carbon combustion rely on the global reactions and usually assumes that the surface is impervious to diffusion. Depending upon the assumption made for both the surface and gas phase chemistry, different scenario emerge which are generally classified as one film, two film or continuous film models (Turns, 2000).

In the one film model there is no flame in the gas phase and the maximum temperature occurs at the carbon surface. In the two film models, a flame sheet lies at some distance from the surface, where the CO produced at the surface reacts with incoming O_2 .In the continuous film models, a flame zone is distributed within the boundary layer .rather than occurring in the sheet.

3.1.1 One film model

The one film model is quite simple to illustrate conveniently and clearly the combined effects of heterogeneous kinetics and gas-phase diffusion. The two film model, although also still quite simplified, is more realistic in that it shows the sequential production and oxidation of CO. We then use these models to obtain estimates of carbon – char burning times (Turns, 2000).

The basic approach to the problem of carbon combustion is quite similar to treatment of droplet evaporation expect the chemical reaction at the surface replaces evaporation. The burning of single spherical carbon particle subject to the following assumption (Turns, 2000).

3.1.1.a Assumptions

1. Burning Process is Quasi – Steady

2. The biomass particle burns in a quiescent, infinite ambient medium that contain only oxygen and inert gas such as nitrogen. There are other no interactions with others particle and the effect of convections are ignored

3. At the particle surface the oxygen react with carbon particle to produce Carbon-di-oxide. In general this reaction is not a particular good since carbon-di-oxide is preferred byproduct at combustion temperature.

4. The gas phase consists of only O_2, CO_2 and inert gases. The O_2 diffuses inward; react with surface to form CO_2, which then diffuse outward. The inert gas forms a stagnant layer as in the Stefan Problem.

5.The gas phase Thermal Conductivity ,K, Specific Heat, Cp , and the product of density and mass diffusivity ,ρD are all constant .Further more we assume that the Lewis Number is Unity, i.e $Le = k /(\rho CpD) = 1$.

6. The biomass particle is impervious to gas-phase species i.e. intra particle diffusion is ignored.

7. The particle is of uniform temperature and radiates as a gray body to the surroundings without participation of the intervening medium (Turns, 2000).

Fig. 3.2 illustrate the basic model embodied by the above assumption ,showing how the species mass fraction and temperature profile vary with the radial coordinates .Here we see that the CO_2 mass fraction is a maximum at the surface and is zero far from the particle surface. Later we will see that if the chemical kinetics rate of O_2 consumption is very fast, the oxygen concentration at the surface, Yo_2,s approaches zero. If the kinetics is zero, there will be an appreciable concentration of O_2 at the surface. Since we assume that there are no reaction occurring in the gas phase and the entire heat rate occurs at the surface, the temperature monotonically falls from a maximum at the surface, Ts to its value far from the surface, $T\infty$.

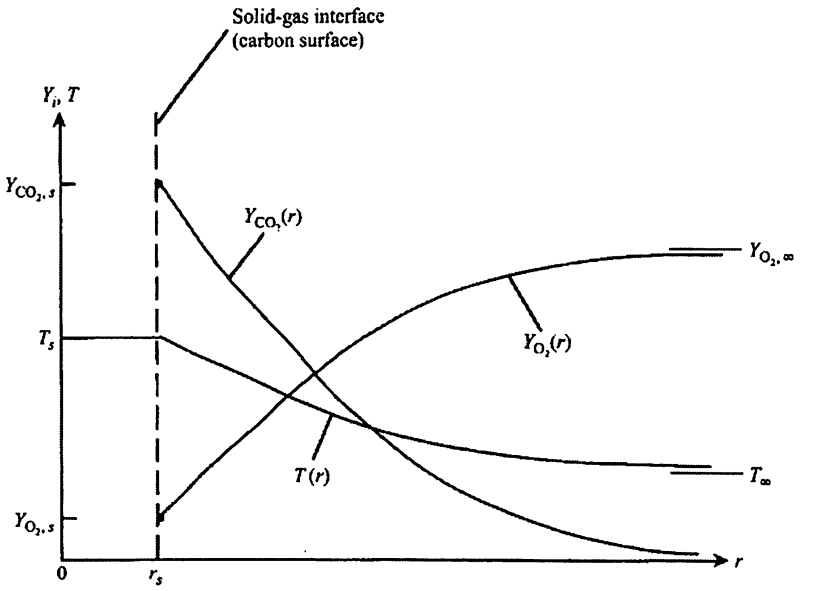

Fig. 3.2 Species and Temperature Profile of Carbon Particle of Biomass assuming that CO_2 is only product of combustion at the Biomass Carbon Particle Surface.

Our primary objectives in the following analysis is to determine expression that allow evaluation of the mass burning rate of the biomass carbon, mc and the surface temperature, Ts. Intermediate variable of interest are the mass fraction of O_2 and CO_2 at the carbon surface. The problem is straight forward and required dealing with only species and energy conservation.

3.1.1.b Overall mass and species conservation

The relationship among the three species mass fluxes, $m_C^{''}$, $m_C^{''}$ and $m_{CO2}^{''}$ is illustrated in the Fig. 3.3. At the surface the mass flow of carbon must equal the difference between the outgoing flow of CO_2 and incoming flow of O_2, i.e

$$m_C^{''} = m_{CO2}^{''} - m_{o2}^{''} \qquad (3.6)$$

Similarly at any arbitrary radial position, r, the next mass flux is the difference between the CO_2 and O_2 fluxes.

$$m_{net}^{''} = m_{CO2}^{''} - m_{o2}^{''} \qquad (3.7)$$

Since the mass flow rates of each species are constant with respect to both radial position (no gas-phase reactions) and time (steady state), we have

$$m_C'' \, 4\pi \, r_s^2 = m_{net}'' \, 4\pi \, r^2 \qquad (3.8)$$

or

$$m_C'' = m_{net}'' = m_{CO2}'' - m_{o2}'' \qquad (3.9)$$

Thus, we see that the outward flow rate is just the carbon combustion rate, as expected. The CO_2 and O_2 flow rate can be related by the stoichiometry associated with the reaction at the surface

12.01 Kg C + 31.99 Kg O_2 = 44.01 Kg CO_2

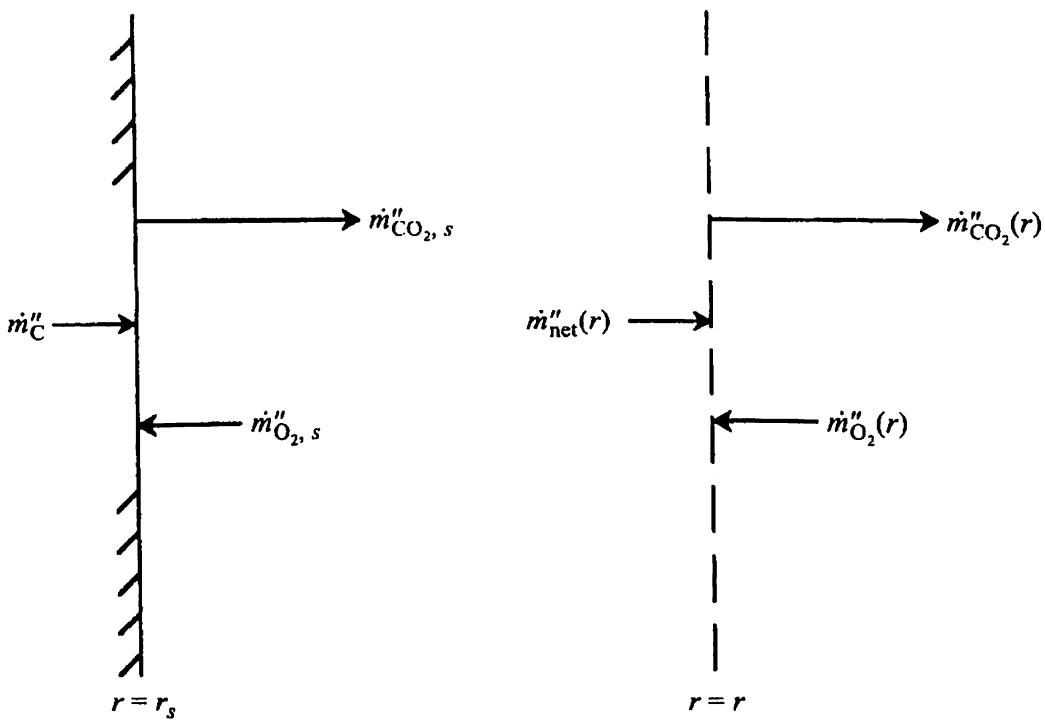

Fig. 3.3 Species mass flux at the carbon surface and at an arbitrary radial location

On a per kg of carbon basis, we have

$$1\ kg\ C + \vartheta_1\ Kg\ O_2 = (\vartheta_1 + 1)\ Kg\ CO_2$$

Where the mass stoichiometric coefficient is

$$\vartheta_1 = \frac{31.99\ Kg\ O_2}{12.01\ Kg\ C} = 2.664$$

The subscript 1 is used to denote this coefficient applies to the one- film model. A different value of the stoichiometric coefficient results for the two film model (Turns, 2000).

We can now relate the gas-phase species flow rates to the carbon burning rate:

$$mO_2 = \vartheta_1\ m_c \qquad (3.10)$$

and

$$mCO_2 = (\vartheta_1 + 1)m_c \qquad (3.11)$$

Thus the problem now is to find any one of the species flow rates. To do this, we can apply Fick's Law to express the conservation of O_2

$$m''_{O2} = Y_{O2}\left(m''_{O2} + m''_{CO2}\right) - \rho D\ \frac{d\,Y_{O2}}{dr} \qquad (3.12)$$

Recognizing that the mass fluxes are simply related to the mass flows as $m_i = 4\pi\ r^2 m''_i$ and substituting equation 3.10 and 3.11, taking care to account for the direction of the flows (inward flow is negative, outward flow is positive) (Turns, 2000)

Equation 3.12 became, with some additional manipulation,

$$m_C = \frac{4\pi r^2 \rho D}{\left(1+\frac{Y_{O2}}{\vartheta_1}\right)}\ \frac{d\left(\frac{Y_{O2}}{\vartheta_1}\right)}{d_r} \qquad (3.13)$$

The boundary condition that apply to the equation are

$$Y_{O2}(r_s) = Y_{02,S} \qquad (3.14.a)$$

and

$$Y_{O2}\ (r \rightarrow \infty) = Y_{O2,\infty} \qquad (3.14.b)$$

Having two boundary condition for our first order ordinary differential equation allows us to determine an expression for mc, the eigenvalue of the problem. Separating equation 13.3 and integrating between the two limits given by the equation 3.14a and b yields

$$m_c = 4\pi r_s \rho D\ In\ \left[\frac{1 + Y_{O2,\infty}/\vartheta_1}{1 + Y_{O2,s}/\vartheta_1}\right]$$

Since $Y_{O2,\infty}$ is treated as a given quantity, our problem would be solved if we knew the value of $Y_{O2,s}$, the oxygen mass fraction at the carbon surface (Turns, 2000).

We can determine the burning rate of biomass carbon by

$$mc = \frac{(Yo2,\infty - 0)}{Rkin + Rdiff}$$

Where,

$$Rkin = \frac{1}{K_{kin}} = \frac{\vartheta 1 RuTs}{4\pi r^2 MW_{mix} K_c P}$$

$\vartheta 1$ = Stchiometric air requirement, Kg O_2/Kg C

Ru = Universal Gas Constant (J/ kmol-K)

Ts = Surface Temperature, K

r = Radius of particle, m

MWmix = Molecular Weight (Kg/ kmol)

Kc = Kinetic rate constant coefficient (m/s)

P = Pressure (Pa)

$$R\ diff = \frac{\vartheta 1 + Yo2s}{\rho D 4\pi rs}$$

$\vartheta 1$ = Stchiometric air requirement , Kg O_2/Kg C

$Yo2s$ = $Oxygen\ molar\ concentration\ \left(\frac{kmol}{m3}\right)$

ρD = Product of density ($\frac{kg}{m3}$) and mass diffusitivity (m^2/s)

r = Radius, m

Since Rdiff involves the unknown value of Yo_2, s. Some iteration is still required in this approach (Turns, 2000).

Table 3.1 Combustion Regime of biomass

Regime	**Rkin/Rdiff**	**Burning Rate Law**	**Condition of Occurrence**
Diffusionally Controlled	<<1	mc = Yo2,∞/ Rdiff	rs large,Ts high, P high
Intermediate	~ 1	mc = Yo2,∞/ (RKin + Rdiff)	-
Kinetically Controlled	>> 1	mc = Yo2,∞/ RKin	rs Small, Ts Low, P Low

Rkin / Rdiff << 1.In this case ,the burning rate is said to be diffusionally controlled .

$$\frac{R_{Kin}}{R_{diff}} = \left(\frac{\vartheta 1}{\vartheta 1 + Y02,s}\right)\left(\frac{Ru\,Ts}{P\,MW_{mix}}\right)\left(\frac{\rho D}{kc}\right)\left(\frac{1}{r_s}\right)$$

Turns, 2000 said that this ratio can be made small in several ways. First, Kc can be very large; this implies a fast surface reaction. We also see that a large particle size, rs or high pressure, P, has the same effect. Although the surface temperature appears explicitly in the numerator of the equation. It effect is primarily through the temperature dependence of Kc where Kc typically increase rapidly with temperature Since Kc = A exp (- EA/RuT).As a result of burning being diffusionally controlled, we see that none of the chemical Kinetic parameter influence the burning rate and the O_2 concentration at the surface approaches zero.

The other limiting case, kinetically controlled combustion occurs when R kin / Rdiff >> 1.In this case, the Rdiff is small and the nodes YO_2, s and YO_2, ∞ are essential at the same value i.e. concentration of O_2 at the surface is large. Now the chemical Kinetic parameters control the burning rate and the mass transfer parameter is unimportant. Kinetically controlled combustion occurs when particle sizes are small, pressure low and temperature low (a low temperature cause Kc to be small) (Turns, 2000).

3.1.1.c Energy Conservation Equation application for Biomass Particle

So far in our analysis we have treated the surface temperature Ts as a known parameter; however this temperature cannot be any arbitrary value that depend energy conservation at the particle surface. As we will see, the controlling surface energy balance depends strongly on the burning rate i.e the energy and mass transfer processes are coupled (Turns,2000).

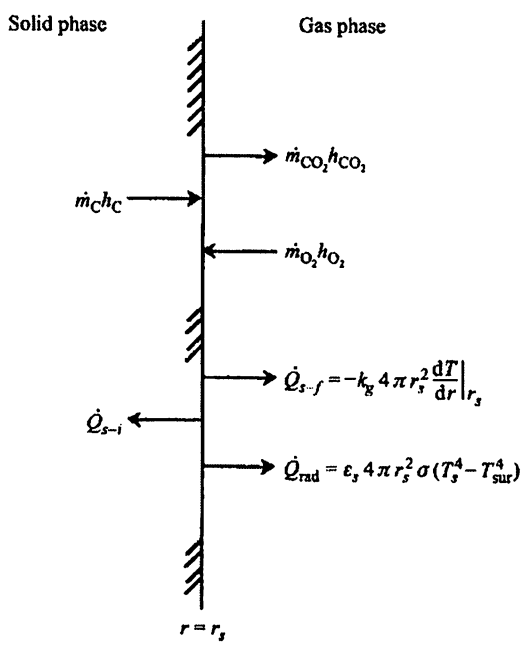

Fig. 3.4 Energy Flow at the surface of Biomass Carbon Particle burning in air

Above equation illustrate the various energy fluxes associated with the burning carbon surface. Writing the surface energy balance yields.

$$\dot{m}_c h_c + \dot{m}_{o2} h_{o2} - \dot{m}_{co2} h_{co2} = \dot{Q}_{S-i} + \dot{Q}_{s-f} + \dot{Q}_{rad}$$

Since we assume combustion occurs in steady state, there is no heat conducted in particle interior, thus Qs-i = 0.

$$\dot{m}_c h_c = -k_g 4\,\pi r_s^2 (\frac{dT}{dr})_{rs} + \varepsilon_s 4\pi r_s^2 \sigma\,(T_s^4 - T_{sur}^4)$$

Where,

$\dot{m}$ = Mass Flowrate (Kg/s)

h = Enthalpy (J/Kg)

s = Surface

i = Interior

rad = radiation

Ts = Surface Temperature, K

Tsur = Surroundings Temperature, K

To obtain an expression for the gas-phase temperature gradient at the surface requires that we write an energy balance within the gas phase and solve for the temperature distribution.

Where,

$$(\frac{dT}{dr})_{rs} = \frac{Z_{\dot{m}c}}{r_s^2} \left[\frac{(T\infty - Ts)\exp(-Z_{mc}/rs)}{1 - \exp(-Z_{mc}/rs)}\right]$$

Where,

$$Z = Cpg / (4\,\pi\, Kg)$$

Where,

Cpg = Specific Heat of gas (J/Kg-K)

T∞ = Freestream or Radiation Temperature

Ts = Surface Temperature

Rearranging, the final output will be

$$\dot{m}_c \Delta h_c = \dot{m}_c c_{pg} \left[\frac{\exp(\frac{-\dot{m}_c c_{pg}}{4\pi k_g r_s})}{1 - \exp(\frac{-\dot{m}_c c_{pg}}{4\pi k_g r_s})} \right] (T_s - T_\infty) + \varepsilon_s 4\pi r_s^2 \sigma (T_s^2 - T_{sur}^2)$$

The above equation gives heat release rate of biomass carbon particle (Turns, 2000).

3.1.2 Particle Burning Time

For diffusion controlled burning, it is a simple matter to find particle burning time. The particle diameter can be expressed as a function of time as follows (Turns, 2000)

$$D^2(t) = D_0^2 - K_B z$$

Where the burning rate constant, KB is given by

$$K_B = \frac{8\rho D}{\rho c} In\,(1 + B)$$

Where,

KB = Burning Rate Constant, m^2/s

Setting D = 0 in first equation, it gives the particle lifetime,

$$t_c = D_0^2 / K_B$$

Where,

t_c = Burning time of biomass particle, s

Do = Diameter of Biomass Particle, m.

The transfer number B is either Bo, m or BCO_2, m with the surface mass fractions set to Zero. Thus far, our analyses have assumed a quiescent gaseous medium. To take in to account the effect of a convective flow over a burning carbon particle, the film theory analysis is applied.

For diffusion controlled conditions with convection, the mass burning rate are augmented by the factor Sh/2,where Sh is the Sherwood number and plays the same role for mass transfer as the Nusselt number does for heat transfer. For unity Lewis number, Sh =Nu, thus

$$(m_{c,diff})_{with\ convection} = \frac{Nu}{2}\,(m_c)_{without\ convection}$$

3.2 Modeling of biomass combustion on grate

In modeling of grate fired furnaces, it is essential to develop a sub-model of grate bed (in chemical engineering, grate bed also called fuel bed, fixed-bed or packed-bed), where the interaction of the solid phase and the gas phase is very complicated Generally, a combustible element in the fuel bed is heated primarily by radiation from the over-bed region and from the burning fuel bed.

As its temperature rises, it loses its free moisture at 100 °C, pyrolyses at 260 °C, ignites at 316 °C and then burns vigorously until either the oxygen surrounding the element is depleted or all the element is devolatized, leaving a carbonaceous char.

The residual charred or partly charred element may undergo further pyrolysis, be gasified by CO_2 or H_2O to yield CO, or CO and H_2, or be oxidized by free oxygen directly to CO_2.Figure 3.1 shows a typical grate fired furnace. In the heterogeneous grate bed, all the above processes may be occurring simultaneously within a section of the bed, since neighboring fuel elements vary widely in size and composition.

In addition, complexity is also introduced by the substantial temperature and concentration gradients that may be present in the larger fuel elements.It seems convenient for the purposes of bed modeling to divide the bed combustion mechanisms as physical process and chemical process .

The physical process includes heating-up and drying of fuel particles, motion of particles on the moving grate, and interaction between gas and solid phases, while the chemical process includes pyrolysis and de volatilization of fuel particles and char gasification and combustion (Wei Dong, 2000).

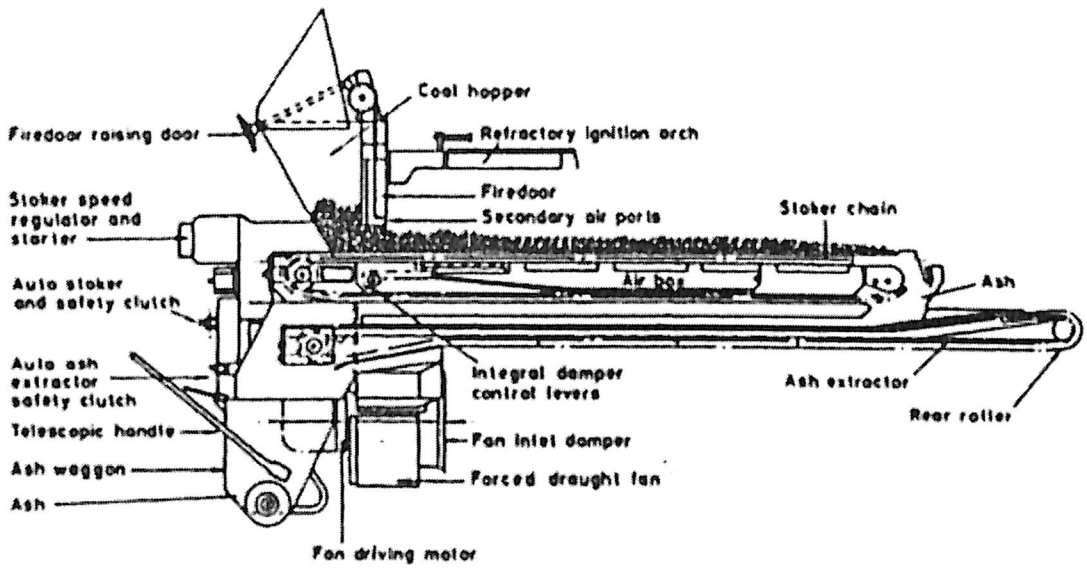

Fig. 3.5 Chain Grate assembly Fired Boiler

3.3 Characteristics of solid particle

A particle may be defined as a small object having a precise physical boundary in all directions. The particle is characterized by its volume and interfacial surface in contact with the environment (Prabir, 2006).

3.3.1 Solid particles

Solid particles are rigid and have a definite shape. A sphere is a natural choice to define a particle, though most natural particles are not spherical. Hence, natural particles are characterized by their degree of deviation from spherical shape, Sphericity, and an equivalent diameter (Prabir, 2006).

3.3.2 Equivalent diameters

Let us take a non-spherical particle having a surface area S, and a volume V. Several types of equivalent diameter of the particle can be defined to describe the particle, as shown in Fig. 3.6. Four more frequently used definitions are (Prabir, 2006)

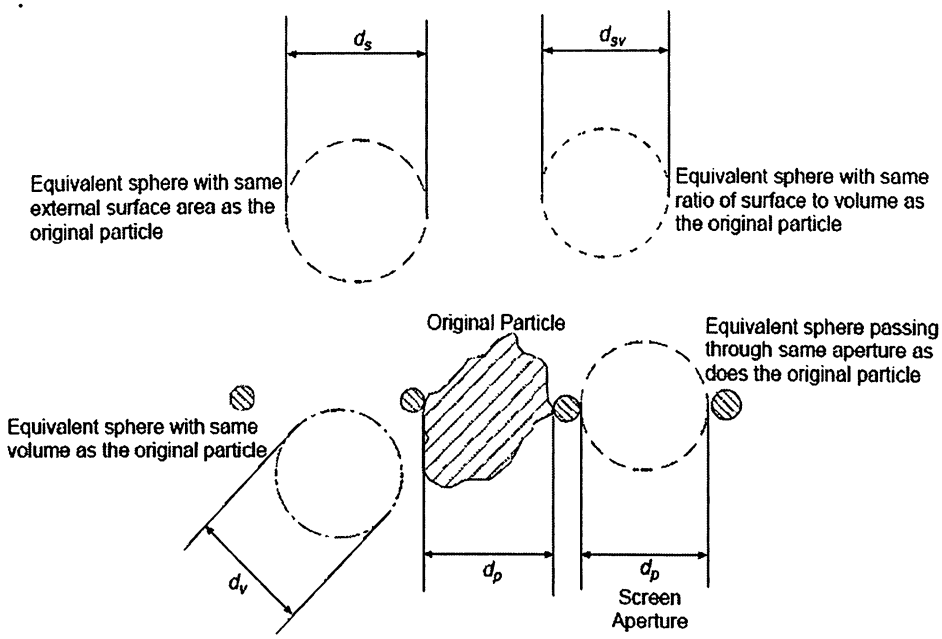

Fig.3.6 Different representations of a non-regular shaped particle

3.3.3 Volume Diameter (dv)

Volume diameter is the diameter of a sphere that has the same volume as the particle:

$$d_v = (\frac{6}{\pi} \times Volume\ of\ particle)^{\frac{1}{3}} = (\frac{6V}{\pi})^{\frac{1}{3}}$$

3.3.4 Surface Diameter (ds)

Surface diameter is the diameter of a sphere that has the same external surface area as the particle. Thus,

$$d_s = (\frac{Surface\ area\ of\ particle}{\pi})^{\frac{1}{2}} = (\frac{S}{\pi})^{\frac{1}{2}}$$

3.3.5 Sieve Size (dp)

Sieve size is the width of the minimum square aperture of the sieve through which the particle will pass (Prabir, 2006).

3.3.6 Surface-Volume Diameter (dsv)

Surface-volume diameter is the diameter of a sphere having the same surface to volume ratio as that of the particle:

$$\frac{6\pi d_{sv}^2}{\pi d_{sv}^3} = \frac{S}{V}$$

$$d_{sv} = 6\,\frac{S}{V}$$

3.3.7 Sphericity (Ø)

Sphericity describes the departure of the particle from a spherical shape. For example, a spherical particle has a sphericity of 1.0.The relationship between the above sizes and the sieve size dp can be derived through experiments for irregular particles and through calculations for geometrically shaped particles (Prabir, 2006).

3.3.8 Packing characteristics

In a particulate mass, particles rest on each other due to the force of gravity to form a packed bed. Depending on the shape of particles and packing characteristics, a certain volume of space in between the particles remains unoccupied. Such space is called a void volume and is specified as voidage or porosity, defined as

$$Voidage, \varepsilon = Porosity = \frac{Void\ Volume}{Volume\ of\ (particles + Voids)}$$

The measurement of particle volume is simple, but the precise measurement of its surface area is very difficult. This problem compounds when one attempts to define the Sphericity of a mass of a large number of dissimilar particles. The packing characteristics of particles are important parameters that depend on the particle's shape and mode of packing. In some special situations, such as in the vicinity of a sphere or a plane wall, the distribution of local voidage becomes important. Unlike bulk voidage, it is not uniform or monotonically varying. It follows a damped oscillatory pattern (Prabir, 2006).

3.4 Biomass Characterizations

Magasiner *et al*, 2001 says, The Maximum grate heat release rates are obtained when burning a high proportion of the fuel in suspension. As fuel moisture increases piles tend to form on the grate. These inhibit combustion. They can be prevented from forming by reducing grate loading or by drying them by passing hot primary air through them. They cannot be dried within a reasonable time scale by radiation from the furnace.

The grate heat release rate is a function of

- Fuel moisture
- Primary air temperature
- Excess air required to complete combustion
- Furnace temperature
- Gas up-flow velocity
- Particle terminal velocity

Furnace temperature and gas up-flow velocity are calculated from the knowledge of the furnace geometry and fuel chemistry. The particle terminal velocity is a function of gas viscosity, gas and particle densities and particle drag coefficient. In correctly designed furnaces having proper over fire air systems, unburned carbon losses vary from 1 to 5% depending on fuel moisture. Losses, as with excess air requirements, rise very steeply when fuel effective moisture goes over 52% (Magasiner *et al*, 2001).

3.5 Fundamental of Grate Fired Boiler Design and Operation

An understanding of the combustion process for grate boiler can assist in evaluating operating procedures and changes or additions to the installation which might improve performance or lower certain emissions. A boiler should release the combustion energy evenly over the entire grate surface. Then the controlling guideline for design is heat release/m^2 of grate, which when multiplied by the grate area results in the maximum input from fuel fed for a given unit. Fuel should be spread evenly over the grate surface (Neil, 2002).

To achieve uniform combustion it is necessary to distribute the air uniformly through the grates to release the energy under optimum combustion conditions. Stratification should be reduced to a minimum so the oxygen content of the flue gases and the combustion temperatures remain uniform and thus, the velocities rising in the furnace are also as uniform as possible.

A grate design that is highly resistant to air flow is desirable to achieve even air distribution across the surface and even combustion conditions. Differential pressure across the grates should be on the order of 2 inch to 3 inch of water column. Grates existing today are probably of the continuous ash discharge type.

Intermittent dumping grates are probably no longer in existence except for small low ash refuse burning applications due to the difficulty in meeting opacity requirements with intermittent ash dumping. The continuous ash discharge grate types are the traveling grate and vibrating grate types discharging the ashes off of the front end of the grate. A continuous ash discharge grate will have virtually no ash at the rear and the ash bed depth will slowly increase as the grate moves forward.

A desirable depth of ash discharging off of the front of the grates is 4" to 6". The increase in ash depth from the rear to the front changes the resistance of the fuel bed plus the ash to the air flow. Having a highly air resistant grate surface will minimize this affect (Neil, 2002).The physical features of grate boiler are produced in Annexure A.

3.5.1 Combustion air system and temperature

Since the goal of combustion on a grate fired boiler is to achieve even burning over the entire active grate surface, it is necessary to obtain even air flow through the grates. Careful attention should be paid to the design of the forced draft system supplying the plenum chamber under the grates. Avoid changes in direction or other duct designs which might unbalance the flow of air to the grates. A highly resistant grate which puts most of the resistance to air flow across the grates rather than across the ash bed will materially aid the goal of even air distribution (Neil, 2002).

When designing for bituminous or sub-bituminous coal, the air temperature can be either ambient or preheated to a maximum air temperature of 177° C. Boilers designed to produce steam for electrical generation will normally require both an economizer and an air heater for maximum efficiency. Boilers designed for process and/or heating steam can be designed with just an economizer to achieve the desired flue gas end temperature. If the moisture content of the fuel exceeds 25%, preheated air is recommended. Therefore, wood requires preheated air and, because of the lower combustion temperature with the higher moisture, 205° C is permissible The over fire air systems for grate has undergone major changes over the years. The very old units had systems designed for 7.5 % to 10% of total air. Later units had systems capable of 15% to 18% of total air supply (Neil, 2002).

Staging has been found to reduce the emissions of NOx. The amount of air that has been used in these three level systems is approximately 35% of total air. This air must be delivered with sufficient energy to produce turbulence and mix the burning fuel with oxygen to complete combustion. The temperature of the over fire air can be either ambient or preheated. The choice should be that of the boiler designer. It is essential to design the over fire air system with sufficient static pressure to produce the required penetration into the combustion chamber for a given nozzle size. Nozzle shape is very important for the most efficient utilization of the fan energy. Units have been equipped with nozzle sizes up to 3 inches in diameter. Further test work has shown that up to 30 inches static pressure is required to produce the needed energy for penetration and good turbulence (Neil, 2002).

3.5.2 Moving Grate Boiler Grate Design

David, 2010 said that the grate angle depend on fuel type particularly fuel moisture content. The wetter the fuel, steeper the grate angle. Grate spacing is usually very close to allow wood pellets and associated wood dust to be burned completely. Grate components contain up to 40% chromium to provide corrosive resistance. The wide tolerance of fuel type and particle size can be used. It can accept fuel with moisture content up to 55%.Moving grate design will avoid clinkering and blockages. The ceramic lining can be modified to cater for wetter or drier fuel and it can burn all biomass type fuel. But the problems are, slow respond to load swing because of high fuel loading on grate and slumber mode heat output can be up to 30% when burning wet fuel. Long warm and cool down time associated because of significant thermal lining.

3.5.3 Fuel Bed Thickness

The correct fuel bed thickness for a plant depends on

a. Size and kind of fuel

b. How much ash it contain

c. Type of combustion equipment utilized

d. Boiler load

The optimum depth only can be gauged by experience. It is difficult to get good results of combustion with fire bed less than 75mm (3in) thick, the primary air passing through the grate will tend to create blow-holes resulting in uneven combustion and too much excess air. Generally fire bed thickness is between 100 mm (4in) and 150 mm (6in) (NIFES, 1989).

3.5.4 Furnace Design

Kefa *et al*, 2000 said that there are two aspect of the design of a furnace. The fast part is concern with the generation of heat; second part involves the absorption of heat inside the furnace. The first part ensures that the designed amount of fuel can be burnt in the given furnace volume, liberating the given amount of heat. Practical designs are based on a permissible firing

rate, which depend on number of factor; these are explained below. The second part ensures that the enclosing furnace wall absorbs the required fraction of the generated heat.

3.5.5 Firing Rate of Furnace

Heat release rate and furnace exit gas temperature are some of the important parameters used for the design of the furnace size. The following section presents methods for selection and calculation of these parameters. Unlike volume in the circulating fluidized bed furnace, the volume of the furnace is greatly influenced by the type of fuel fired (Prabir *et al*,2000). For each type of fuel there is a special heat release rate. The furnace cross section area and height is influenced by the type of fuel used.

The heat release rate is expressed on three different bases, furnace volume (qv), and furnace cross section area (qF) and water wall area in the burner region (qb).

3.5.5. a Heat Release Rate per unit volume (qv)

The volumetric heat release rate (qv) is the amount of heat generated by the combustion of fuel in a unit effective volume of the furnace (Louis *et al*,2000) .It is given as

$$q_v = \frac{B.LHV}{V} \frac{KW}{m^3}$$

Where,

B = Designed fuel consumption rate, Kg/s

V = Furnace Volume, m^3

LHV = Lower Heating Value of fuel, KJ/Kg

A Proper choice of volumetric heat release rate will ensure that

- Fuel particle are burnt substantially
- The flue gas is cooled to the required safe temperature before leaving the furnace

This temperature is known as Furnace Exit Gas Temperature (FEGT), is critical for safe operation of downstream heat exchanger surfaces.

For smaller boiler capacity (> 220 TPH Steam) a volumetric heat release rate, chosen on the basis of complete combustion of fuel, is close to the chosen on the basis of cooling of flue gas. However, that is not the case for larger capacity boiler because with increasing boiler capacity, the area of the enclosing furnace wall does not increase at the same rate as does the furnace volume. For example if the boiler capacity is doubled, the furnace height cannot be doubled because of cost consideration. So the available furnace wall area would not be twice as much. The volumetric heat release rate also depends on the ash characteristics, firing method and arrangement of burner. Some typical values of qv are shown in table below.

Table 3.2 Typical Value of Volumetric Heat Release Rate (q V) in MW/m^3

Fuel Type	**Dry Bottom Furnace, qv(MW/m^3)**	**Wet slagging bottom furnace ,qv (MW/m^3)**		
		Open Furnace	**Half open furnace**	**Slagging pool**
Anthracite	0.110 – 0.140	≤ 0.145	≤ 0.169	0.523 – 0.598
Semi Anthracite	0.116 – 0.163	0.151 - 0.186	0.163 – 0.198	0.523 – 0.698
Bituminous	0.14 – 0.20	-		
Lignite	0.09 – 0.15	≤ 0.186	≤ 0.198	0.523 – 0.640
Wood	0.114 – 0.230	0.145 - 0.180	0.160 – 0.190	0.520 – 0.670

3.5.5.b Heat Release Rate per Unit Cross Sectional Area (qF)

This is the amount of heat released per unit cross section of the furnace. It is also at the time called grate heat release rate (Kefa *et al*, 2000). It is given by

$$q_F = \frac{B.LHV}{F_{grate}} \; KW/m^2$$

Where,

F = Cross sectional area of the furnace grate m^2

The grate heat release rate ,qf, reflects the temperature level in the furnace to some degree. When qf increases, the temperature in the burner region rises. Which helps stability of the flame but it increases the possibility of slagging in the furnace. For small boiler (steam capacity < 220 TPH) it is not essential to check qf because compared to the volume, the cross section area of the furnace is very large. Since this is not the case for large capacity boiler, the qf must be carefully chosen. Thus it depend on both the capacity of boiler and the softening temperature (ST) of the fuel. Typical value of upper limit of qf value are given in table for a wide range of coal in boiler up to 1500 TPH capacity. Beyond this capacity the limit of qf changes only marginally.

The volume of the furnace can be determined from the chosen value of q, while the height of the furnace is calculated from the qf.

Table 3.3 Typical Value of Upper Limit of qF in MW/m^2

Boiler Capacity (TPH)	**Upper Limit of qF in MW/m^2**		
	ST ≤ 1300 ° C	**ST = 1300 ° C**	**ST ≥ 1300 ° C**
130	2.13	2.56	2.59
220	2.79	3.37	3.91
420	3.65	4.49	5.12
500	3.91	4.65	5.44
1000	4.42	5.12	6.16
1500	4.77	5.45	6.63

ST = Softening temperature of ash. ° C

3.5.5.c Heat Release Rate per Unit Wall Area of the Burner Region (qb)

The burner region of the furnace is the zone of most intense heat (Prabir *et al*, 2000). So this area is designed separately using a third type of heat release rate qb, called burner zone heat release. It is based on the water wall area in the burner region. It is defined by

$$q_b = \frac{B.LHV}{2(a+b)\,H_b} \; KW/m^2$$

Where,

a and b = Width and depth of the furnace

Hb = Distance between the top edge of the uppermost burner and lower edge of the lowest burner, m

The parameter qb represents the temperature level and heat flux in the burner region .This additional parameter is often used for judging the general condition of the burner region in the larger boiler. It depends on the fuel ignition characteristics, ash characteristics, firing method and arrangement of the burner .Some recommended value of qb are given in table

Table 3.4 Recommended values of burner region heat release rate, qb

Fuel	**qb in MW/m^2**
Brown Coal	0.93 – 1.16
Anthracite and Semi anthracite	1.4 -2.1
Lignite	1.4 – 2.32

3.5.6 Furnace Depth

(Louis *et al*, 2000) Heat release rate helps determining the volume as well as the cross section area of the furnace. They do not define the depth to breadth proportion of the furnace. Which is an important parameter from both combustion and heat absorption standpoint. For example in a narrow (low depth to depth ratio), the flame emerging from the front wall can hit the opposite wall. This would severely damage the tubes. So for a given furnace cross section, the depth to breadth ratio of the furnace should be calculated to avoid this possibility. There is however a minimum value of the furnace depth, b min, which depends on the capacity of the boiler and the type of fuel fired. The arrangement of burner, heat release rate per unit furnace area, power output of each burner, and flame length are some of the factor the influence the breadth and depth of the furnace. While choosing the depth the flue gas velocity in convective pass and steam velocity in super heater should be consider. So the periphery of the furnace

should also consider the steam –water velocity through these tubes. It is essential important for boiler pressure above 9.8 MPa.

3.5.7 Furnace Height

The furnace should be sufficiently high so that the flame does not hit the super heater tubes. Height must exceed the minimum value, depending on the type of fuel used and capacity of the boiler. The shorter the furnace height, the worse the natural circulation. Thus a minimum furnace height also needed for the required degree of natural circulation (Louis *et al*, 2000).

3.5.8 Furnace Exit Gas Temperature

The furnace exit gas temperature (FEGT) is the important design parameter. It defines the ratio of heat absorption by the radiant heating surface in the furnace and that by the convective heating surfaces downstream of the furnace. This parameter is governed by both technical and economical factor. A higher FEGT would make the furnace compact but the convective section larger (Louis *et al*, 2000).

3.6 Heat and Mass Transfer in Furnace

It is important to study the heat and mass transfer to understand the energy performance of furnace. The mass flow rate of flue gas ad its temperature decides the quantity of heat transfer by convection and mass of fuel burning decides the Radiative heat transfer to the water wall.

3.6.1 Furnace Heat Transfer

Kumar, 2009 said that Heat conductivity coefficient is a physical parameter of substance. In general, heat conductivity coefficient depends on temperature, pressure and substance. Heat Transfer by conduction in flue gases occurs through transport of the kinetic energy of molecular motion resulting from the random movement and collision of the molecules. From the concept of kinetic theory, mean travel velocity V of the gas molecules is prescribed by the relation

$$V = \sqrt{\frac{3\,G\,T}{M}}$$

Where,

V = Velocity of gas molecule (m/s)

G = Universal Gas Constant (8.314 Kg m^2 / s^2 mol K)

M = Molecular weight of the gas (Kg/ mol)

T = Absolute Temperature (° K)

Thermal Conductivity is worked from the relation

$$k = \frac{1}{3} V C_v (l\rho)$$

Where,

l = Mean free path (average distance travelled by a molecule before experiencing collision)

C_v = Specific Heat at constant volume

ρ = Mass Density

Experimental investigation shows that with increase in pressure within the furnace the gas density increases; while the mean free path diminishes in the inverse proportion. However the product ($l\rho$) practically remains constant there by that thermal conductivity of gases does not depend upon the pressure. An increase in thermal conductivity of mixture of gas (flue gas) with rise in temperature may be attributed to an increase in mean travel velocity and specific heat at elevated temperature. The increased agitations of gaseous molecules at elevated temperature also results in greater frequency contact and an attendant increase in molecular exchange rate.

3.6.2 Determining Heat Transfer Coefficient to the fuel particle in Fuel bed

The overall gas-side heat transfer coefficient ho can be written as a sum of the contributions of three components: particle convection or conduction hcond, gas convection hconv, and radiation hrad (Vernbanck, 1997).

$$h_o = h_{cond} + h_{conv} + h_{rad}$$

For a gas passing at a superficial velocity V through a fixed bed with a large number of particles, Gas convection may be calculated using the following equations

$$(Nu)_{conv} = \frac{h_{conv} d_t}{K_g} = 0.05\, R_e\, P_r \qquad R_e < 2000$$

$$(Nu)_{conv} = \frac{h_{conv} d_t}{K_g} = 0.18\, R_e\, P_r \qquad R_e > 2000$$

Where,

$$Reynolds\ Number, R_e = \frac{\rho\, v\, d_t}{\mu}$$

$$Prandtl\ Number, P_r = C_p\, \mu\, / K_g$$

This situation is different from one in which the whole bed of particles is involved in exchanging heat with the fluidizing gas. At a low Reynolds number, the gas–particle heat transfer coefficient on bulk solids in the bed is lower than that on single (isolated) particles. It can be as much as three orders of magnitude below the single-particle heat transfer coefficient. However, in coarse-particle beds the gas–particle heat transfer coefficients for both bulk solids and isolated particles are closer.

3.6.3 Heat Transfer to the wall of the furnace near bed

Vernbanck, 1997 said that by analyzing data from commercially-operating boilers, practicing engineers often develop and use rough but simple correlations for overall heat transfer to the water wall h. One such empirical relation is

$$h = 5\, \rho_{avg}^{0.391}\, T_b^{0.408}\ \ W/m^2\, K$$

Where,

ρ_{avg} = Average density of fuel bed in furnace

T_b = Average temperature of fuel bed

3.6.4 Gas temperature at furnace exit

The model uses the combustion heat balance equation whereby the total net heat input into the furnace equates the sum of the heat absorbed by the furnace walls and the heat carried by the gases leaving the furnace (Vernbanck, 1997). The model uses the ambient air temperature as its reference temperature, therefore the net heat input into the furnace per kilogram of fuel burnt can be written as

$$H_{in} = Heat\ in\ fuel\ burnt + Heat\ in\ hot\ combustion\ air$$
$$= NCV + m_{ha}\,(c_{ha}t_{ha} - c_a t_a)$$

Where,

H_{in} = Net heat input in the furnace in kJ/kg fuel burnt

NCV = Net calorific value of the fuel in kJ/kg

m_{ha} = Hot combustion air flow in kg/kg fuel burnt

c_{ha} = Specific heat of the air at t_{ha} in kJ/kg °C

t_{ha} = Temperature of the hot air in °C

c_a = Specific heat of the ambient air in kJ/kg °C

t_a = Ambient air temperature in °C

The heat absorbed by the surrounding walls can be defined by the corrected Stefan-Boltzmann equation and thus the following equation can be written

$$H_{out} = Heat\ absorbed\ by\ firnace\ wall + Hea\ carried\ by\ the\ gas\ leaving\ the\ furnace$$
$$= \frac{20.53\,.\,Fr.\,BBSA}{m_f}\left[\left(\frac{T_e}{100}\right)\text{^}4 - \left(\frac{T_w}{100}\right)\text{^}4\right] + m_g\,(c_e\,t_e - c_a\,t_a)$$

Where,

20.53 = Stefan-Boltzmann constant in kJ/h m^2 °K^4

Fr = correction factor for geometry and emissivity

(Dimensionless); (0.72 for wood)

BBSA = Total effective black body surface area of the furnace in m^2

m_f = Amount of fuel burnt in kg/h

T_e = Absolute temperature of the exit gas in ° K

T_w = Absolute temperature of the furnace walls in ° K

m_g = Mass of flue gas produced per kg fuel burnt in kg/kg

c_e = Specific heat of the gas at temperature t, in kJ/kg ° C

t_e = Exit gas temperature in °C.

3.6.5 Determining flue gas property

Molar specific heats Cp, in kJ/(kmol K) at atmospheric pressure for various common gases as a function of temperature (Vernbanck, 1997) which can be determined from

$$C_p = a + b\,T + cT^2 + dT^3 \qquad KJ/(kmol\,K)$$

Where,

T = Gas Temperature in ° K

Value of a,b,c and d are given in Annexure D.

3.6.6 Thermal Conductivity of flue gas

The thermal conductivity of the flue gas can be determined by the formula (Vernbanck, 1997).

$$K_g = \left(\sum K_i \times r_i\right) \times Z \times 1.085$$

Where,

K_g = Thermal conductivity of the flue gas in W/ m° C

K_i = Thermal conductivity of the flue gas component in W/ m° C

r = Volumetric fraction of the component in m^3/m^3

Z = $1 + 0.402\,y^{0.511}\,(1 - y)$

y = Volumetric fraction of H_20 in m^3/m^3

The volumetric fraction of the component is determined from the mass fraction of the component, from:

$$r_i = m_i \times \frac{R_i}{R_g}$$

Where,

r_i = Volumetric fraction of the component in m3/m3

m_i = Mass fraction of the component in kg/kg

R_i = Gas constant of the component in *Nmlkg* °C

$RCO_2 = 188$; $RO_2 = 260$; $RH_2 = 4120$; $RSO_2 = 130$

$RN_2 = 297$; $RH_2O = 462$

R_g = Gas constant of flue gas Nm/Kg°C

= $S\, m_k \times R_k$

m_k = Mass fraction of flue gas component in kg/kg

3.6.7 Determining Dynamic Viscosity of flue gas

Vernbanck, 1997 said that the dynamic viscosity of the flue gas can be determined from

$$\mu_g = \frac{\sum \mu_k . m_k / \sqrt{M_k}}{\sum m_k / \sqrt{M_k}}$$

Where,

μ_g = Dynamic viscosity of flue gas in kg/ms

μ_k = Dynamic viscosity of flue gas component in kg/ms

M_k = Molecular mass of flue gas component in kg/ kmol

3.6.8 Determining Non-luminous radiative coefficient

The presence of water vapour and carbon dioxide in the flue gas is important in boiler calculations. They are selective radiators that both emit and absorb radiation in certain wavelengths that are not visible, hence the term non-luminous. The nonluminous radiation is dependent on gas temperature, the partial pressure of the gaseous constituents and the geometry.

The non-luminous coefficient can be calculated as shown below.

$$h_r = h_{rExit\ gas\ temp} \times K_t \times K_E$$

Where,

$$h_{rExit\ gas\ temp} = 4.1868\ P_x \left[\frac{t_g + 71.5 - 28.5\ \frac{\ln(\frac{x}{0.015625})}{ln2}}{1271.5 - 28.5\ \frac{\ln(\frac{x}{0.015625})}{ln2}} \right] KJ/m^2h^o\ C$$

$h_{rExit\ gas\ temp}$ = Radiation coefficient in KJ/m^{2}h °C

t_g = Gas temperature in °C

x = MBL X [PH (Pc + PH)]$^{0.5}$

MBL = Mean beam length in m

PH = Partial pressure of H_2O

PC = Partial pressure of CO_2

PX = $a_o + a_1x + a_2 x^2 + a_3 x^3 + a_4 x^4 + a_5 x^5$

With:

$a_o = 10248755$ $a_1 = 2590015$

$a_2 = -5214298$ $a_3 = 5838360$

$a_4 = -3038581$ $a_5 = 58109$

Kt = Temperature correction factor

Where,

$$K_t = \left[\frac{T_g^4 - T_w^4}{T_g^4 - 573^4}\right] \times \left[\frac{t_g - 300}{t_g - t_w}\right] \text{ for wall temperature} < 300\ ^\circ C$$

$$= (0.73 \times k_t - 0.719) \times \frac{(1100)^{0.25}}{t_g} + 1 \text{ for wall temperature between 300 \& 1000°C}$$

Tg = Log mean temperature of gas in °K

Tw = Log mean wall temperature in °K

KE = Wall emissivity correction factor (taken = 1)

For the boiler model calculation, the total gas pressure can be considered to be atmospheric. Hence, the partial pressures of the H_2O and CO_2 components can be taken equal to their volumetric fractions (Vernbanck, 1997).

3.6.9 Determining Convective coefficient for cross flow

The convective coefficient for gas flow across a bundle of tubes on wall can be determined from

$$N_u = K \,.\, R_e^{0.6}\, P_r^{0.33}$$

or

$$h_c = K \,.\, D^{-0.4} . G^{0.6} . c^{0.33} . \mu^{-0.27} . K^{0.67}$$

Where,

h_c = Convective coefficient in W/m^2 °C

K = 0.287 for in-line tube arrangement

= 0.32 for staggered tube arrangement

D = Outside diameter of tube in m

G = Flue gas mass flux in kg/m^2s

c = Specific heat of flue gas in J/kg °C

μ = Dynamic viscosity of flue gas in kg/ms

k = Thermal conductivity of flue gas in W/m °C.

The properties of the flue gas are in this case determined for the film temperature, defined as follows

$$t_f = \frac{t_w + t_g}{2}$$

Where,

t_f = Film temperature in ° C

t_w = Log mean wall temperature in ° C

t_g = Log mean gas temperature in ° C.

The formula is valid for turbulent flow with a Reynolds number greater than 2000 and for tube banks at least 10 rows deep. An arrangement factor has to be applied to the result to adjust for the geometry of the bank. This factor is dependent on the ratio between longitudinal, as well

as transversal pitching and the diameter of the tube. For normal industrial boiler constructions, this factor is around 0.98 to 1 (Vernbanck, 1997).

3.6.10 Radiative Heat Transfer

The main factor affecting heat transfer during the firing of solid fuel in a bed is radiation of heat from the surface of the bed of burning fuel. This account for as much as 70% of the entire quantity of heat absorbed by the furnace water wall. The determining effect of radiation from the bed of burning fuel manifests itself in the local heat fluxes existing in the individual part of a furnace water wall, which depends on how these parts are situated with respect to bed.

Total average heat flux absorbed by furnace water wall during bed type firing of fuel is equal to the sum of radiant heat flux from the bed surface qb and heat flux absorbed from furnace gases (qrad+qc) by radiation and convection (Kamenetskii ,2008).

$$q = q_b + (q_{rad} + q_c)_g$$

$$q_b = \sigma \varepsilon_{red} (T_b^4 - T_w^4) R/H$$

$$q_{rad} = \sigma \varepsilon_{eff} (\varepsilon_g T_g^4 - a_g T_w^4)$$

Where,

T_b = Average temperature of bed surface, K

T_w = Average temperature of water wall, K

T_g = Average temperature of furnace gases, K

R = Fire bed (grate) surface area, m^2

H = Surface area of heat transfer (water wall), m^2

σ = Stefan-Boltzmann constant

ε_{red} = Emissivity of bed

ε_{eff} = Emissivity of wall

ε_g = Emissivity of furnace gas

a_g = Absorptivity of furnace gas

3.6.11 Mass Transfer

The mass balance of combustion air supplied and resultant combustion product can be useful tool to quantify the energy transfer associated with the combustion products that evolved in the furnace (D.S.Kumar, 2009)

The mass transfer operations can be classified in to the following categories;

(i) Diffusion mass transfer; molecular or eddy diffusion
(ii) Convective mass transfer: free or forced
(iii) Mass transfer by change of phase

Inside the furnace the mass transfer of gases are occurring through diffusion and convective mass transfer. So we are not taken in to account of phase change mechanism.

3.6.12 Diffusion mass transfer; molecular or eddy diffusion

The molecular diffusion is the transport of matter on a microscopic level as a result of diffusion from a region of high concentration in a system of a mixture of liquid or gases. The diffusion mas transfer occurs when a substance diffuses through a layer of stagnant fluid. It is independent of any convection within the system (D.S.Kumar, 2009).

The molecular diffusion is further categorized in to;

- Ordinary diffusion resulting from concentration gradient; the diffusing substance moves from a position of high concentration to one of low concentration.
- Thermal diffusion which may occur by virtue of temperature gradient
- Pressure diffusion resulting from hydrostatic pressure difference that provides the driving potential
- Forces diffusion which results from the action of external forces

The eddy diffusion occurs when one of the diffusing fluids is in turbulent motion. The eddying motion greatly increases the speed of the mass transfer as it is in additional to molecular diffusion.

3.6.13 Convective mass transfer: free or forced

Mass transfer due to convection involves transfer between a moving fluid and a surface or between two relatively immiscible moving fluids. The convective mass transfer depends both on the transport properties and on the dynamic (laminar or turbulent) characteristics of the flowing fluid.

3.6.14 Determining Velocity, concentration and flux of flue gas mixture

Some of the terms associated with different species in a multi-component mixture are defined below for better understanding of the phenomenon of mass transfer (D.S.Kumar,2009).

3.6.14.1 Concentrations

The mass concentration or mass density ρ_a of species A in a multicomponent mixture is defined as the mass of species A per unit volume of the mixture.

$$\rho_a = \frac{mass\ of\ species\ A}{Volume\ of\ the\ mixture}$$

The mass concentration is quite often represented by the symbol C also. In that case $\rho_a = C_a$

The molar concentration or molar density represents the number of moles of species A per unit volume of the mixture.

$$n_a = \frac{number\ of\ molecules\ of\ species\ A}{Volume\ of\ the\ mixture}$$

Since the number of moles equal the mass divided by the molecular weight,

$$n_a = \frac{mass\ of\ species\ A}{Volume\ of\ the\ mixture} \times \frac{1}{mol.wt.of\ species\ A} = \frac{\rho_a}{M_a}$$

The mass fraction ρ_a^* prescribes the ratio of mass concentration of species A to the total mass density of the mixture

$$\rho_a^* = \frac{\rho_a}{\rho} = \frac{C_a}{C}$$

The mole fraction n_a^* prescribes the ratio of number of moles of species A to the total number of moles of the mixture.

$$n_a^* = \frac{n_a}{n_a + n_b} = \frac{n_a}{n}$$

Where n is the molar density of the mixture, i.e., number of moles in the mixture per unit volume

By summation of fraction overs species,

$$\sum \rho^* = \rho_a^* + \rho_b^*$$

$$= \frac{\rho_a}{\rho} + \frac{\rho_b}{\rho} = \frac{\rho_a + \rho_b}{\rho} = 1$$

and

$$\sum n^* = n_a^* + n_b^*$$

$$= \frac{n_a}{n} + \frac{n_b}{n} = \frac{n_a + n_b}{n} = 1$$

Further,

$$M = \frac{\rho}{n} = \frac{\rho_a + \rho_b}{n}$$

$$= \frac{n_a M_a + n_b M_b}{n}$$

$$= n_a^* M_a + n_a^* M_b$$

Thus the molecular weight of the mixture can be worked out by adding the molecular weights of the individual species in proportion to their mole fractions.

For a gaseous phase, the concentrations are usually expressed in term of partial pressures. Invoking the perfect gas law,

$$p_a V = N_a G T$$

The molar concentration is

$$n_a = \frac{N_a}{V} = \frac{\rho_a}{G T}$$

Where,

ρ_a = Pressure of species A

N_a = Total number of moles of species A in the volume V

T = Absolute temperature

G = Universal Gas Constant (G = 8314 Nm /Kg mol K)

Likewise the mole fraction for ideal gas is

$$n_a^* = \frac{n_a}{n} = \frac{{}^{p_a}/_{GT}}{{}^{p}/_{GT}} = \frac{p_a}{p}$$

Where,

p = Total pressure exerted by the gas mixture; $p = p_a + p_b$

3.6.14.2 Velocities

Each component/species of a multi – component mixture has a different mobility rate and the bulk velocity of the mixture is computed either on mass – average or molar – average basis. For a binary mixture of species A and B,

The mass-average velocity V mass is defined as

$$V_{mass} = \frac{\rho_a V_a + \rho_b V_b}{\rho_a + \rho_b}$$

$$= \frac{\rho_a V_a + \rho_b V_b}{\rho} = \rho_a^* V_a + \rho_b^* V_b$$

The molar – average velocity V molar is defined as

$$V_{molar} = \frac{n_a V_a + n_b V_b}{n_a + n_b}$$

$$= \frac{n_a V_a + n_b V_b}{n} = n_a^* V_a + n_b^* V_b$$

3.6.14.3 Fluxes

The existence of different velocities and concentration causes flux of mass transfer. For species A of the multi – component mixture,

Absolute flux = $\rho_a V_a$

Bulk motion flux = $\rho_a V\,mass$

Diffusion flux = $\frac{m_a}{A}$

The quantity $\frac{m_a}{A}$ represents mass flow per unit time.

The absolute flux of any constituent as seen by a stationary observer equals the sum of diffusion flux and the bulk motion flux. That is,

$$\rho_a V_a = \frac{m_a}{A} + \rho_a V_{mass}$$

Accordingly the diffusion flux is,

$$\frac{m_a}{A} = \rho_a (V_a - V_{mass})$$

The diffusion flux is thus proportional to the difference is the velocity of component and the bulk velocity. This velocity difference is called the diffusion velocity.

Therefore Mass-diffusion velocity of species A = $V_a - V_{mass}$

Similarly on molar basis;

Molar-diffusion velocity $= V_a - V_{molar}$

Diffusion flux $= n_a (V_a - V_{molar})$

3.7 Determining Pressure drop across bed of fuel in grate

A fixed or packed bed refers to a bed of stationary particles residing on a perforated grid, through which a gas flows. Here, the particles do not move relative to each other. When the gas flows through a packed bed of solids it exerts a drag force on the particles, causing a pressure drop across the bed. The pressure drop per unit height of a packed bed, ΔP/L of uniformly sized particles, dp is correlated as (Prabir, 2006)

$$\frac{\Delta P}{L} = 150 \frac{(1-\varepsilon)^2}{\varepsilon^3} \frac{\mu U}{(\emptyset d_p)^2} + 1.75 \frac{(1-\varepsilon)}{\varepsilon^3} \frac{\rho_g U^2}{\emptyset d_p}$$

Where

$\frac{\Delta P}{L}$ = N/m^2 per meter of fuel bed depth

ε = Void fraction in the bed

$\emptyset$ = Sphericity of bed solids

μ = Dynamic Viscosity of gas, Kg/m s

ρ_g = Density of gas, Kg/m^3

U = Gas flow rate per unit cross section of the bed, m/s

dp = Surface Volume diameter, m

Results and Discussion

CHAPTER IV

RESULTS AND DISCUSSION

The results obtain from the model study on biomass burning rate, particle burning time, heat release from fuel bed, flue gas property, convective and radiative heat transfer, flue gas exit temperature and pressure drop across fuel bed are given in this chapter under the following major subheadings. The discussions made on the results in the study are also presented here.

4.1 Selected boiler design

4.2 Biomass burning rate

4.3 Particle burning time

4.4 Heat Release Rate per unit volume (qv)

4.5 Heat Release Rate per Unit Cross Sectional Area (qF)

4.6 Flue Gas molecular Velocity

4.7 Stoichiometric air requirement for combustion

4.8 Property of flue gas

4.9 Heat release from fuel bed to near water wall

4.10 Determining furnace wall temperature for selected boiler design

4.11 Non- Luminous Radiative Coefficient

4.12 Convective coefficient for cross flow

4.13 Determining internal heat transfer coefficient

4.14 Determining heat transfer to cavity wall

4.15 Radiative heat transfer

4.16 Pressure Drop across fuel bed

4.1 Selected boiler design

The steam Generator mainly consists of furnace, super heater, boiler bank, economizer and air heater

4.1.1 Grate

Bio-mass is fed into furnace with the help of mechanical or pneumatic fuel feeders and spreaders. Fuel burns on firing grate generating heat. Some of the fuel is burnt as soon as it enters the furnace in air and is called suspension firing. This heat is absorbed by various boiler heat transfer sections and used to convert water into steam. Depending up on the fuel type and it's characteristics, a suitable grate is selected for firing purpose. There are various types of Grates available like Travelling grate, chain grate, inclined water cooled grate, pin hole grate, dumping grate, fixed grate..etc. Travelling Grate is widely used for high ash content fuels and medium range boilers and traveling grate design is used in this study.

4.1.2 Furnace

Furnace is usually vertical and water tube type (Fig.4.1). Furnace water walls are either membrane wall type or tangent tube wall or space tube type. Furnace absorbs major portion of the heat generated during fuel combustion through radiation heat transfer. Proper residence time is selected during furnace design in order to ensure that the fuel gets enough time to burn completely inside the furnace. Boiler furnace parts include furnace bottom headers and top headers on four walls connected with furnace wall tubes which absorb radiation in the furnace. Headers are usually made up of carbon steel pipes and tubes are also of carbon steel. Furnace has a provision for secondary air, fuel feeders. Furnace headers are connected to down comer pipes from Lower drum (water drum). Furnace top headers are connected to Steam/water drum or Top drum with the help of riser tubes/pipes thus completing the circuit. So water from lower drum enters the furnace lower headers and then passes through furnace tubes absorbing heat. Part of the water converts to steam on account of heat absorption and this two phase water/steam enters furnace top headers. This steam and water mixture then enters Steam Drum through risers thus completing the circuit. This process is called circulation and the term to describe this water to steam ratio is called circulation ratio. In water tube boiler furnaces this ratio ranges from 15 to 25 in the case of natural circulation boilers. In assisted circulation or forced circulation boilers,

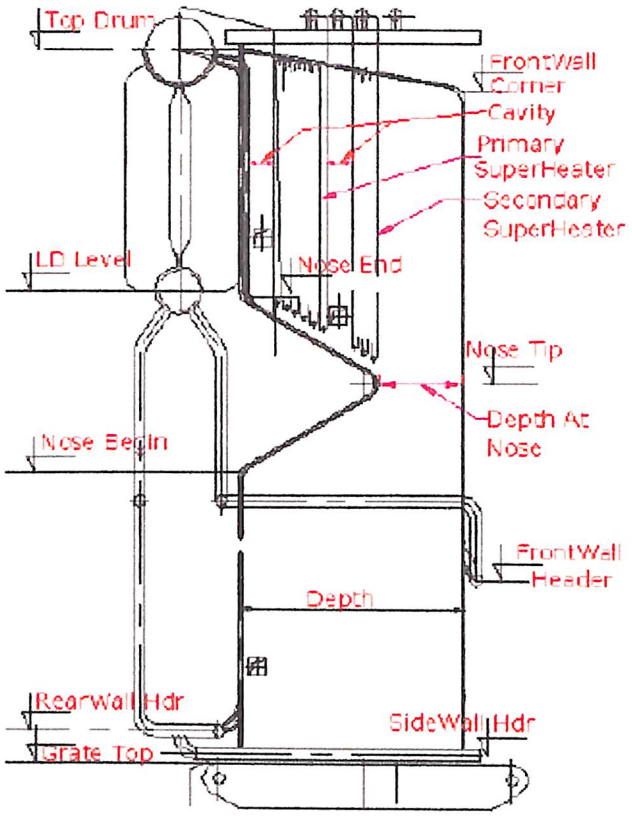

Fig. 4.1 Furnace different level

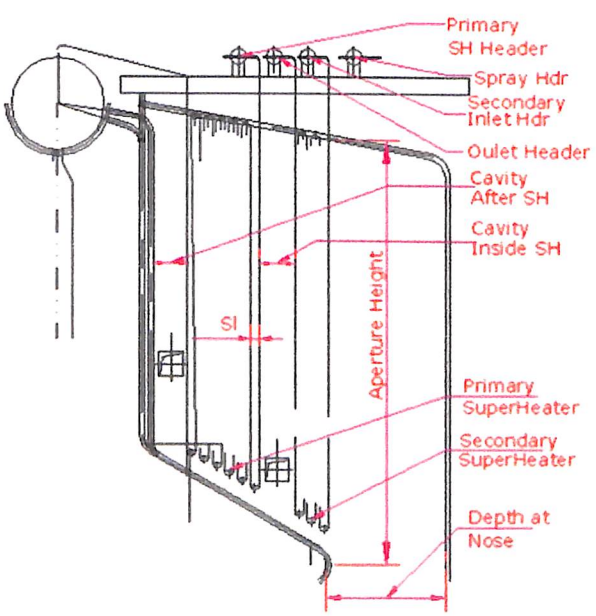

Fig. 4.2 Two stage superheater - Primary and Secondary

steam water mixture is circulated with the help of a pump unlike natural circulation boiler where it happens because of density difference between steam and water. So forced circulation is required for only high pressure boilers above 150 bar or so and the circulation ratio is much lower and less than 10. In single drum boilers, the furnace is made very tall to absorb the additional heat load required because of the absence of the boiler bank.

4.1.3 Boiler Bank

Boiler bank absorbs heat from hot gases through convection (Fig.4.3). Usually Boiler bank is bulky as it has to absorb heat by convection at relatively low temperature. Most of the grate fired boilers are of Bi-Drum construction where the lower drum is always filled with the water and the upper drum is half full with water and the rest with steam. Both the drum are connected by hundreds of tubes and sometimes thousands of tubes. Material of construction is carbon steel for both the drums and tubes. Now-a-days single drum boilers are gaining popularity as this expensive boiler bank can be avoided. Rotary soot blowers are provided to dust-off the soot.

4.1.4 Superheater

Superheater is the prime section in any boiler (Fig. 4.2). Right design of the superheater is very critical in the boiler. Superheater absorbs heat by direct radiation from furnace, by non-luminous radiation and by convection. Superheater section is generally protected by furnace nose in many industrial boilers. some superheaters, called platten type, kept directly hanging in the furnace to absorb more heat. Superheater consists of Inlet outlet headers connected with superheater coils. Inter-stage desuperheater / attemparetor is generally provided to control the steam outlet temperature. Depending up on the steam temperature and resultant metal temperature of the superheater coils either carbon steel or low alloy material is used. Superheaters are also provided with steam or sonic soot soot blowers of retractable type.

4.1.5 Economizer

Economizer is used downstream of Boiler bank to preheat the feed water absorbing heat from hot exhaust gases. Economizers are always water tube type. Bare tubes in Economizers are widely used in Industrial boilers. Finned tubes are popular in HRSG applications. Economizers

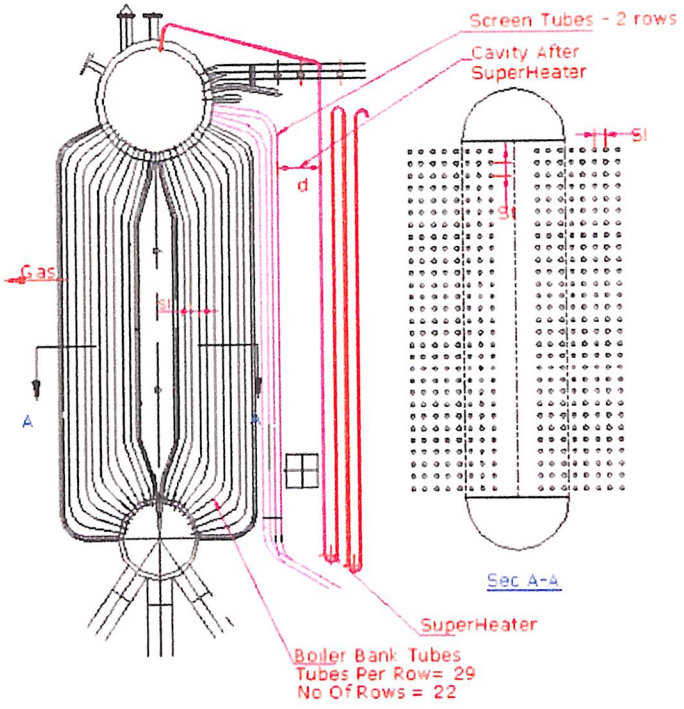

Fig. 4.3 Boiler Bank - Cross Flow (Typical)

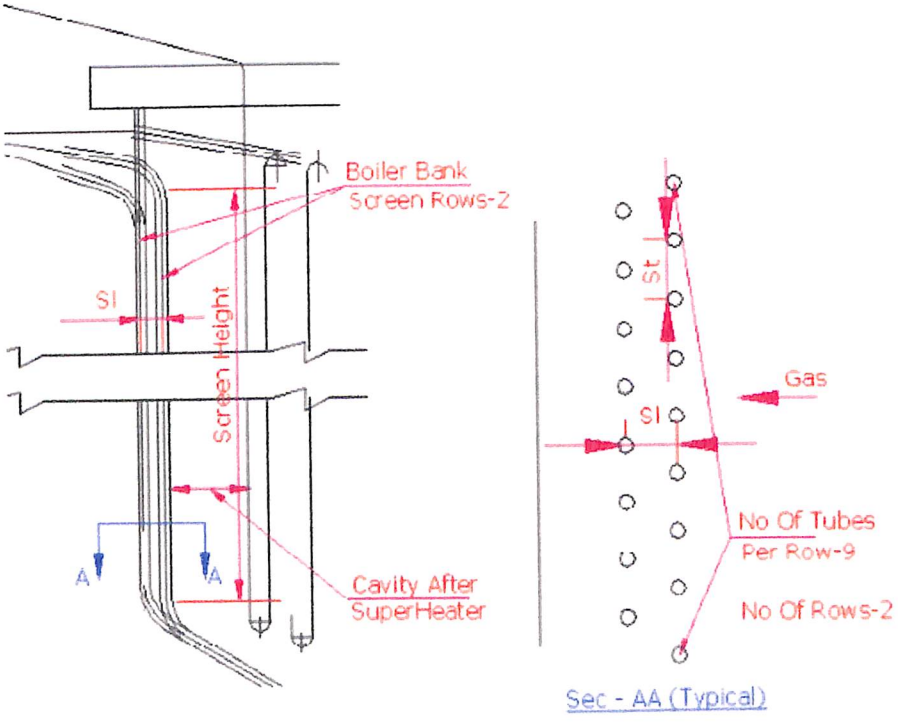

Fig. 4.4 Boiler Bank Screen (Typical)

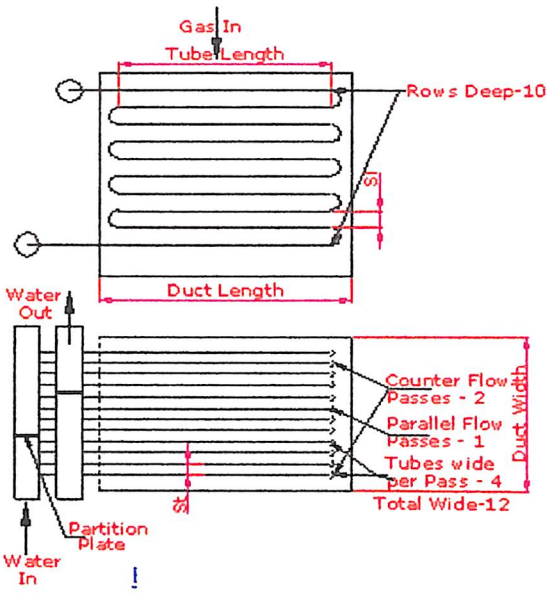

Fig. 4.5 Economizer

are retrofitted to many old boilers to increase the fuel efficiency of the boiler. Feed water can be heated up to a level about 20 - 30 ° C below saturation temperature of the boiler. Economizers need hot water input to reduce condensation of corrosive gases like SO_2 on tubes. Depending up on the sulfur content in the fuel, water inlet temperature of 80 ° C up to 150 ° C is required for economizers. Typical economizer is shown in Fig.4.5.

4.1.6 Air heater

Air heater is used to preheat the combustion air before sending it to furnace for combustion. This also recovers heat from the exhaust gases and reduces the boiler outlet gas temperatures to a level of 130 to 170 ° C. Hot air helps combustion and hot air temperatures of 150 to 220 c are common in many industrial boilers. Hot air temperature is especially important, if fuel contains inherent moisture, like bagasse.

4.1.7 Boiler Parts

Boiler parts include boiler sections like furnace, superheater, boiler bank, economizer, air heater, steam and water drums. Fuel feeding section includes fuel storage, fuel bunker or silo, rotary, reciprocating or pneumatic fuel feeder, grate and ash discharge chutes.

4.1.8 Highlighted design parameters of selected boiler

The main design parameters of the selected boiler of 12 MW capacity are discussed here. Detail design of the boiler components are produced in annexure.

4.1.8.a Boiler Rating

Steam Capacity (Actual)	:	80	TPH
Steam Pressure (g)	:	65	Kg/Cm^2
Steam Outlet temperature	:	485	Deg C
Water inlet temperature	:	105	Deg C
Grate Type	:	Travelling	
Furnace	:	Nose type	
Furnace Wall	:	Membrane	
Super Heater	:	Two Stages – Primary Counter, Secondary Parallel	
Boiler Bank	:	Water Tube	
Boiler Bank Flow	:	Cross Flow	
Fuel Name	:	Wood	

4.1.8.b Performance Detail

Efficiency(GCV)	:	83.46	
Efficiency(NCV)	:	89.27	
Gross Cal Value	:	3,985.88	Kcal/Kg
Net Cal Value	:	3,726.49	Kcal/Kg
Fuel Sensible Heat	:	0.00	Kcal/Kg

Fuel Consumption	:	17,054.88	Kg/hr
Gross Heat Input	:	6.798×10^7	Kcal/ hr
Net Heat Input	:	6.355×10^7	Kcal/ hr
Total Heat Load	:	5.673×10^7	Kcal/ hr
Gas Flow	:	1.290×10^5	Kg/ hr
FGR Flow	:	0.000	
Total DraftLoss(Gas)	:	7.749X10	mm of WC
Boiler Heating Surface Area	:	3,983.62	m^2

4.1.8.c Furnace

Exit Gas Temp	:	996.11	Deg C
Eff Proj Rad Surface(EPRS):		317.12	m^2
Volumetric Heat Rel Rate	:	192,926.44	$Kcal/m^3$

Further design parameters and working parameters of primary, secondary super heaters, boiler drum, boiler bank, boiler bank screen, economizer and air preheater are produced in Annexure E which is designed using FIRE CAD Tool.

4.2 Biomass burning rate

Generally the biomass which are less than < 5 cm are used in boiler. The biomass size more than these size will result in poor and prolonged combustion. For our study purpose the wood aspects are iterated by starting with size equals 5cm diameter and then less.

Wood diameter = 5 Cm

Wood piece Length = 6 Cm

Particle temperature = 1800 K

Kinetic Rate constant ,Kc = 13.9 m/s

Assume molecular weight of gases at surface = 30 Kg / Kmol

Assume wood are in cylindrical shape

Volume of wood single piece $= \pi r^2 h$

$= 3.14 \times 0.025^2 \times 0.06$

$= 1.17 \times 10^{-4}\ m^3$

Surface area of wood piece $= 2\pi rh$

$= 2 \times 3.14 \times 0.025 \times 0.06$

$= 9.42 \times 10^{-3}\ m^2$

Volume diameter (dv)

$$d_v = [\left(\frac{6}{\pi}\right) \times Volume\ of\ particle\ ]^{\frac{1}{3}}$$

$$= [\left(\frac{6}{\pi}\right) \times 1.17 \times 10^{-4}\ ]^{\frac{1}{3}}$$

$= 0.060\ m^3$

Surface diameter (ds)

$$d_s = [\frac{Surface\ area\ of\ particle}{\pi}]^{\frac{1}{2}}$$

$$= [\frac{9.42 \times 10^{-3}}{\pi}]^{\frac{1}{2}}$$

$= 0.0547\ m^2$

Sphericity (Ø)

$$Sphericity\ (\emptyset) = \frac{Surface\ area\ of\ a\ sphere\ with\ the\ volume\ same\ as\ the\ particle}{Actual\ surface\ area\ of\ the\ particle}$$

$$= \frac{\pi dv^2}{S}$$

$$Sphericity\ (\emptyset) = \frac{3.14 \times (0.060)^2}{9.42 \times 10^{-3}} = 1.2$$

Spherical particle has a sphericity = 1

Since the wood is chopped in to smaller pieces which merely resembles cylindrical structure .So its sphericity value is 1.2 which shows its deviation from spherical shape.

Since the wood shape doesn't resembles spherical structure, assuming the mean diameter of the selected wood as 5 cm for our study iteration.

Mean diameter of wood = 5 Cm

= 5×10^{-2} m

Density of gas by ideal gas law at surface temperature, $\rho = \frac{P}{\left(\frac{R_u}{MW_{mix}}\right)T_s}$

$$= \frac{101325}{\left(\frac{8315}{30}\right)1800}$$

$= 0.20$ Kg / m^3

Mass diffusivity is estimated using a value for CO_2 in N_2 from Annexure C, corrected to 1800 K

$$D = \left(\frac{1800\ K}{293\ K}\right)^{1.5} \times 1.6 \times 10^{-5}\ \frac{m^2}{s}$$

$= 2.4 \times 10^{-4}$ m^2/s

Assuming $Yo_2,S = 0$ for the time being

$$R\,diff = \frac{\vartheta 1 + Yo2s}{\rho D 4\pi rs}$$

$$= \frac{2.664 + 0}{0.20\,(2.4 \times 10^{-4}) \times 4 \times 3.14 \times 2.5 \times 10^{-2}}$$

$$= \frac{2.664}{1.5072 \times 10^{-5}}$$

$$= 1.76 \times 10^{5}\ \text{s/kg}$$

The chemical kinetic resistance

$$Rkin = \frac{1}{K_{kin}} = \frac{\vartheta 1 RuTs}{4\pi r^2 MW_{mix} K_c P}$$

$$= \frac{2.664\,(8315)1800}{4 \times 3.14 \times (2.5 \times 10^{-2})^2 \times 30 \times 13.9 \times 101325}$$

$$= 120.21\ \text{s/kg}$$

From the above calculation, we see Rdiff is more than the value of Rkin, the combustion is nearly diffusion controlled

$$mc = \frac{(Yo2, \infty - 0)}{Rkin + Rdiff}$$

$$= \frac{0.233}{(1.76 \times 10^5) + (120.21)}$$

$$= 1.35 \times 10^{-6}\ \text{kg/s}$$

4.2.1 Two Film Method

Kinetic Rate constant for C-CO_2 reaction is

$$K_c = 4.016 \times 10^8 \exp[\frac{-29790}{T_s}]$$

$$= 4.016 \times 10^8 \exp[\frac{-29790}{1800}] = 26.07\ m/s$$

The combustion rate can be expressed in term of surface CO_2 Concentration

$$m_c = 4\pi r_s^2 K_c \frac{MW_C MW_{mix}}{MW_{CO2}} \frac{P}{R_o T_s} Y_{CO2,S}$$

$$= \frac{4 \times 3.14 \times (2.5 \times 10^{-2})^2 \times 26.07 \times 12 \times 30 \times 101325}{44.01 \times 8315 \times 1800}$$

$$= 0.01133\, Y_{co2,s} \left(\frac{Kg}{s}\right)$$

Another equation which governs the burning rate is

$$m_c = 4\pi r_s \rho D \ln(1+B)$$

$$= 4 \times 3.14 \times (2.5 \times 10^{-2})^2 \times 0.2 \times 1.57 \times 10^{-4} \ln(1+B)$$

$$= 9.85 \times 10^{-6} \ln(1+B) \left(\frac{Kg}{s}\right)$$

$$B = \frac{2\, Yo2\alpha - \left[\frac{\vartheta_s - 1}{\vartheta_s}\right] Yco2,s}{\vartheta_s - 1 + \left[\frac{(\vartheta_s - 1)}{\vartheta_s}\right] Yco2,s}$$

$$= \frac{2(0.233) - \left[\frac{3.664-1}{3.664}\right] YCo2\, s}{3.664-1+\left[\frac{3.664-1}{3.664}\right] Y\, co2,s}$$

$$= \frac{0.466 - 0.727\, Yco2,s}{2.664 + 0.727\, Yco2,s}$$

Solving equation a,b,c iteratively. We start the iteration assuming YCO_2,s is zero, the diffusion controlled limit.

Table 4.1 shows the iteration results of two film model

Table 4.1 Iteration results of two film model

Iteration	$YCO_{2,s}$	B	mc (kg/s)
1	0	0.1749	1.61×10^{-6}
2	0.1003	0.1436	1.37×10^{-6}
3	0.0835	0.1521	1.41×10^{-6}
4	0.0863	0.1513	1.41×10^{-6}

Giving two significant figure accuracy, the solution converges to

$$m_c = 1.41 \times 10^{-6}$$

4.3 Particle burning time

The biomass particle burning time are calculated as follows

Wood mean diameter $= 5\ cm = 5 \times 10^{-2}\ m$

Density of wood $= 800\ kg / m^3$

Burning rate constant

$$K_B = \frac{8\,\rho\, D}{\rho_{wood}} \ln(1 + Bco2m)$$

$$= \frac{8\,(0.20) 1.57 \times 10^{-4}}{800} \ln(1 + 0.1488)$$

$$= 4.35 \times 10^{-8} \frac{m^2}{s}$$

Burning time of wood piece $= \frac{D_O^2}{K_B}$

$= 57472$ Sec

The burning rate and burning time of wood pieces are carried out at different aspect whose results are tabulated in table 4.2.

Table 4.2 Burning rate and burning time of different wood piece size

Mean diameter of wood	Burning Rate, mc (Kg/s)		Burning Time
	One film model	Two film model	
5 cm	1.35×10^{-6}	1.42×10^{-6}	15.37 Hrs
4 cm	1.086×10^{-6}	1.13×10^{-6}	9.8 Hrs
3 cm	0.81×10^{-6}	0.85×10^{-6}	5.5 Hrs
2 cm	0.54×10^{-6}	0.56×10^{-6}	2.4 Hrs
1 cm	0.27×10^{-6}	0.28×10^{-6}	36.9 Minutes
5 mm	0.13×10^{-6}	0.14×10^{-6}	9.2 Minutes
4 mm	0.10×10^{-6}	0.113×10^{-6}	5.9 Minutes
3 mm	0.08×10^{-6}	0.085×10^{-6}	3.3 Minutes
2 mm	0.053×10^{-6}	0.056×10^{-6}	1.47 Minutes
1 mm	0.026×10^{-6}	0.028×10^{-6}	22.14 Seconds

It's observed from the Fig.4.6 that the burning time of wood particle will be low when its aspect is minimum.

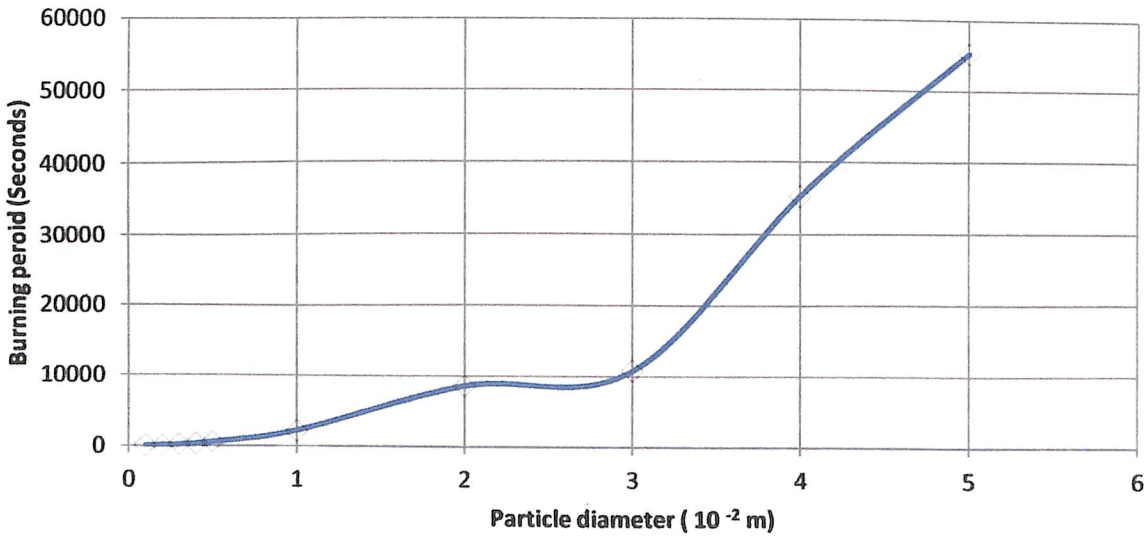

Fig. 4.6 Behavior of particle burning time with respect to biomass size

The burning rate will greatly depend on the pressure of primary air imparting on the biomass particle whose behavior at different striking pressure are charted below in table 4.3.

Table 4.3 Behavior of burning rate with impinging primary air pressure

S.No	Burning rate of biomass by one film model ($\times 10^{-6}$ Kg/s)					
	Diameter of wood particle					
	Pressure, atm	*5 cm*	*4 cm*	*2 cm*	*3 cm*	*1 cm*
1	1	1.35	1.08	0.81	0.54	0.27
2	4	5.43	4.34	3.25	2.17	1.08
3	6	8.14	6.51	4.88	3.25	1.62
4	8	10.86	8.68	6.51	4.34	2.16
5	10	13.57	10.86	8.14	5.42	2.70
6	12	16.29	13.03	9.77	6.51	3.24
7	14	19.01	15.20	11.40	7.59	3.79
8	16	21.72	17.37	13.03	8.68	4.33
9	18	24.44	19.55	14.65	9.76	4.87
10	20	27.15	21.72	16.28	10.85	5.41
11	22	29.87	23.89	17.91	11.93	5.95
12	26	35.30	28.24	21.17	14.10	7.04
13	28	38.02	30.41	22.80	15.11	7.58
14	30	40.73	32.58	24.43	16.27	8.12

It's observed from the above calculated result that, the burning rate seems to increase with increase in primary air pressure. But as the aspect of biomass reduces, burning rate also seems to get reduce. Because in above calculation, constant Kc value is taken for both the larger and smaller particle. But in actual, the burning rate will increase with decrease in biomass aspect. Smaller particle will quickly achieve de-moisture, de-volatize cum ignition temperature than larger one and have Kc value more than the larger particle Kc value .

Because of larger Kc value with smaller particle, it achieve higher burning rate in actual condition. Since determining the Kc for smaller particle is quite difficult .So the results of burning rate is produced as per model assumption which is the reason for showing higher burning rate for higher biomass particle size. So, both the biomass aspect and primary air pressure have its own role in deciding the burning rate of particle which is shown in Fig.4.7.

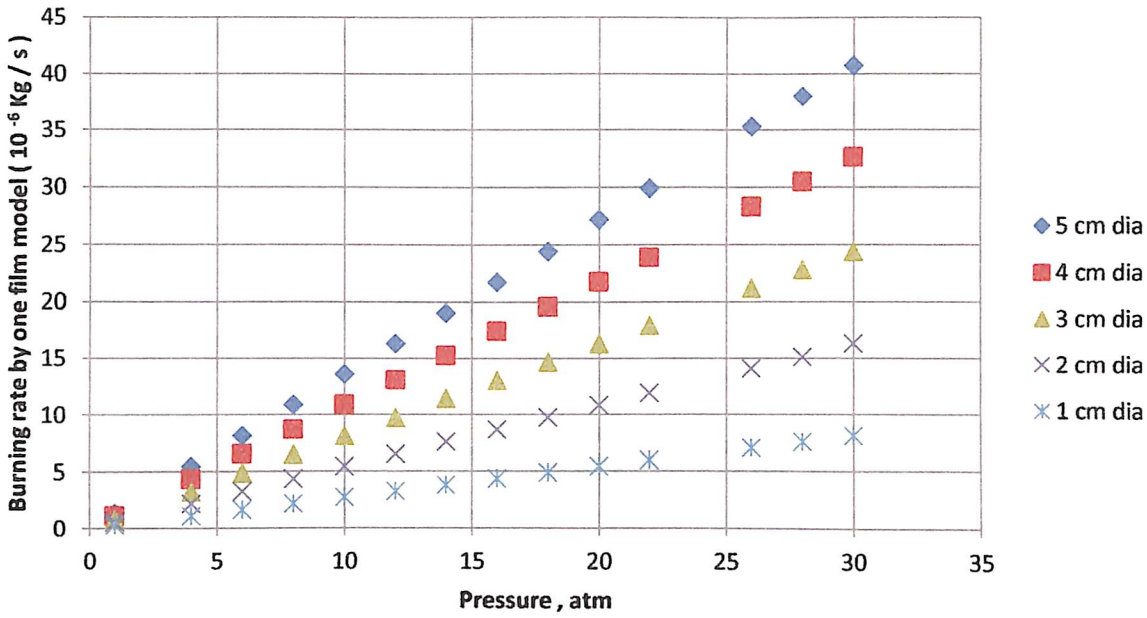

Fig. 4.7 Variation of burning rate as the function of biomass aspect and pressure

4.4 Heat Release Rate per unit volume (qv)

The quantity of energy released per unit volume of selected boiler design is calculated as follows

$$q_v = \frac{B.LHV}{V} \ \frac{KW}{m^3}$$

Designed fuel consumption rate, B = 4.73 Kg/s

Furnace Volume, V = 4.48 m × 6.73 m × 12.08 m

= 364 .21 m3

Lower Heating Value of fuel, LHV = 15592 KJ/Kg

$$q_v = \frac{4.73 \times 15592}{364.21} \ \frac{KW}{m^3}$$

$$q_v = 202.49 \ \frac{KW}{m^3}$$

4.5 Heat Release Rate per Unit Cross Sectional Area (qF)

The quantity of energy released from unit area of fuel bed is calculated as follows

$$q_F = \frac{B.LHV}{F_{grate}} \; KW/_{m^2}$$

Cross sectional area of the furnace grate, F $= 6.73 \times 4.48 \; m^2$

$$q_F = \frac{4.73 \times 15592}{6.73 \times 4.48} \; KW/_{m^2}$$

$$q_F = 2446 \; KW/_{m^2}$$

4.6 Flue Gas molecular Velocity

The velocity of flue gas molecules and its existing velocity inside the furnace are calculated as follows. Design velocities of boiler fluids are given in Annexure B.

Flue Gas Component	Molecular Weight (Kg/Kmol)
CO_2	44
N_2	28
O_2	32
H_2O	18

Gas temperature = 1000 ° C = 1273 K

Mean travel velocity by kinetic theory,

$$V = \sqrt{\frac{3\,G\,T}{M}}$$

Where,

V = Velocity of gas molecule (m/s)

G = Universal Gas Constant (8.314 Kg m^2 / s^2 mol K)

M = Molecular weight of the gas (Kg/ mol)

T = Absolute Temperature ($^{\circ}$ K)

Mean travel velocity of flue gas components

$$V, CO_2 = \sqrt{\frac{3 \times 8.314 \times 1273}{0.044}}$$

= 849.48 m/s

$$V, N_2 = \sqrt{\frac{3 \times 8.314 \times 1273}{0.028}}$$

= 1064.88 m/s

$$V, O_2 = \sqrt{\frac{3 \times 8.314 \times 1273}{0.032}}$$

= 996.10 m/s

$$V, H_2O = \sqrt{\frac{3 \times 8.314 \times 1273}{0.018}}$$

= 1328.13 m/s

Vmass = (0.31 × 849.48) + (0.61 × 1064.88) + (0.04 × 996.10) + (0.028 × 1328.13)

= 989.92 m/s

Actual velocity of flue gas inside the furnace is established below,

Volumetric flow rate of flue gas (m^3/s) = Furnace cross sectional area (m^2) × Velocity (m/s)

119.60 m^3/s = 30.20 m2 × Velocity

Velocity = 3.96 m/s

4.7 Stoichiometric air requirement for combustion

4.7.1 Wood Composition

Carbon	:	45.6 %
Hydrogen	:	4 %
Nitrogen	:	0.5 %
Oxygen	:	37.45 %
Sulphur	:	0.07 %
Moisture	:	9.33 %
Ash	:	3.05 %

4.7.2 Carbon Combustion:

$C+O_2 = CO_2$

12kg C + 32 Kg O_2 = 44 Kg O_2

1 Kg C + 2.66 Kg CO_2 = 3.6 Kg CO_2

In 1 kg of fuel 0.45 kg of carbon presents

Therefore,

O_2 required for carbon combustion = 2.66 × 0.45

= 1.197 Kg O_2

CO_2 produced as byproduct = 3.6 × 0.45

= 1.62 Kg CO_2

4.7.3 Hydrogen Combustion:

$2H_2+O_2 = 2H_2O$

1 kg H_2 + 8 Kg O_2 = 9 Kg H_2O

In 1 Kg of wood 0.04 kg of hydrogen presents

O_2 required for combustion of this hydrogen = 0.04 × 8

= 0.32 Kg o_2

H_2O Produced as byproduct = 9 × 0.04

= 0.36 Kg H_2O

Since sulphur is negligible we are neglecting its combustion and we assume nitrogen reactivity is nil at low temperature.

For 1 Kg of wood

Total O_2 required = 1.197 + 0.32

= 1.517 Kg

O_2 presents in the fuel = 0.37 Kg /Kg fuel

Therefore actual O_2 required = 1.517 – 0.37

= 1.147 Kg

For obtaining 1 Kg of O_2, amount of air required = 100/23

= 4.35 Kg

(Air by mass: 23% Oxygen, 77% Nitrogen)

For 1 Kg of fuel, air required = 4.35 × 1.147

= 4.98 Kg air

Amount of nitrogen in supplied air = 4.98 × 0.77

= 3.83 Kg N_2

Amount of nitrogen in fuel = 0.5 %

Total nitrogen in byproduct = 3.83 + (0.5/100)

= 3.835 Kg N_2

4.7.4 Excess Air

Let's take excess air for wood = 30%

Stoichiometric air = 4.98 Kg

Now total air = 4.98 + (4.98 × 0.30)

= 6.47 Kg of air

Nitrogen mass in byproduct = 6.47 × 0.77

= 4.98 Kg N_2

4.7.5 Summary of stoichiometric and excess air calculation

Total air required = 6.47 Kg air / Kg of fuel

Byproduct formation by burning of 1 Kg of fuel

CO_2 = 1.62 Kg

H_2O = 0.36 Kg

N_2 = 4.98 Kg

Required actual fuel firing rate in boiler = 17055 Kg /hr

Mass flow of air = 17055 Kg/ hr × 6.47 Kg air /Kg fuel

= 110346 Kg air / hr

Mass flow rate of byproduct

CO_2 = 1.62 × 17055 = 27629 Kg/hr

H_2O = 0.36 × 17055 = 6140 Kg/hr

N_2 = 4.98 × 17055 = 84934 Kg/hr

Table 4.4 shows the mass flow rate of flue gas for actual boiler operational condition

Table 4.4 Mass flow rate of flue gas

S.No	Mass flow in combustion	For unit mass of wood	For actual fuel firing rate (17055 Kg/hr)
1	Combustion air required (In)	6.47 Kg	110346 Kg / hr
2	CO_2 (Out)	1.62 Kg	27629 Kg /hr
3	H_2O (Out)	0.36 Kg	6140 Kg / hr
4	N_2 (Out)	4.98 Kg	84934 Kg /hr
5	Excess O_2(Out)	-	5800 Kg/hr

While operation of boiler 40 % of combustion air is passed as primary air and 60 % of remaining as secondary air. It is taken in account that, due to supply of excess air about 4 – 5% of O_2 is observed in flue gas exit.

Total mass flow of flue gas = Mass flow of $CO_2+H_2O+N_2+O_2$, Kg/hr

= 27629 + 6140 + 84934 +5800

= 124503 Kg/hr

The flue gas composition on the weight basis is shown in table 4.5

Table 4.5 Flue gas composition by weight basis

S.No	Composition	Calculation of % by weight	% by weight
1.	CO_2	(27629/124503) × 100	22.19
2.	H_2O	(6140 / 124503) × 100	4.93
3.	N_2	(4934 / 124503) × 100	68.2
4.	O_2	(5800 / 124503) × 100	4.65

4.8 Property of flue gas

It's important to know the flue gas property which plays a basic role in heat transfer mechanism. So the flue gas properties are calculated as follows

4.8.1 Determining molar concentration, mass density and average molecular weight of flue gas

The average molecular weight of flue gas is independent of temperature, pressure exit in the furnace but its proportional to percentage composition of species in flue gas. In case of mass density and molar concentration of flue gas, it's purely dependent factor of temperature and pressure.

Table 4.6 The partial pressure ratio and molecular weight of flue gas species are

S.No	Flue gas components	Partial pressure ratio, δ	Molecular Weight, MW
1.	CO_2	0.22	44
2.	N_2	0.68	28
3.	O_2	0.046	32
4.	H_2O	0.049	18

The calculation are carried out for 1037°C (1310 K) at 1×10^5 N/m^2 furnace pressure. Though slightly negative pressure is maintained inside the furnace, we are taking the atmospheric pressure for convenient in calculation.

Molar Concentration of flue gas species are

$$n_{co_2} = \frac{0.22 \times 10^5}{8314 \times 1310} = 2.02 \times 10^{-3}\ Kg\ mol/m^3$$

$$n_{N_2} = \frac{0.68 \times 10^5}{8314 \times 1310} = 6.24 \times 10^{-3}\ Kg\ mol/m^3$$

$$n_{o_2} = \frac{0.046 \times 10^5}{8314 \times 1310} = 4.22 \times 10^{-4}\ Kg\ mol/m^3$$

$$n_{H2O} = \frac{0.049 \times 10^5}{8314 \times 1310} = 4.49 \times 10^{-4}\ Kg\ mol/m^3$$

4.8.1.a Mass Density

$$\rho_{co_2} = 44 \times 2.02 \times 10^{-3}$$

$$= 0.0888\ {}^{Kg}/_{m^3}$$

$$\rho_{N_2} = 28 \times 6.24 \times 10^{-3}$$

$$= 0.1747\ {}^{Kg}/_{m^3}$$

$$\rho_{o_2} = 32 \times 4.22 \times 10^{-4}$$

$$= 0.0135\ {}^{Kg}/_{m^3}$$

$$\rho_{H2O} = 18 \times 4.49 \times 10^{-4}$$

$$= 8.082 \times 10^{-3}\ {}^{Kg}/_{m^3}$$

Overall mass density $\rho = \rho_{co_2} + \rho_{N_2} + \rho_{o_2} + \rho_{H2O}$

$$= 0.0888 + 0.1747 + 0.0135 + 8.082 \times 10^{-3} = 0.2850\ {}^{Kg}/_{m^3}$$

The mass fraction of flue gas components

$$\rho^*_{co_2} = \frac{\rho_{co_2}}{\rho} = \frac{0.0888}{0.2850} = 0.31$$

$$\rho^*_{N_2} = \frac{\rho_{N_2}}{\rho} = \frac{0.1747}{0.2850} = 0.61$$

$$\rho^*_{o_2} = \frac{\rho_{o_2}}{\rho} = \frac{0.0135}{0.2850} = 0.04$$

$$\rho^*_{H2O} = \frac{\rho_{H2O}}{\rho} = \frac{8.08 \times 10^{-3}}{0.2850} = 0.028$$

4.8.1.b Average Molecular weight of flue gas

$$A_{MW} = \sum \varphi_S \times MW_S$$

Where

A_{MW} = Avg molecular weight of flue gas

$\varphi_S = Partial\ pressure\ of\ \ flue\ gas\ species\ (\varphi_{CO2}, \varphi_{N2}, \varphi_{O2}, \varphi_{H2O})$

$MW_S = Molecular\ weight\ of\ flue\ gas\ species\ (MW_{CO2}, MW_{N2}, MW_{O2}, MW_{H2O})$

$$A_{MW} = (0.22 \times 44) + (0.68 \times 28) + (0.046 \times 32) + (0.049 \times 18)$$

$$= 31.07$$

4.8.2 Adiabatic Flame Temperature of Wood

The adiabatic flame temperature of wood burning in air would be 1900 K. Hardly it ranges between 1800 K to 1900 K which is depends on deviation from equivalents ratio. The flame temperature decreases as the equivalents ratio moves away from unity. The property of flue gas is shown in the table 4.7.

Table 4.7 Calculated property of flue gas for selected boiler design over wide range of temperature

S.No	Temperature °C	Molecular Weight	Density, Kg/m^3	Enthalpy, Kcal/Kg	Specific Heat, Kcal/Kg °C	Thermal Conductivity, Kcal/hr m °C	Viscosity, Cp
1	1700	31.24	0.1938	489.96	0.1775	0.0502	0.0612
2	1650	31.24	0.1987	473.98	0.1775	0.0494	0.0603
3	1600	31.24	0.2035	458.01	0.1773	0.0486	0.0594
4	1550	31.24	0.2083	442.05	0.1771	0.0477	0.0585
5	1500	31.24	0.2147	426.12	0.1768	0.0468	0.0575
6	1450	31.24	0.2211	410.22	0.1764	0.0464	0.0566
7	1400	31.24	0.2274	394.37	0.1759	0.0451	0.0556
8	1350	31.24	0.2339	378.56	0.1753	0.0442	0.0547
9	1300	31.24	0.2419	362.81	0.1746	0.0433	0.0537
10	1250	31.24	0.2499	347.12	0.1739	0.042	0.0526
11	1200	31.24	0.2579	331.51	0.1730	0.0413	0.0516
12	1150	31.24	0.2676	315.97	0.1721	0.0404	0.0506
13	1100	31.24	0.2772	300.53	0.1711	0.0394	0.0495
14	1050	31.24	0.2884	285.17	0.1703	0.0383	0.0484
15	1000	31.24	0.2996	269.93	0.1688	0.0373	0.0473
16	950	31.24	0.3108	254.79	0.1675	0.0360	0.0462
17	900	31.24	0.3253	239.76	0.1662	0.0352	0.0450
18	850	31.24	0.3397	224.86	0.1648	0.034	0.0438
19	800	31.24	0.3557	210.08	0.1634	0.032	0.0426
20	750	31.24	0.3710	195.45	0.1618	0.0318	0.0413
21	700	31.24	0.3910	180.95	0.1602	0.030	0.0400
22	650	31.24	0.4134	166.60	0.1583	0.028	0.0380
23	600	31.24	0.4350	152.42	0.1566	0.02819	0.0374
24	550	31.24	0.4631	138.39	0.1549	0.0264	0.0360
25	500	31.24	0.4935	124.52	0.1530	0.025	0.0345

4.9 Heat release from fuel bed to near water wall

The heat release rate from biomass bed varies according to its temperature of combustion and fuel bed density. The fuel bed density is decided by the size of the biomass i.e. fuel density on bed is fix by the void fraction of biomass which is again the factor of size and the temperature of combustion will be nearly equals to adiabatic flame temperature, but this temperature exist only at fuel bed not at furnace wall because of heat loss from furnace surface.

Adiabatic temperature of wood as Tb= 1900 K (1627 °C)

Density of wood = 800 Kg / m^3

Void fraction exits in fuel bed, ε = 0.87

Density of fuel bed at this void fraction = 700 Kg / m^3

Heat release rate from fuel bed, $h = 5\ \rho_{avg}^{0.391}\ T_b^{0.408}\ \ W/m^2\ K$

$= 5\times 700^{\,0.391} \times 1900^{\,0.408}$

$= 87.94\ W/m^2\ K$

It's impossible to say that the fuel bed will always retain the temperature near Adiabatic Flame Temperature (AFT). As it varies according to heat loss to surrounding, the heat release rate from bed is carries out at different temperatures deviate from AFT (Table 4.8).

Table 4.8 Fuel bed temperature Vs. Fuel bed heat release rate.

S.No	Temperature of Bed		Heat release from bed (W/m^2 K)
1	1900 K	1627 °C	87.94
2	1850 K	1577 °C	87.84
3	1800 K	1527 °C	87.74
4	1700 K	1427 °C	87.54
5	1500 K	1227 °C	87.09
6	1300 K	1027 °C	86.59
7	1200 K	927 °C	86.30

From Fig.4.8 that over wide temperature difference between the fuel bed (i.e. 1900 K to 1200 K) ,the heat release rate from bed doesn't vary greatly. So the only deciding factor of heat release rate from fuel bed is average fuel bed density which depends on void fraction or size of fuel selected. To study this phenomenon, calculations are carried out at different fuel bed density at AFT whose results are tabulated in table 4.9.

Table 4.9 Fuel bed density Vs. Heat release rate

S.No	Fuel bed density ,Kg/m^3	Heat release from bed (W/m^2 K)
1	800	92.8
2	750	90.55
3	700	88.14
4	650	85.62
5	600	82.98
6	550	80.20
7	500	77.27

Fig.4.9 shows that as the fuel density goes down, the heat release rate also goes down proportionally. So the particle size plays the key role in deciding heat rate from fuel bed. But as the combustion proceed, the size of biomass piece starts shrinking. So the void fraction will change which keeps the density of fuel bed vary .To maintain the density nearly constant in the bed, the vibrating reciprocating system is provided in the furnace grate.

4.10 Determining furnace wall temperature for selected boiler design

It's known from the selected boiler design that the exit gas temperature of furnace is 996.11 ° C which can be used in FEGT energy balance equation of furnace to determine the furnace wall temperature.

NCV of fuel = 3726.49 Kcal / kg

= 15592 KJ / Kg

m_{ha} = 6.47 kg /kg of fuel

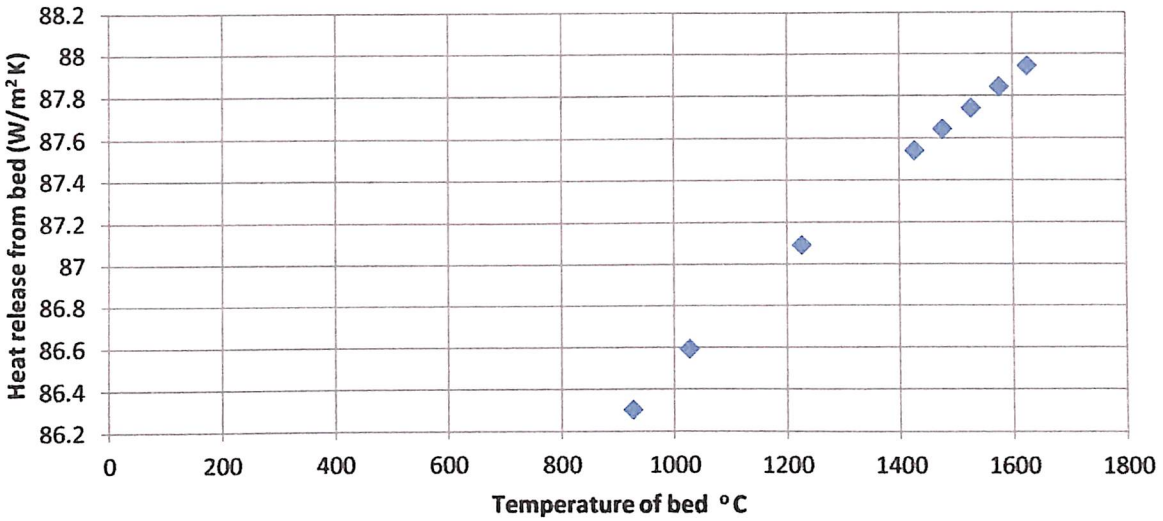

Fig. 4.8 Least variation of heat release from bed with corresponding bed temperature

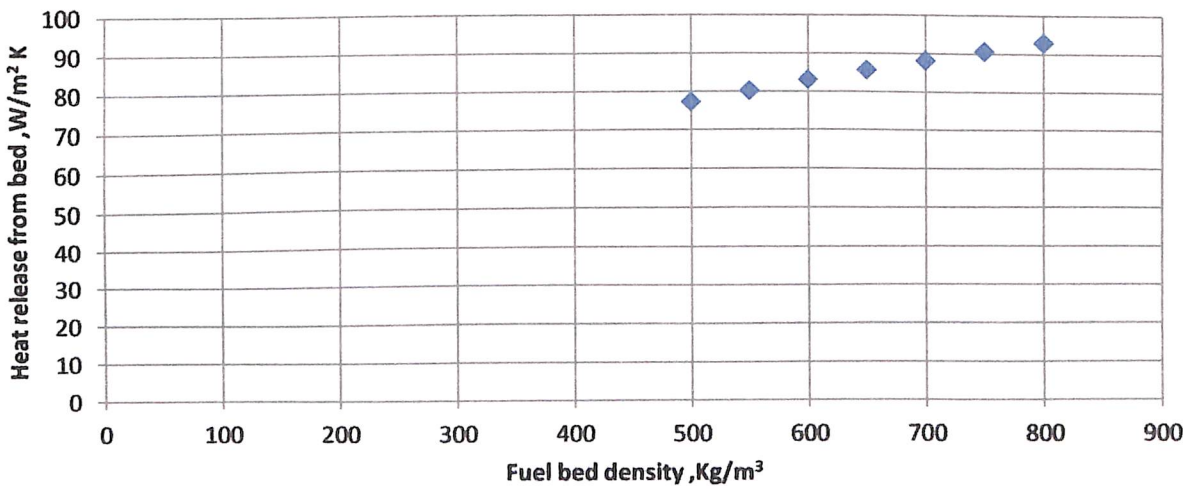

Fig. 4.9 Fuel bed density Vs. Fuel bed heat release to near furnace wall

Specific heat of air at 150 ° C (423 K) is calculated as follows

$Cp = a + b\,T + c\,T^2 + d\,T^3$

$= 28.11 + (0.1967\times 10^{-2} \times 423) + (0.4802 \times 10^{-5} \times 423^2) + (-1.966 \times 423^3)$

$= 29.65$ KJ / Kmol K

$= 29.65/28.97$ KJ/Kg K

$= 1.023$ KJ/Kg K

$c_{ha} = 1.023\ KJ/Kg^oC$

$t_{ha} = 150\,^\circ C$

$c_a = 1.004KJ/Kg^oC$

$t_a = 28^o\ C$

Fr = 0.72

m_f = 17055 Kg/hr

T_e = 1269.11 ° K

m_g = 7 kg/kg

c_e = 0.9623 kJ/kg ° C

t_e = 996.11 °C

$$NCV + m_{ha}\,(c_{ha}t_{ha} - c_a t_a) = \frac{20.53\,.Fr.BBSA}{m_f}\left[\left(\frac{T_e}{100}\right)\text{^}4 - \left(\frac{T_w}{100}\right)\text{^}4\right] + m_g\,(c_e\,t_e - c_a\,t_a)$$

$$15592 + 6.47(1.023\times150 - 1.004\times28) = \frac{20.53\times0.72\times3984}{17055}\left[\left(\frac{1269.11}{100}\right)\text{^}4 - \left(\frac{T_w}{100}\right)\text{^}4\right] + 7(0.962\times 996.11 - 1.004\times 28)$$

Solving the equation gives T_w value.

$$T_w = 1232.48^oK$$
$$= 959.48\,^oC$$

4.11 Non- Luminous Radiative Coefficient

The Non-luminous coefficient of flue gas is calculated as follows

Flue gas temperature in °C , $t_g = 996.11^o\ C$

Mean Beam Length (MBL) calculation

MBL for selected boiler dimension can be obtain by choosing the appropriate dimension ratio from table 4.10.

Table 4.10 Mean Beam Length for furnace dimension

S.no	Dimensional Ratio (length, width, height in any ratio)	Mean Beam Length(MBL) ,L (m)
	Rectangular Furnace	
1	1-1-1 to 1-1-3 1-2-1 to 1-2-4	2/3 × (Furnace Volume) $^{1/3}$
2	1-1-4 to 1-1-infinite	1 × smallest dimension
3	1-2-5 to 1-2-8	1.3 × smallest dimension
4	1-3-3 to 1-infinite-infinite	1.8 × smallest dimension
	Cylindrical furnace	
5	d × d	2/3 × diameter
6	d × 2d to d× infinite	1 × diameter

Furnace geometry of selected boiler is

Depth = 4.48 m

Width = 6.73 m

Height = 12.08 m

Ratio of dimension: 1.12 – 1.68 – 3.02

Therefore, Mean Beam Length (MBL) = 2/3 (Furnace Volume) $^{1/3}$

= $2/3\ (4.48 \times 6.73 \times 12.08)^{1/3}$

= 4.76 m

PH = 0.049

PC = 0.22

x = $MBL\ X\ [PH\ (Pc + PH)]^{0.5}$

= $4.76 \times [0.049\ (0.22 + 0.049)]^{0.5} = 0.546$

PX = $ao + a1x + a2\ x^2 + a3\ x^3 + a4\ x^4 + a5\ x^5$

= $(10.24) + (259.0015 \times 0.546) + (-521.4298 \times 0.546^{2}) + (583.8360 \times 0.546^{3}) + (-303.85 \times 0.546^{4}) + (58.10 \times 0.546^{5})$

= 67.055

$$h_{r-gas\ temp} = 4.1868\ P_x \left[\frac{t_g + 71.5 - 28.5\ \frac{\ln(\frac{x}{0.015625})}{ln2}}{1271.5 - 28.5\ \frac{\ln(\frac{x}{0.015625})}{ln2}} \right] KJ/m^2h^o\ C$$

$$h_{r\ 996.11} = 4.1868 \times 67.055 \left[\frac{996.11 + 71.5 - 28.5\ \frac{\ln(\frac{0.546}{0.015625})}{ln2}}{1271.5 - 28.5\ \frac{\ln(\frac{0.546}{0.015625})}{ln2}} \right]$$

$$h_{r\ 996.11} = 229.877\ KJ/m^2h^o\ C$$

Log mean temperature in °K, Tg = 1269.11 °K

Log mean wall temperature in °K, Tw = 1232.48 °K

Mean wall temperature in ° C , $t_w = 959.48^oC$

$$K_t = \left[\frac{126.11^4 - 1232.48^4}{1269.11^4 - 573^4}\right] \times \left[\frac{996.11 - 300}{996.11 - 959.48}\right]$$

$$= 2.186 \text{ (For wall temperature} < 300 \text{ ° C)}$$

For existing wall temperature 996.11 ° C

$$= (0.73 \times k_t - 0.719) \times \frac{(1100)^{0.25}}{t_g} + 1$$

$$= (0.73 \times 2.186 - 0.719) \times \frac{(1100)^{0.25}}{996.11} + 1$$

$$= 1.00506$$

Taking wall emissivity correction factor = 1

$$h_r = h_{r-gas\ temp} \times K_t \times K_E$$

$$h_r = 229.877 \times 1.00506 \times 1$$

$$= 231.88 \text{ KJ/m}^2\text{h °C or } 64.41 \text{ W/ m}^2 \text{ °C}$$

Non luminous Radiative coefficient is depend on flue gas temperature exist inside the furnace. Above calculation is carried out at FEGT where there is wide gap exist between AFT and FEGT. So let's see the behavior of non-luminous Radiative coefficient within this temperature range which is charted in table 4.11.

Table 4.11 Non-luminous radiative coefficient of flue gas

S.No	Temperature of gas inside furnace	Non-luminous Radiative coefficient (W/m^2 °C)
1	1627 ° C	108.18
2	1500 ° C	99.37
3	1400 ° C	92.44
4	1300 ° C	85.50
5	1200 ° C	78.57
6	1100 ° C	71.64

Its infer from the Fig.4.10 that there is considerable loss of non- luminous radiant coefficient with loss in temperature from flue gas

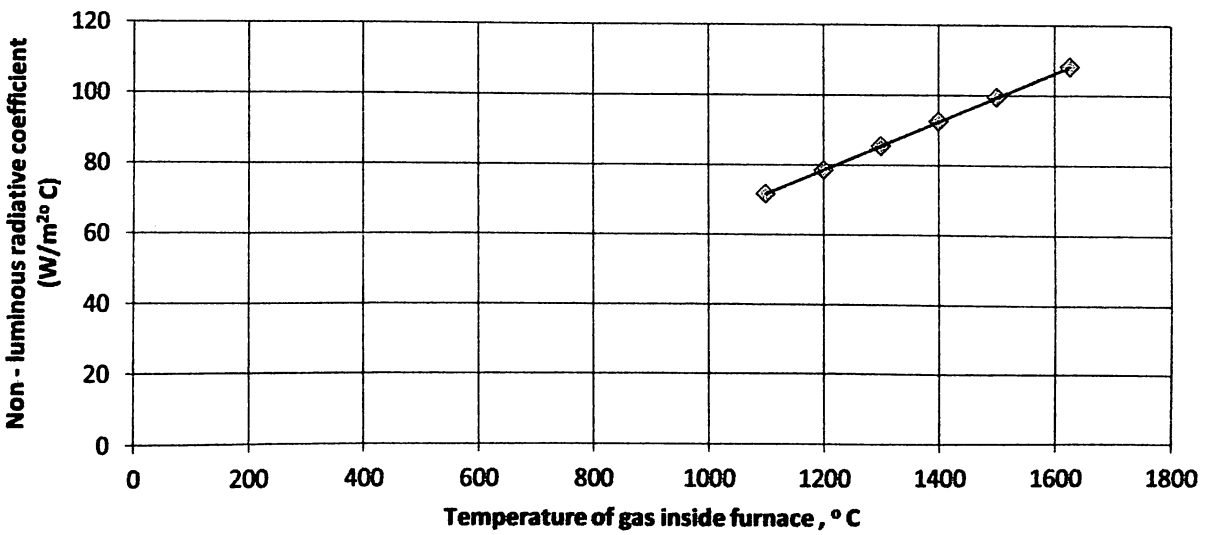

Fig. 4.10 Variation of Non-luminous radiant coefficient with gas temperature

4.12 Convective coefficient for cross flow

The convective coefficient of membrane wall, boiler bank, boiler screen, super heaters and economizer are calculated as follows

4.12.1 Film temperature

The property of flue gas is determined at film temperature

Log mean wall temperature in ° C , t_w = 959.58 ° C

Log mean gas temperature in ° C, t_g = 1000 ° C

Film temperature in ° C , t_f $= \frac{959.58+1000}{2}$

= 980 ° C

4.12.2 Flue gas mass flux

The mass flux or mass velocity of flue gas at super heaters, boiler bank screen, boiler bank and economizer are provided below form Fire Cad design at Annexure E.

Gas mass velocity of primary super heater, G = 3575.95 Kg/h m^2

Gas mass velocity of secondary super heater, G = 3218.71 Kg/h m^2

Gas mass velocity of boiler bank screen, G = 4706.35 Kg/h m^2

Gas mass velocity of boiler bank, G = 6788.46 Kg/h m^2

Gas mass velocity of economizer, G = 20500 Kg/h m^2

4.12.3 Specific heat

Specific heat of flue gas, °C at 980 ° C = 0.1688 Kcal / Kg ° C

= 0.706 KJ /Kg ° C

= 706 J / Kg ° C

4.12.3 Thermal Conductivity

The thermal conductivity of flue gas at operating gas temperature is as follows

Thermal conductivity of flue gas at 980 ° C, k = 0.0373 Kcal /h m ° C

= 0.156 KJ / h m ° C

= 4.33×10^{-5} KJ/s m ° C

= 0.0433 W /m ° C

4.12.4 Viscosity

Viscosity of flue gas at 980 ° C,μ = 0.0473 Cp (Dynamic viscosity)

(Kinematic Viscosity) = 0.0473×10^{-3} Kg / m s

Convective coefficient for cross flow is

$$h_c = K \cdot D^{-0.4} \cdot G^{0.6} \cdot c^{0.33} \cdot \mu^{-0.27} \cdot k^{0.67}$$

4.12.5 Convective coefficient for primary super heater

Outer diameter OD of membrane tube, D = 50.80 mm

= 50.80×10^{-3} m

K = 0.287 (Inline tube arrangement)

$$h_c = (0.287)(50.80 \times 10^{-3})^{-0.4}(0.9933)^{0.6}\,(706)^{0.33}\,(4.73 \times 10^{-5})^{-0.27}\,(0.0433)^{0.67}$$

= 14.72 W / m^2 ° C

4.12.6 Convective coefficient for secondary super heater

Outer diameter OD of membrane tube, D = 44.50 mm

= 44.50×10^{-3} m

K = 0.287 (Inline tube arrangement)

$$h_c = (0.287)(44.50 \times 10^{-3})^{-0.4}(0.8940)^{0.6}\,(706)^{0.33}\,(4.73 \times 10^{-5})^{-0.27}\,(0.0433)^{0.67}$$

= 14.57 W / m^2 ° C

4.12.7 Convective coefficient for boiler bank screen

Outer diameter OD of membrane tube, D = 76.20 mm

= 76.20×10^{-3} m

K = 0.302 (Staggered tube arrangement)

$$h_c = (0.302)(76.20 \times 10^{-3})^{-0.4}(1.3073)^{0.6}\,(706)^{0.33}\,(4.73 \times 10^{-5})^{-0.27}\,(0.0433)^{0.67}$$

$= 15.54\ W/m^2\,^\circ C$

4.12.8 Convective coefficient for Boiler bank

Outer diameter OD of membrane tube, D = 50.80 mm

= 50.80×10^{-3} m

K = 0.287 (Inline tube arrangement)

$$h_c = (0.287)(50.80 \times 10^{-3})^{-0.4}(1.8856)^{0.6}\,(706)^{0.33}\,(4.73 \times 10^{-5})^{-0.27}\,(0.0433)^{0.67}$$

$= 21.63\ W/m^2\,^\circ C$

4.12.9 Convective coefficient for economizer

Outer diameter OD of membrane tube, D = 50.80 mm = 50.80×10^{-3} m

K = 0.287 (Inline tube arrangement)

$$h_c = (0.287)(50.80 \times 10^{-3})^{-0.4}(5.6944)^{0.6}\,(706)^{0.33}\,(4.73 \times 10^{-5})^{-0.27}\,(0.0433)^{0.67}$$

$= 41.99\ W/m^2\,^\circ C$

Over the range of wide temperature difference, the conductivity, viscosity and specific heat remain constant. So the convective coefficient for cross flow highly dependent on mass flux of flue gas and outer diameter of tube. But the outer diameter for existing boiler can't be changed; it has to handle at design stage itself. Here the mass flux of flue gas plays a critical role in deciding the convective coefficient which is proportional to quantity of fuel fired.

The effect of tube diameter in convective coefficient is presented in table 4.12.

Table 4.12 Primary Super Heater tube diameter Vs. Convective Coefficient

S.No	Tube OD for Primary Super Heater, mm (Inline arrangement)	Convective Coefficient, $W/m^2\,^oC$
1	50.8 (actual OD)	14.72
2	50	14.82
3	49	14.94
4	47	15.19
5	45	15.45
6	40	16.20
7	35	17.09

It's observed from Fig.4.11 that with about 30 % reductions in OD of superheater, the convective coefficient tends to increase about 14 %. So these functional behaviors have to take care while designing the OD of superheater for efficient energy transfer and also it seems the convective coefficient get reduce with the boiler loading. As the fuel firing rate reduces, the mass flux of flue gas also gets down and it will result in reduced convective coefficient.

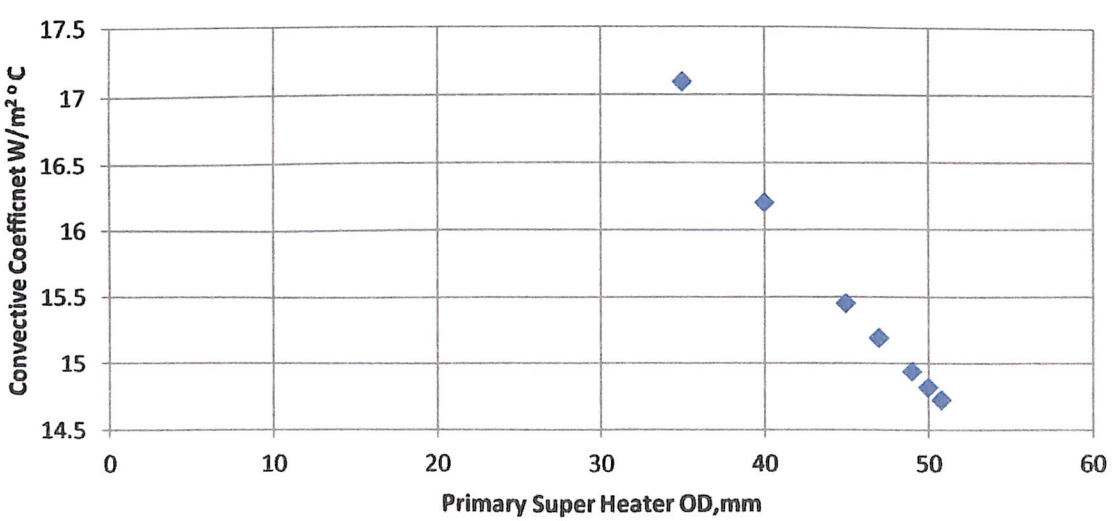

Fig. 4.11 Primary super heater tube OD vs. Convective Coefficient

4.13 Determining internal heat transfer coefficient of air preheater

$$h_i = 0.023\, d^{-0.2}\, k^{0.6} G^{0.8} c^{0.4} \mu^{-0.4}$$

Thermal conductivity, k = 0.043 W/m ° C

Gas mass flux tube side, G = 8.4120 Kg / m^2s (30283 Kg/h m^2 from Annexure E)

Specific heat, c = 706 J /Kg ° C

Dynamic Viscosity, μ = 4.73× 10^{-5} Kg/ m s

Internal heat transfer coefficient can be applicable to air preheater.

OD = 63.50 mm

Tube thickness = 2.03 mm

Internal diameter, d = 63.50 – 2.03 = 61.47 mm

= 61.47 × 10^{-3} m

$$h_i = 0.023\,(61.47 \times 10^{-3})^{-0.2}\,(0.043)^{0.6}(8.4120)^{0.8}(706)^{0.4}(4.73 \times 10 - 5)^{-0.4}$$

= 24.74 W / m ° C

Table 4.13 Air preheater internal tube diameter Vs. Internal Heat transfer Coefficient

S.No	Tube internal diameter for air preheater, mm	Internal heat transfer coefficient, W/m^2 ° C
1	61.47 (Existing)	24.74
2	60	24.86
3	59	24.95
4	58	25.03
5	57	25.12
6	55	25.30

The variation of internal heat transfer coefficient with tube internal diameter is shown in table. It's observed from Fig 4.12 that, with 10 % reduction in air preheater OD, the internal heat transfer coefficient raise only by about 2.3 %.So here design parameter doesn't cause much impact on heat transfer mechanism. Here, the heat transfer is purely the function of mass velocity of flue gas.

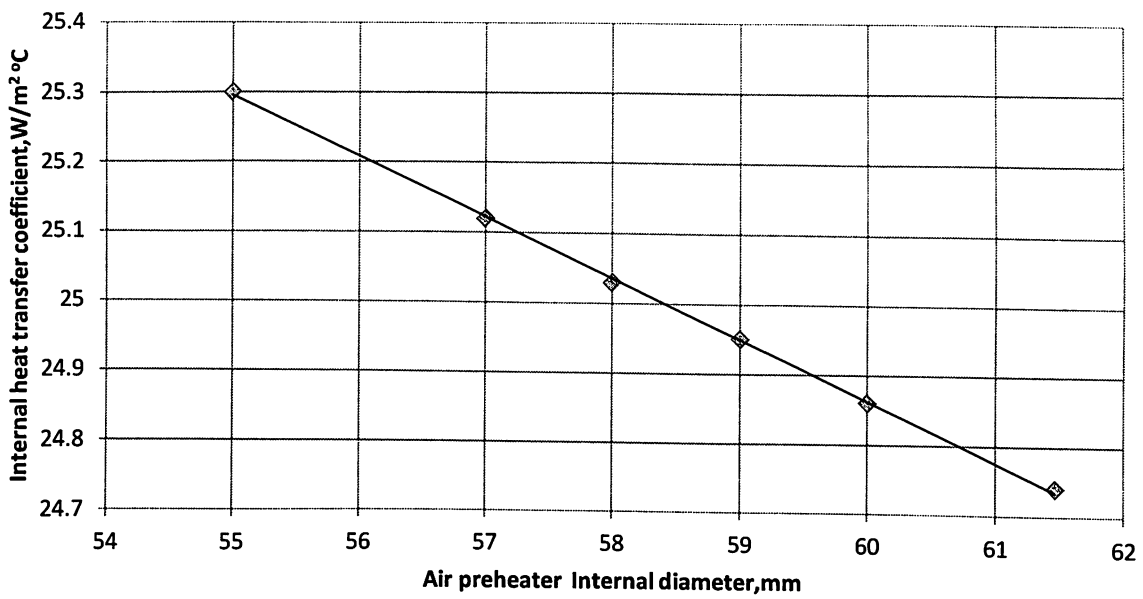

Fig. 4.12 Air preheater internal diameter Vs. Internal heat transfer coefficient

4.14 Determining heat transfer to cavity wall

The heat transfer to cavity wall from flue gas is calculated as follows

Hydraulic diameter, Dh

$$= 4 \times \left[\frac{Volume\ of\ furnace, m^3}{Peripheral\ Surface\ area\ of\ furnace, m^2}\right]$$

$$= 4 \times \left[\frac{4.48 \times 6.73 \times 12}{30.20}\right] = 48 \text{ m}$$

Flue gas mass flux, G	=	3300	Kg / hr m^2
Dynamic Viscosity, μ	=	4.73×10^{-5}	Kg/ m s
Specific heat, Cp	=	0.706	KJ /Kg ° C

$$h_c = 0.161\, D_h^{-0.2}\; G^{0.8}\, \mu^{0.2}\, c_p$$

$$h_c = 0.161 \times 48^{-0.2}\; 3300^{0.8}\, (4.73 \times 10 - 5)^{0.2}\, 0.706$$

= 4.66 KJ / h m^2 ° C or

= 1.29 W/m^2 ° C

4.15 Radiative heat transfer

The radiative heat transfer inside the furnace is established in following calculation, also the convective heat transfer is included.

Average temperature of bed surface, T_b	=	1523	K (1250 ° C)
Average temperature of water wall, T_w	=	1232.48	K (959.48 ° C)
Average temperature of furnace gases, T_g	=	1273	K (1000 ° C)
Fuel bed area, R = 6.73 m × 4.48 m	=	30.15	m^2
Surface area of heat transfer (water wall), H	=	3984	m^2
Stefan-Boltzmann constant, σ	=	5.67×10^{-8} W/m^2 K^4	
Emissivity of bed, ε_{bed}	=	0.95	
Emissivity of wall, ε_{eff}	=	1	
Emissivity of furnace gas, ε_g	=	0.45	
Absorptivity of furnace gas, a_g	=	0.2	

4.15.a Radiation received by water wall tubes from fuel bed

$$q_b = \sigma\, \varepsilon_{bed}\, (T_b^4 - T_w^4) R/H$$

$$= 5.67 \times 10^{-8} \times 0.95\,(1523^4 - 1232.48^4) \times \frac{30.15}{3984}$$

$= 1253$ W / m^2

4.15.b Radiation from flue gas

$$q_{rad} = \sigma\, \varepsilon_{eff}\, (\varepsilon_g T_g^4 - a_g T_w^4)$$

$$= 5.67 \times 10^{-8} \times 1 \times (0.45 \times 1273^4 - 0.2 \times 1232.48^4)$$

$= 40839.59$ W /m^2

4.15.c Convective heat transfer

Average convective heat transfer coefficient, h = 30 W / m^2 °C

$$q_c = h \times (T_g - T_w)$$

$$= 30 \times (1000 - 960)$$

$= 1200$ W/m^2

Total average heat flux absorbed by water wall = (1253 + 40839.59 + 1200) W/m^2

$= 43292.59$ W/m^2

$= 43.29$ KW/m^2

4.16 Pressure Drop across fuel bed

The pressure drop across the fuel bed is produced in following calculations

$$\frac{\Delta P}{L} = 150\, \frac{(1-\varepsilon)^2}{\varepsilon^3}\, \frac{\mu\, U}{(\emptyset\, d_p)^2} + 1.75\, \frac{(1-\varepsilon)}{\varepsilon^3}\, \frac{\rho_g\, U^2}{\emptyset d_p}$$

For wood piece of size 6 cm long and 5 cm diameter

ε = 0.70

$\emptyset$ = 1.23

μ = 1.13×10^{-5} Kg/m s at 150 ° C

ρ_g = 2.33 Kg/m3 for inlet air at 150 ° C

U = 2 (m/s)

dp = 0.075 m

$$\frac{\Delta P}{L} = 150 \frac{(1-0.70)^2}{0.70^3} \frac{1.13 \times 10-5 \times 2}{(1.23 \times 0.075)^2} + 1.75 \frac{(1-0.70)}{0.70^3} \frac{2.33 \times 2^2}{1.23 \times 0.075}$$

= 157.93 N/m^2 per meter of fuel bed depth

(or)

= 15.73 mm of WC per meter of fuel bed depth

The pressure drop across the fuel bed in grate is calculated at wide range of primary air velocity and whose results are tabulated in table 4.14.

Fig.4.13 shows with increase in velocity, the pressure drop across the fuel bed also increase correspondingly which is due to the assumption that the void of the fuel bed will remain constant throughout the combustion process, but in actual condition once the primary air started supplying below the grate, due to its force of lifting, disturbance of fuel bed will occur which will change the void fraction of bed with respect to supplying velocity. So the pressure drop also changes considerably. But over certain level of velocity, the void fraction tend to stay remain closely (Fig 4.18) which results in close values of fuel bed pressure drop with increasing velocity which is shown in Fig. 4.14.

Fig.4.15 shows the variation of bed void fraction with respect to primary air velocity

Table 4.14 Pressure drop across fuel bed in grate with initial staged void value

Length (cm)	**Diameter (cm)**	**Void, ε**	**Pressure drop ΔP/L, mm of WC per meter of fuel bed height**														
			Velocity (m/s)														
			1	***2***	***3***	***4***	***5***	***6***	***7***	***8***	***9***	***10***	***11***	***12***	***13***	***14***	***15***
6	5	0.70	4	15.7	35.4	62.9	98.3	141	192	251	318	393	476	566	665	771	885
	4	0.65	7.7	30.8	69.4	123	192	277	378	493	625	771	933	1111	1304	1512	1736
	3	0.54	26	104	234	415	649	934	1272	1662	2103	2596	3141	3738	4387	5088	5840
	2	0.45	92	370	830	1476	2305	3319	4516	5898	7464	9214	11149	13267	15576	18056	20727
	1	0.30	1023	4040	9049	16052	25048	36037	49019	63999	80963	99924	120879	143827	168768	195702	224629
5	5	0.68	4.3	17.2	38.7	69	108	155	211	276	349	430	521	620	727	843	968
	4	0.63	8.4	33	75	134	210	303	413	539	682	843	1020	1214	1424	1652	1896
4	4	0.50	21.2	85	190	338	530	761	1036	1354	1713	2115	2560	3046	3575	4146	4760
	3	0.35	118	472	1060	1884	2944	4239	5769	7534	9535	11771	14243	16949	19891	23069	26481
3	3	0.30	183	733	1647	2928	4574	6586	8964	11707	14815	18290	22129	26335	30906	35843	41145
2	2	0.30	276	1100	2474	4395	6866	9884	13450	17566	22230	27442	33202	39511	46368	53775	61729

Table 4.14 is the pressure drop values across the bed with the assumption that the void volume will remain constant with respect to fuel size. But in actual the void volume keeps changes with respect to superficial gas velocity i.e. inlet air velocity due to its fluidization effect which is govern by the simple empirical relation

$$Void\ , \varepsilon = \frac{U+1}{U+2}$$

Table 4.15 Pressure drop across fuel bed in grate with varied void value with respect to varying primary air velocity

Length (cm)	**Diameter (cm)**	**Pressure drop ΔP/L, mm of WC per meter of fuel bed height with varying voidage**														
		Velocity (m/s)														
		1	***2***	***3***	***4***	***5***	***6***	***7***	***8***	***9***	***10***	***11***	***12***	***13***	***14***	***15***
6	5	5	10.6	15.8	20.7	25.5	30.2	34.8	39.4	44	48.6	53.2	57.7	62.3	66.8	71.3
	4	7	14.3	21.2	27.9	34.3	41	47	53	59.3	65	72	78	84	90	96
	3	10	21	31.2	41	50.3	60	69	78	87	96	105	114	123	132	141
	2	17	36	54	70	87	102	118	114	150	165	180	196	211	227	242
	1	44	92	135	177	218	258	298	338	377	416	455	494	533	572	610
5	5	5	10	15	19	24	28	33	37	42	46	50	54	59	63	67
	4	7	14	20	26	32	38	44	50	55	62	67	73	79	85	91
4	4	6	13	19	24	30	35.5	41	46	52	57	63	68	73	79	84
	3	9	18	27	36	44	52	60	68	76	84	92	100	107	155	123
3	3	8	17	25	33	40	47.3	54.6	62	69	76	83	91	98	105	112
2	2	11.9	25.1	37.2	48.7	60	71	82	92.8	103	114	125	136	147	157	168

Table 4.16 shows the voidage will remain same for all the fuel size, because the void equation governs only with the velocity.

Table 4.16 Behavior of void fraction with respect to primary air velocity in fuel bed

Velocity (m/s)	1	2	3	4	5	6	7	8	9	10	11	12	13	14	15
Void ,ε	0.66	0.75	0.80	0.83	0.85	0.87	0.88	0.90	0.90	0.91	0.92	0.92	0.93	0.93	0.94

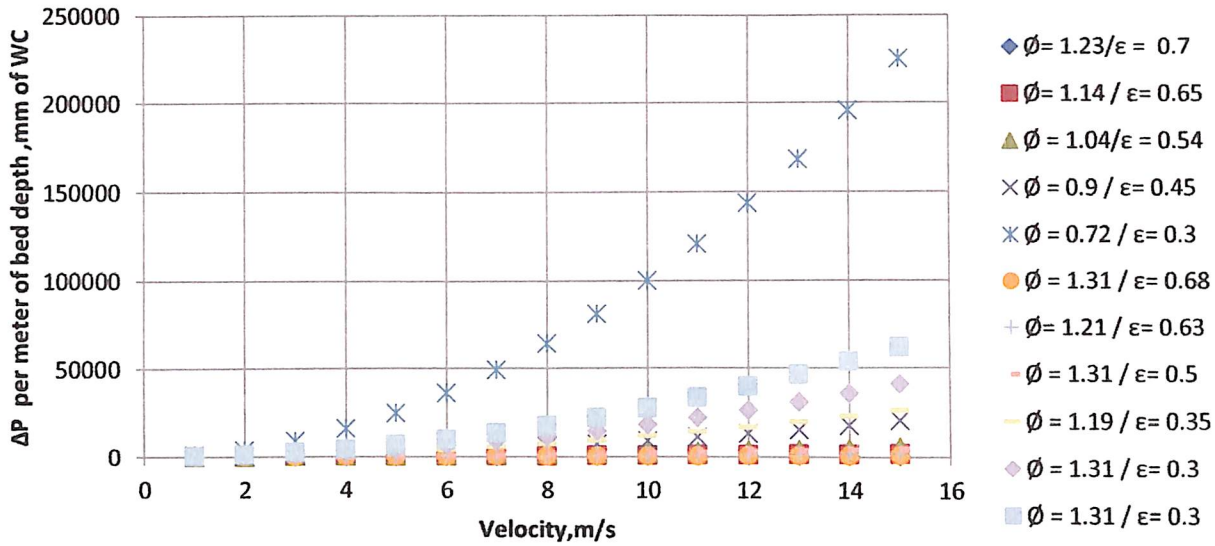

Fig. 4.13 Pressure drop in fuel bed with initial staged void value of wood particle

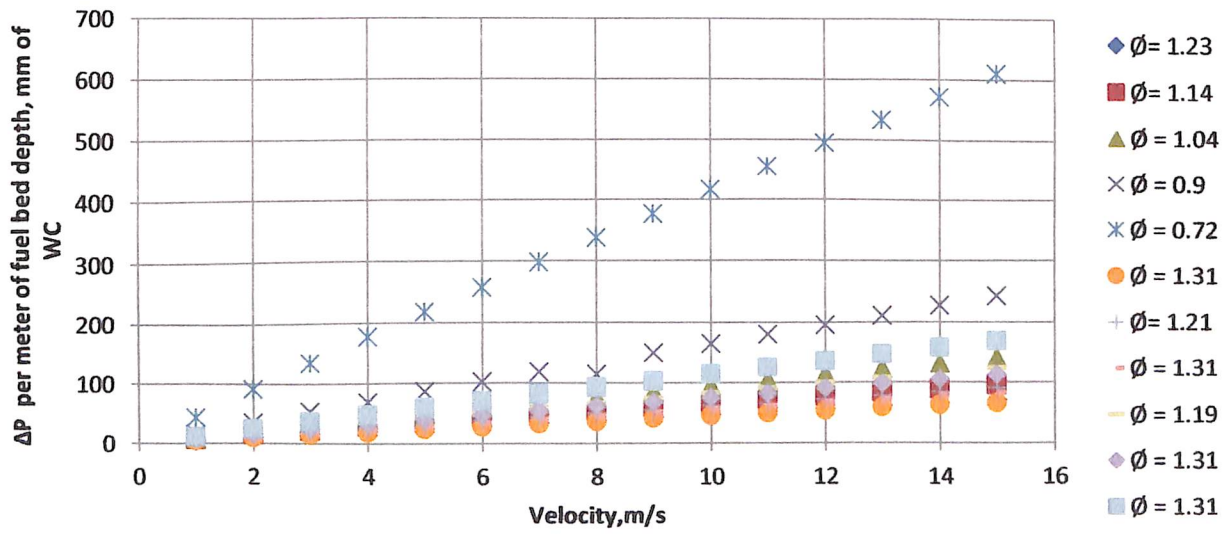

Fig. 4.14 Pressure drop in fuel bed with varying void value with respect to primary air velocity

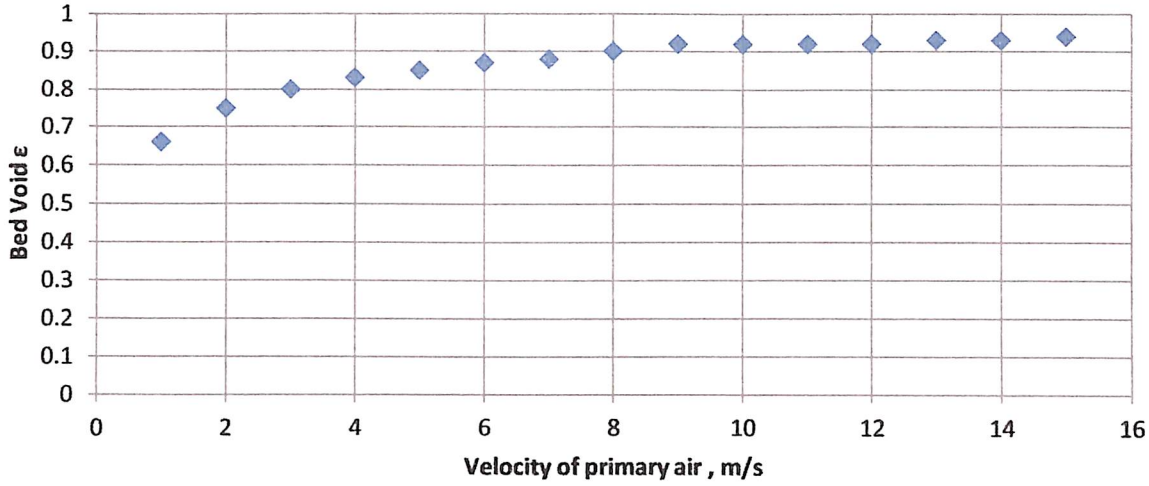

Fig. 4.15 Bed void fraction Vs. Velocity of primary air

Thus the velocity of primary air plays the important role in providing the turbulence to the fuel bed which will results in enhanced combustion. So the customized pressure drop of about 3mm to 5mm of WC of H_2O per mm of fuel bed depth is maintained in order to ensure the uniform air distribution and absence of blow holes created in the bed in grate.

Summary and Conclusions

CHAPTER V

SUMMARY AND CONCLUSIONS

In this chapter the result obtained from the study are summarized and conclusion is drawn based on the results.

At various range of primary air pressure, the burning rate increase tremendously with respect to increase in pressure. But as the aspect of biomass reduces, the steepness of burning rate curve begins to lower. So both the biomass aspect and primary air pressure have its own role in deciding the burning rate of particle. For a particular size of biomass piece, the burning rate of fuel in the boiler grate can be varied by increasing the impinging pressure of the primary air which is achieved by passing the air from air box below the grate at various velocities. By doing this, good turbulence is provided to fuel bed combustion which may result in less requirement of excess air also.

Over wide temperature range of the fuel bed (i.e. 1900 K to 1200 K), the heat release rate from bed doesn't vary greatly i.e. the change is between 87.94 $W/m^2 K$ to 86.30 $W/m^2 K$ which is very less difference. So the only deciding factor of heat release rate from fuel bed is average fuel bed density which depends on void fraction or size of fuel selected where the change in heat release is observed between 92.8 $W/m^2 K$ to 77.27 $W/m^2 K$ when the fuel bed density vary from 800 to 500 Kg / m^3

The Non-Luminous radiative coefficient is the way of heat transfer to super heater from radiation of tri molecule especially H_2O and CO_2 in flue gas. It's observed from the study that, with maintaining the temperature of flue gas loss at considerable range, the effect of heat transfer by non-luminous radiative coefficient is high. But, once the loss of heat from boiler surface is high, considerable reduction in non-luminous radiative coefficient is observed which affects the heat transfer especially in primary and secondary super heater. For a case at flue gas temperature of 1627 ° C the coefficient value is 108.18 W/m^2 °C, but when the temperature falls to 1100 ° C, the non-luminous coefficient value is 71.64 W/m^2 °C.

The convective coefficient tends to increase about 14 % with about 30 % reductions in OD of superheater. The convective coefficient ranges from 14.72 to 17.09 W/m^2 ° C when the

primary super heater OD reduces from 50.8 mm to 35 mm and the same coefficient tends to reduce with reduction in fuel firing rate. The flue gas mass flux reduces with reduction in fuel firing rate which contributes to fall in convective coefficient value.

From the study of internal heat transfer coefficient with tube internal diameter of air preheater, it's observed that, with 10 % reduction in superheater OD, the internal heat transfer coefficient raise only by about 2.3 %.So here it doesn't have much impact on heat transfer mechanism with respect to sizing of super heater tube. Internal heat transfer coefficient is variable with respect to flue gas mass velocity inside the tube.

The cavity wall heat transfer is observed as 1.29 W/m^2 ^{o} C which is also the function of gas mass velocity.

Out of total heat absorbed by the water wall in the furnace, the radiative heat transfer contributing the major percentage of heat transfer. The selected boiler design receives about 43.29 KW/m^2 of water wall area out of which nearly 30-40 KW/m^2 is received by heat radiation mainly from flue gas and from fuel bed as well as flame.

With increase in velocity, the pressure drop across the fuel bed also increase correspondingly which is due to the assumption that the void of the fuel bed will remain constant throughout the combustion process, but in actual condition once the primary air started supplying below the grate, due to its force of lifting, disturbance of fuel bed will occur which will change the void fraction of bed with respect to supplying velocity. So the pressure drop also changes considerably. But over certain level of velocity, the void fraction tend to stay remain closely which results in close value of bed pressure drop with increasing velocity.

The velocity of primary air plays the important role in providing the turbulence to the fuel bed which will results in enhanced combustion. So the standard pressure drop of about 3mm to 5mm of WC per mm of fuel bed depth is maintained in order to ensure the uniform air distribution and absence of blow holes created in the bed in grate.

For a case, the wood piece of 6 cm long and 3 cm diameter have well defined customized pressure drop between 3mm to 5 mm of WC per mm of fuel bed depth between 11 m/s to 15 m/s velocity. As the wood piece goes down from the above size (Say 2mm), the pressure drop across

the bed increases to about 60 mm of WC per mm of fuel bed at maximum velocity of 15 m/s. So the particle size is chosen based on the estimated pressure drop to have the undisturbed combustion on the furnace grate.

When the pressure drop is high, it shows that the wood pieces are loaded unevenly or overloaded .Both the condition will result in reduction of turbulence on fuel particle which leads to the deposition and cover up of ash on the fuel bed which may sometime lead to fall of fuel bed temperature or even quench the fire at some portion of bed by blocking the passage of oxygen for combustion and very minimal pressure drop also sometimes lead to blow holes creation or quenching of flame on fuel bed too.

The following recommendations are made for future work of research area

a. Fluidized combustion of biomass is the effective method than grate fired system. The incorporation of the same system in grate fired boiler with charcoal as the fluidizing medium will provide better combustion and overall improvement in grate boiler performance with lower emission.
b. The above said fluidization principle can be look for adopting in batch feed grate fired fuel bed .But even partial achievement of fluidization on fuel bed with charcoal as medium may result in enhanced combustion.
c. The heat transfer coefficient determined in this study is based on the model developed, but in actual these coefficient values will differ because of deposition of ash and other minerals on the heating surface over the period of time. These heat transfer barrier analysis have to consider in detail while designing and determining the heat transfer mechanism inside the furnace.

References

REFERENCES

Report on "Renewable Energy in India: Progress, Vision and strategy" by Ministry of New and Renewable Energy (MNRE), Govt of India; March 2011.

Energy efficiency in thermal utilities book II, Boiler, Chapter 2, Bureau of Energy Efficiency (BEE) under Ministry of Power, Govt of India; 2005.

Sridharan S. Boiler for firing renewable fuels. Paper published in BEE; 2008.

Yang YB, Sharif VN ,Swithenbank J. Effect of air flow rate and fuel moisture on the burning behaviours of biomass and simulated municipal solid wastes in packed beds. Fuel 83 (2004) 1553–1562;2004.

Yang YB, Ryu C,Khor A,Yates NE,Sharifi VN,Swithenbank J. Effect of fuel properties on biomass combustion.Part II.Modelling approach-identification of controlling factor;2005.

Gort R. On the propagation of a reaction front in a packed bed: thermal conversion of municipal waste and biomass. Academic Dissertation, University of Twente; 1995.

Goh YR, Siddall RG, Nasserzadeh V, Zakaria R, Swithenbank J, Lawrence D, Garrod N, Jones B. Mathematical modelling of the waste incinerator burning bed. J Inst Energy 1998.

Goh YR, Lim CN, Chan KH, Zakaria R, Reynolds G, Yang YB, Siddall RG, Nasserzadeh V, Swithenbank J. Mixing, modelling and measurements of incinerator bed combustion. The Second International Symposium on Incineration and Flue Gas Treatment Technology, Sheffield, UK; 4–6 July 1999.

Zakaria R, Goh Y, Yang Y, Lim C, Goodfellow J, Chan K, Reynolds G, Ward D, Siddall R, Nasserzadeh V, Swithenbank J. Reduction of NOx emission from the burning bed in a municipal solid waste incinerator. The Fifth European Conference on Industrial Furnaces and Boilers, Espinho-Porto-Portugal; 11–14 April 2000.

Ro¨nnba¨ck M, Axell M, Gustavsson L. Combustion processes in a biomass fuel bed—experimental results. Progree in Thermochemical Conversion, Tyrol, Austria; 17–22 September 2000.

Sharifi VN. Optimization study of incineration in a MSW incinerator with a vertical radiation shaft. PhD Thesis. Sheffield University; 1990.

Beckmann M, Scholz R, Wiese C, Busch M, Peppler E. Gasification of waste materials in grate systems. The Fourth European Conference on Industrial Furnaces and Boilers (INFUB), Espinho-Porto-Portugal; 1–4 April 1997.

Thunman H, A ° mand L-E, Ghirelli F, Leckner B. Modelling and verifying experiments on the whole furnace. In: Thunman H, editor. Principles and models of solid fuel combustion. Go¨teborg, Sweden: Chalmers University of Technology; 2001.

Yang YB, Nasserzadeh V, Goodfellow J, Goh YR, Swithenbank J. Parameter study on the incineration of municipal solid waste fuels in packed beds. J Inst Energy 2002;September.

Yang YB, Yamauchi H, Nasserzadeh V, Swithenbank J. Effects of fuel devolatilisation on the combustion of wood chips and incineration of simulated municipal solid wastes in a packed bed. Fuel 2001;82: 2205–21.

Peters B. Thermal conversion of solid fuels. WIT Press; 2003.

Shin D, Choi S. The combustion of simulated waste particles in a bed.Combust Flame 2000;121:167–80.

Adams T. A simple fuel bed model for predicting particulate emissions from a wood waste boiler. Combust Flame 1980;39: 225–39.

Stapf M, Kircherer A, Kolb Th, Wo¨lfert A, Seifert H. Verbrennung im Drehrohrofen: Modellierung, Betriebs—und Technikumsversuche. Volume 15 of VDI-Berichte 1313, Du¨sseldorf: VDI-Verlag; 1997.

Beckmann M, Scholz R. Simplified mathematical model of combustion in stoker systems. The Third European Conference on Industrial Furnaces and Boilers. Porto, Potrugal; 1995. p. 61–70.

Wurzenberger JC. A combined packed bed and single particle model applied to biomass combustion. PhD thesis, Graz University of Technology; 2001. 19. Peters B. A detailed model for devolatilization and combustion of waste material in packed beds. The Third European Conference on Industrial Furnaces and Boilers (INFUB). Lisbon, Portugal; 18–21 April 1995.

Thunman H, Leckner B. Ignition and propagation of a reaction front in cross-current bed combustion of wet biofuels. Fuel 2001;80: 473–81.

Stephen R.Turn. An Introduction to Combustion - concept and application, Second Edition, The Pennsylvania university, USA; McGraw-Hill; 2000.

Wei Dong, Design of advanced industrial furnaces using numerical modeling method, Royal Institute of technology, Stockholm, Sweden, 2000.

Prabir Basu .Combustion and gasification in fluidized beds. Technical University of Nova Scotia, Halifax, CRC/Taylor & Francis, 2006, ISBN 0849333962, 9780849333965.

N Magasiner , C Van Alphen , MB Inkson and BJ Misplon. Characterizing Fuels For Biomass - Coal Fired Co-Generation. Proc S Afr Sug Technol Ass (2001) 75: page 285.

Neil Jhonson (2002). Fundamentals of Stoker Fired Boiler Design and Operation. CIBO Emission Controls Technology Conference July 15 - 17, 2002

David Palmer (2010).Principles and fundamentals of biomass boiler system design .Carbon Trust presentation March 17, 2010.

Boiler operators handbook. National Industrial Fuel Efficiency Service - NIFES (Great Britain).Edition 2, revised, illustrated. Springer, 1989.ISBN 1853332852.

Prabir basu, Kefa cen,Louis Jestin. Boilers and burners: design and theory. Springer 2000.ISBN 0387987037

Kumar D.S, Heat and mass transfer text book,S.K .Kataria and Sons publication,Seventh edition 2009

H Vernbanck (1997). Development Of A Mathematical Model For Watertube Boiler Heat Transfer Calculations. *Proc* S *Afr Sug Technol Ass* (1997) *71:166-171*

B.Ya.Kamenetskii (2008).Calculation of heat transfer in boiler furnace during firing of fuel in a bed.ISSN 0040-6015,Thermal engineering,2008,Vol.55,pp.442-445© Pleiades publishing ,Inc.,2008.

Annexure

ANNEXURE A

Physical features of Grate boiler

S.No	Characteristics	Values
1	Height of bed or fuel burning zone (m)	0.2
2	Superficial velocity (m/s)	1 – 2
3	Excess air (%)	20 – 30
4	Grate heat release rate (MW/m^2)	0.5 – 1.5
5	Fuel size (mm)	32 – 6
6	Turndown ratio	4:1
7	Combustion efficiency (%)	85 – 90
8	Overall voidage	0.4 – 0.5
9	Typical bed to surface heat transfer coefficient (W/m^2 K)	50 – 150

ANNEXURE B

Design Velocities: Range of Velocities Generally Used in Boilers

S.No	Nature of Service	Range of design velocity (m/s)
	Air	
1	Air Heater	5-25
2	Coal and airline ,pulverized coal	15 – 23
3	Compressed air line	7.5-10
4	Forced draft Ducts	7.5 – 18
5	Forced draft ducts, entrance to burner	7.5 – 10
6	Register grill	1.5 – 3
7	Ventilation duct	5 – 15
	Flue gas	
8	Air heater	5 – 25
9	Boiler back -pass	12- 25
10	Induced draft flues and breeching	10 -18
11	Stacks and chimneys	10 – 25
	Steam lines	
12	High pressure	40 – 60
13	Low pressure	60 – 75
14	Vacuum	100 – 200
15	Super heater	10 - 25
	Water	
16	Boiler circulation	0.35 – 3.5
17	Economizer tubes	0.75 – 1.5
18	Water line , general	2.5 – 40

ANNEXURE C

Binary diffusion coefficient at 1 atmosphere pressure

S.No	Substance A	Substance B	T(K)	$D_{AB\ 10^5}\ (\frac{m^2}{s})$
1	Benzene	Air	273	0.77
2	Carbon dioxide	Air	273	1.38
3	Carbon dioxide	Nitrogen	293	1.63
4	Cyclohexane	Air	318	0.86
5	n- Decane	Nitrogen	363	0.84
6	n-Dodecane	Nitrogen	399	0.81
7	Ethanol	Air	273	1.02
8	n-Hexane	Nitrogen	288	0.757
9	Hydrogen	Air	273	0.611
10	Methanol	Air	273	1.32
11	Water	Air	273	2.2

ANNEXURE D

Specific Heat of Gases

Substance	Formula	Molecular Weight (Kg/Kmol)	a	b ($\times 10^{-2}$)	c ($\times 10^{-5}$)	d ($\times 10^{-9}$)	Temperature Range (K)
Nitrogen	N_2	28	28.9	-0.1571	0.8081	- 2.873	273 - 1800
Oxygen	O_2	32	25.48	1.520	-0.7155	1.312	273 – 1800
Air		28.97	28.11	0.1967	0.4802	- 1.966	273 – 1800
Hydrogen	H_2	2	29.11	- 0.1916	0.4003	- 0.8704	273 – 1800
Carbon monoxide	CO	28	28.16	0.1675	0.5372	- 3.595	273 – 1800
Carbon dioxide	CO_2	44	22.26	5.981	- 3.507	7.469	273 – 1800
Water Vapor	H_2O	18	32.24	0.1923	1.055	- 3.595	273 – 1800
Nitrous di oxide	N_2O	44	24.11	5.8632	- 3.562	10.58	273 – 1500
Nitrogen dioxide	NO_2	46	22.9	5.715	- 3.52	7.87	273 - 1500
Sulfur dioxide	SO_2	46	25.78	5.795	- 3.182	8.612	273 - 1800

ANNEXURE E

Design of Grate Fired Boiler using FIRE CAD Tool - Input Data

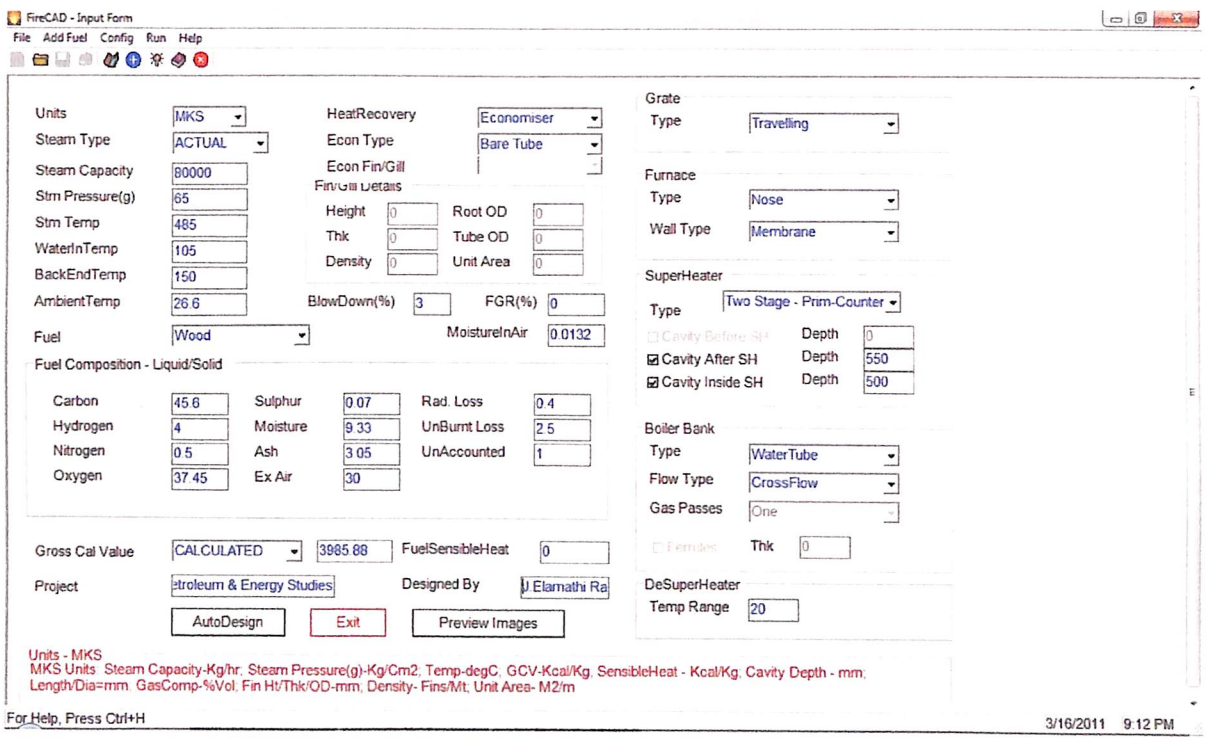

Furnace Design Details – Output Screen

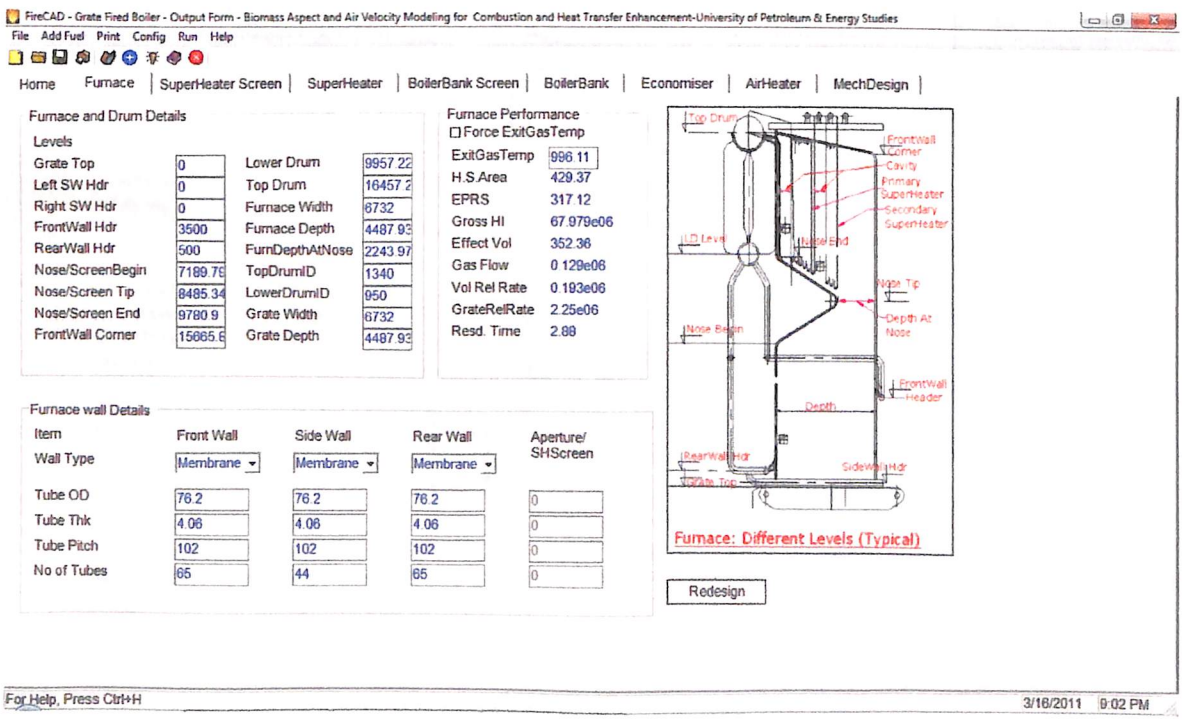

Super Heater Design – Output Screen

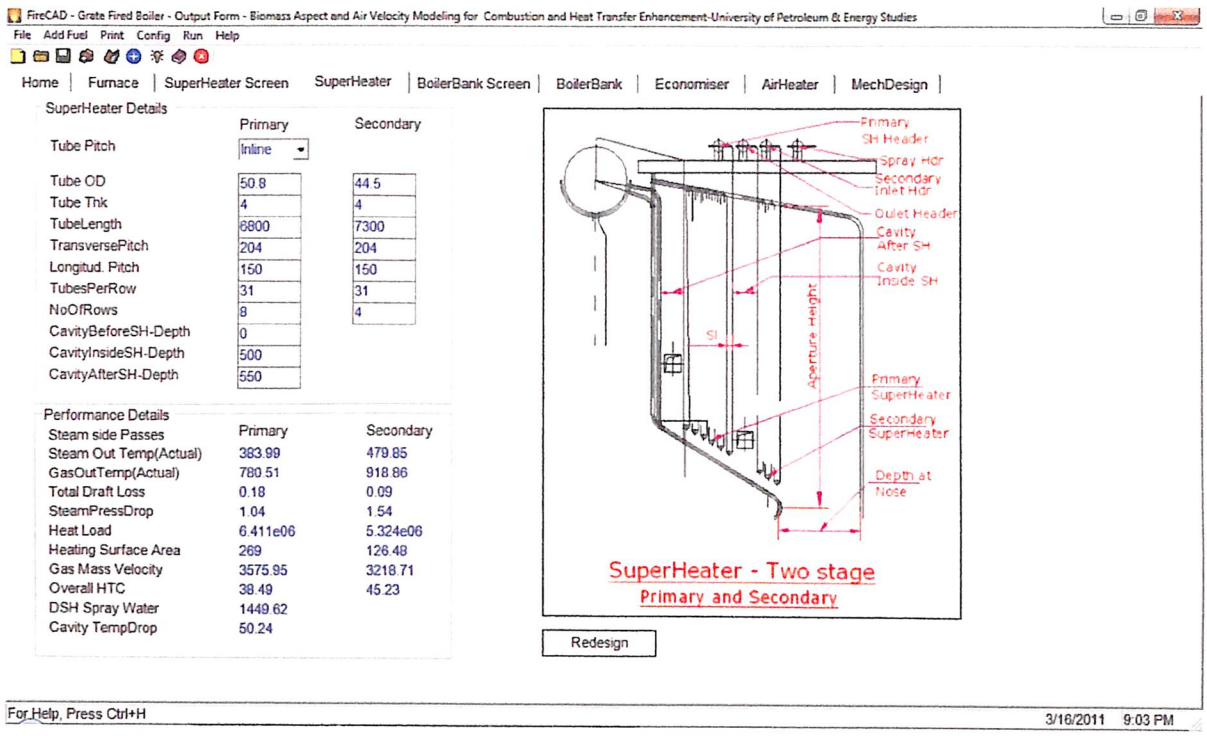

Boiler Bank Screen Design – Output Screen

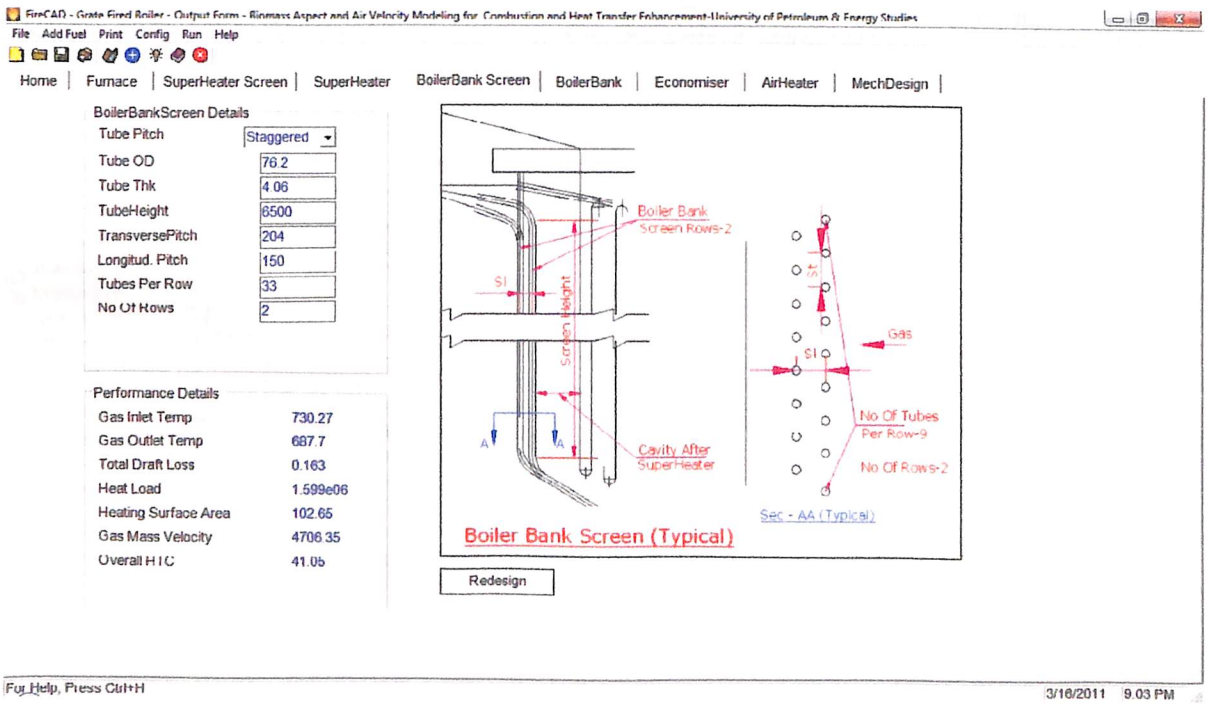

Boiler Bank Design – Output Screen

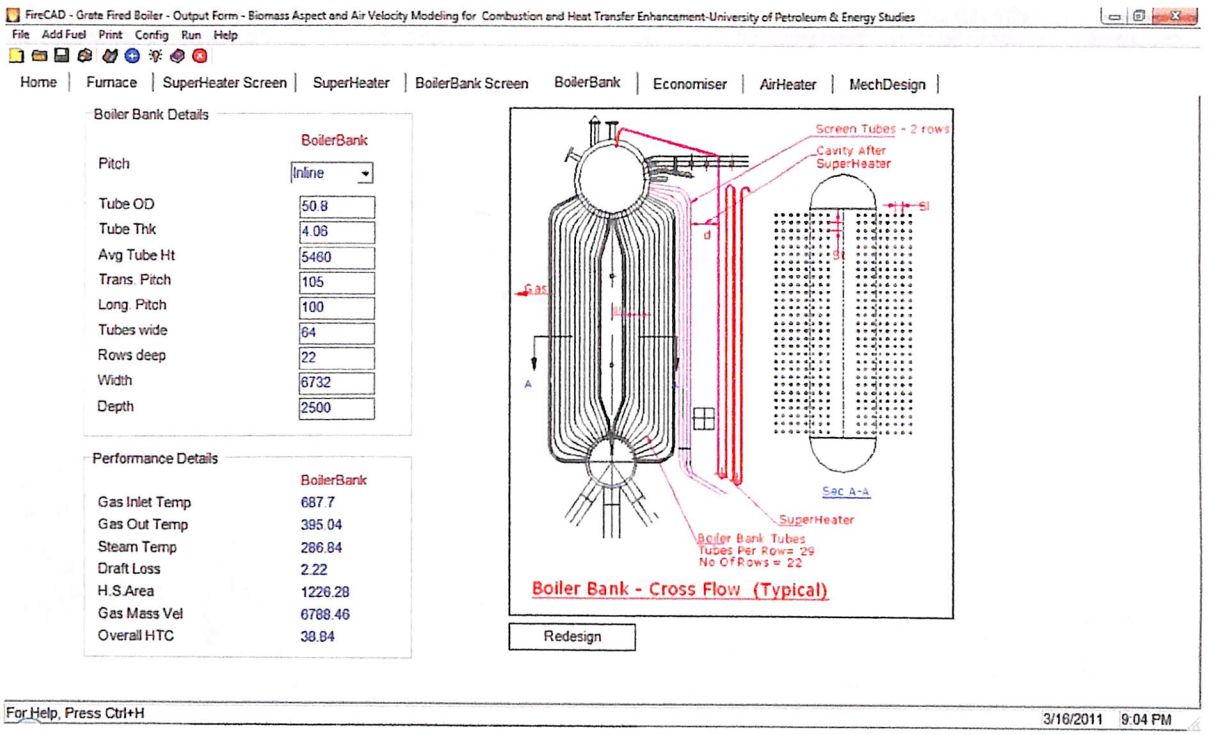

Economizer Design – Output Screen

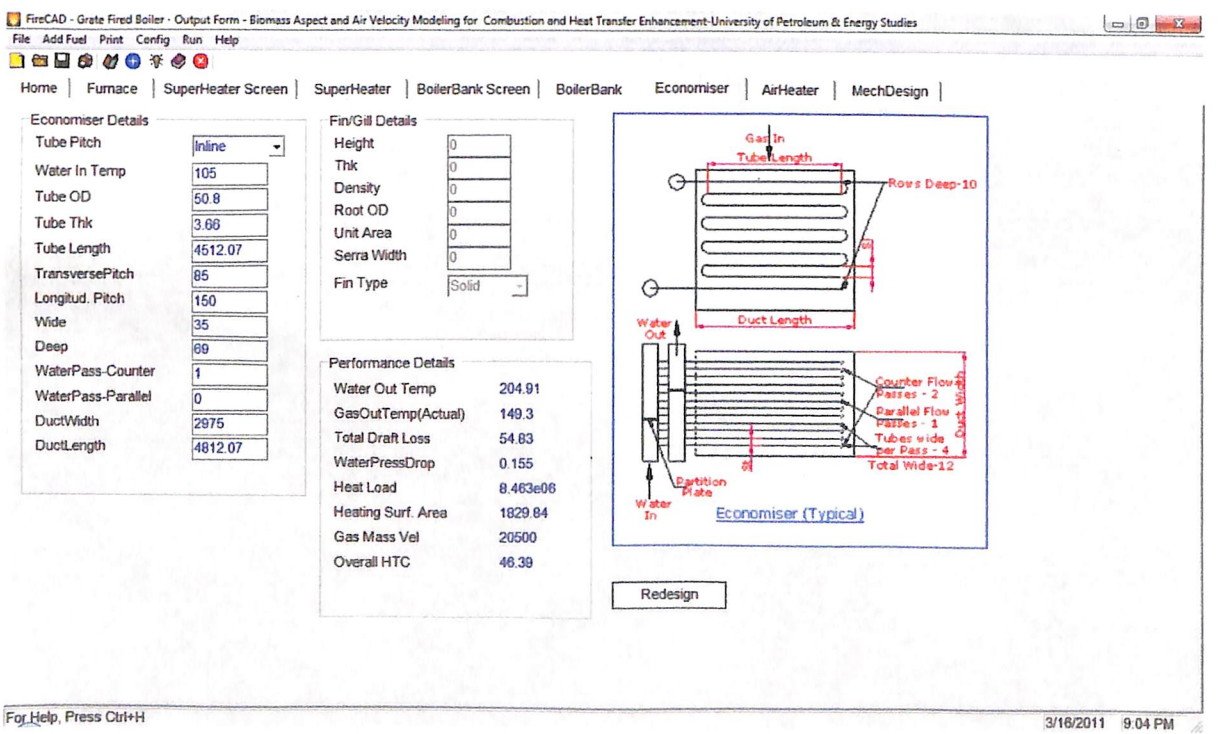

Performance details of Furnace – Output Screen

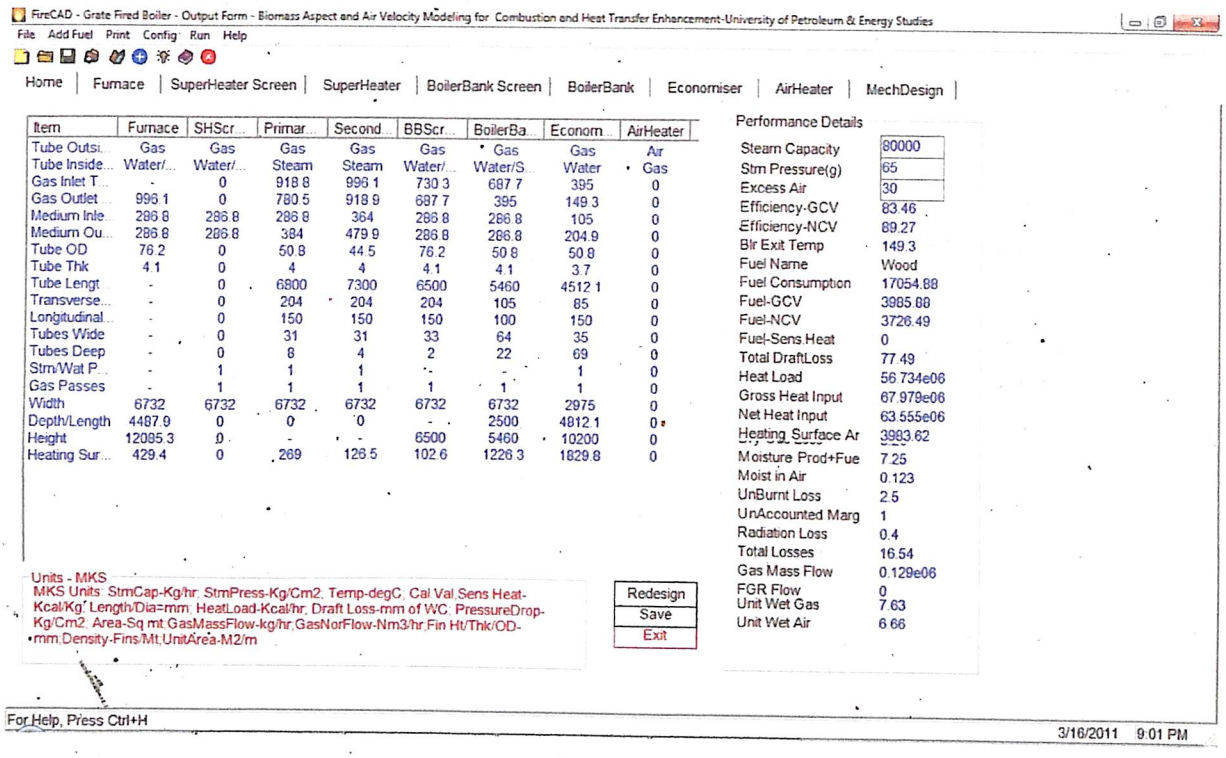

Air Preheater Performance – Output Screen